CHAPTER IV
RESULTS AND DISCUSSION

Effects of operating temperature, zeolite, and zeolite water content were studied here. *KY* and *KBaX* zeolites were chosen as the adsorbents for this study. Roughly, concentration of each C_8 aromatic was varied from 1.24% to 20% by weight at the temperatures of 40, 65, and 90 °C. The zeolite water content, indicated by LOI, was varied from 1.2% to 4.5%.

4.1 Effect of Zeoltie

Figures 4.1 to 4.18 show the adsorption isotherms of *p*-xylene, *m*-xylene, *o*-xylene, and ethylbenzene on *KY* and *KBaX* zeolites at the studied temperatures and water contents. The amount of a C_8 aromatic adsorbed is expressed in gram of the adsorbed species per gram of that species fed, called loading. According to the figures, at high xylene concentration, the zeolite adsorbs *p*-xylene more than the other C_8 aromatics, followed by ethylbenzene, *m*-xylene, and *o*-xylene. At lower concentration, in most cases, both zeolites adsorb more *p*-xylene. However, no definite trend can be observed for the other C_8 aromatics.

The selectivity can be calculated from the ratio of maximum loading of each substance. The selectivity of *p*-xylene relative to the other C_8 aromatics on the *KY* and *KBaX* zeolite is shown in Tables 4.1 – 4.6. On *KY* zeolite, the selectivity of *p*-xylene relative to *o*-xylene is higher than that relative to *m*-xylene and ethylbenzene over the range of studied temperatures. In other words, *KY* zeolite adsorbs *p*-xylene more than ethylbenzene, *m*-xylene, and *o*-xylene, respectively. The selectivity of *p*-xylene relative to *o*-xylene and *m*-xylene are comparable, yet the selectivity over *o*-xylene is slightly higher. The same trend can be observed in the case of *KBaX* zeolite.

However, at the same condition, *KY* zeolite has *p*-xylene selectivity higher than *KBaX* zeolite. The high *p*-xylene selectivity of *KY* zeolite can be explained by the acidity of the zeolite, as discussed by Kulprathipanja (2001). The lower zeolite acidity, the more selective to *p*-xylene. This is a result from a strong acid-base interaction between low acidic zeolite and the least basic xylene isomer, *p*-xylene, which has the weakest electron-donating characteristic among xylenes. Two main factors that govern the zeolite acidity are the ratio of SiO_2/Al_2O_3 and the exchangeable cation.

Y zeolite is more selective to *p*-xylene than *X* zeolite because acidity of a zeolite increases as the ratio of SiO_2/Al_2O_3 decreases. This is because the increase in the AlO_4^- active sites decreases the strength of the electrostatic field in each site. Therefore, *X* zeolite with the SiO_2/Al_2O_3 of 2 is more acidic than *Y* zeolite with the ratio of 5.0.

A zeolite can be ion-exchanged with a variety of metal cations to alter their acidity. There is a strong correlation between the total acidity of a zeolite and the ionic radius or valence of the exchanged cation. Exchanged cations with a lower ionic radius give higher zeolite acidity (Li>Na>K, Co>Zn>Ca> La>Pb>Ba). Di-valence cations give higher zeolite acidity than mono-valence cations (Kulprathipanja, 2001). Accordingly, *KY* zeolite has lower acidity than *KBaX* zeolite.

From Figures 4.1 to 4.18, at the same operating temperature and water content, *KY* zeolite has higher adsorption capacity than *KBaX* zeolite. This result is also supported by the zeolite characteristics as shown in Table 3.2. The BET results show that the micropore volume, surface area and average pore diameter of *KY* zeolite are higher than those of *KBaX* zeolite. Moreover, because *X* zeolite has higher exchange capacity for cations, it may increase the adsorbate and adsorbent interaction. Therefore, *KY* zeolite has an ability to adsorb more C_8 aromatics than *KBaX* zeolite does.

4.2 Effect of Operating Temperature

As shown in Figures 4.1 to 4.8, at the higher operating temperature, the amount of each aromatic adsorbed by *KY* zeolite in the range of water contents and concentrations is less than that at the lower temperature. This can be explained by the known fact that the adsorption process is exothermic; therefore, the zeolite adsorbs all the species less at higher temperature. At high temperature, molecules of the C_8 aromatics and desorbent have higher internal energy and tend to move around rather than being adsorbed on the zeolite. The adsorption capacity of the zeolites is the same at different temperatures. It is the adsorption efficiency that decreases as the temperature increases. Similarly, the adsorption of aromatics by *KBaX* zeolite is less at high temperature.

The selectivity of *p*-xylene relative to the other C_8 aromatics on *KY* and *KBaX* zeolites is shown in Tables 4.1 – 4.6. The results show that in the studied range of concentration and water contents, temperature affects the *p*-xylene selectivity. As the temperature increases, the selectivity to *p*-xylene over the other C_8 aromatics for both *KY* and *KBaX* zeolites decreases. Although the selectivity increases as the operating temperature decreases operation at the low temperature reduces the molecular transfer rate. Thus, the liquid phase adsorption process must be operated at a temperature that balances between the selectivity and transfer rate.

4.3 Effect of Water Content in Zeolite

Water content in zeolite, as is indicated by LOI, is the amount of moisture adsorbed on the zeolite. From Figures 4.1 to 4.18, as the water content in the zeolites increases, the adsorption capacity of both zeolites decreases. This is the result from the active sites of the zeolites are ocupied by water molecules. The same trend was also observed for the *p*-xylene selectivity. That is as the water content in the zeolites increases, the *p*-xylene selectivity of both *KY* and *KBaX* zeolite decreases.

The above statement can be substantiated as follows. Adsorbed water molecules on the zeolite are polarizable due to a strong electrostatic field between the exchanged cation and alumina framework. The polarized water molecule in the zeolite works as a Bronsted acid. The lower the moisture content is, the lower acidity of the zeolite is, which, in turn, increases the selectivity to *p*-xylene.

4.4 Adsorption of Toluene

Comparison of *p*-xylene and toluene adsorption on *KY* and *KBaX* zeolites is shown in Figures 4.19 to 4.27. Both zeolites adsorb more *p*-xylene than toluene. Moreover, *KY* zeolite adsorbs more *p*-xylene and toluene than *KBaX* zeolite does. The adsorption exhibits the same trend over the range of the studied temperatures and water contents. Adsorption of *m*-xylene/toluene and *o*-xylene/toluene on *KY* and *KBaX* zeolites are plotted in Figures 4.28 to 4.45. Unlike the adsorption of *p*-xylene, *KY* and *KBaX* zeolites adsorb more toluene than *m*-xylene and *o*-xylene over the range of the investigated temperatures and water contents. The amount of toluene adsorbed relative to *m*-xylene or *o*-xylene by *KY* zeolite is much higher than that in the case of *KBaX* zeolite. Competitive adsorption of ethylbenzene and toluene at the

studied temperatures and water contents on *KY* and *KBaX* zeolites is shown in Figures 4.46 to 4.54. *KY* zeolite adsorbs more toluene than ethylbenzene over the range of the studied water contents and temperatures. Like *KY* zeolite, *KBaX* zeolite with 1.2% LOI shows the similar behavior. But for the high water contents, *KBaX* zeolite adsorbs about the same amount for both ethylbenzene and toluene.

4.5 Modeling of the Experimental Data

From the statistical model, equation 2.2, the correlation is expressed in terms of mole fraction in the solid and liquid phases. Therefore, as shown in Figures 4.55 to 4.72, the adsorption isotherms were plotted differently from the first part. From the figures, the solid phase and liquid phase mole fraction are linearly dependent on each other. The complicated statistical model can then be simplified by setting A_{12} and A_{21} to unity. And with simple mathematical manipulation, equation 2.2 can be expressed as equation 2.3, where k_1 is a function of temperature as

$$k_1 = K_{01} \exp\left(\frac{-\Delta H_1}{RT}\right) \tag{4.1}$$

where K_{01} is the constant of species 1, ΔH_1 is the heat of adsorption of species 1 on the adsorbent, R is the gas constant, and T is the operating temperature. ΔH_1 and K_{01} are concentration and temperature independent parameters. Each calculation involves a set of data at different concentrations with the same water content and adsorbed species (approximately 15 data). The solver function in Microsoft excel program was used to obtain the most suitable parameters, ΔH_1 and K_{01} from the experimental data. The calculation was based on the least squared method. All the R^2 are in the range of 0.89 to 0.99.

The comparison of the experimental data and prediction from the model of *p*-xylene, ethylbenzene, *m*-xylene, and *o*-xylene on the *KY* and *KBaX* zeolites in the *p*-xylene/toluene, ethylbenzene/toluene, *m*-xylene/toluene, and *o*-xylene/toluene at the studied water contents and temperatures are shown in Figures 4.55 to 4.72. From the figures, it can be clearly seen that the linear model provides a very good fit with a high degree of accuracy to the experimental data. Two important points are worth mentioning here. First, the experiment was carried out at very low concentration thus linear isotherm is not unexpected since it lies in the Henry's law region. Second, at the low concentration the adsorbate molecules are very dilute. Hence, the interaction between molecules is also diminished. That substantiates why such the simple model can well represent the whole range of the experimental data.

4.6 The Multi-Component Pulse Test on *KY* Zeolite

Multi-component pulse test was conducted on *KY* zeolite. The test represents multi-component adsorption of C_8 aromatic system at low concentration. Figures 4.73 to 4.81 show results from the multi-component pulse test. Components leaving the column starts with n-C_9 as it is a tracer, followed by *m*-xylene, *o*-xylene, ethylbenzene, and *p*-xylene. In the presence of other C_8 aromatics, *KY* zeolite is still selective for *p*-xylene because of strong interaction of *p*-xylene with the zeolite as shown by the order of components leaving the column. In other words, the amount of desorbent used to desorb *p*-xylene from *KY* zeolite is higher than that needed to desorb other species at the same conditions. *p*-xylene selectivity is calculated by the Sorbex Database provided by *UOP LLC*. The results are shown in Tables 4.7 to 4.9. The selectivity of *p*-xylene over *m*-xylene is the highest followed by *o*-xylene and ethybenzene. Moreover, the selectivity from the pulse test is higher than that from the single component experiment.

Since *p*-xylene is the least basic species and *m*-xylene is the most basic species among the C_8 aromatics, it would be expected that *KY* zeolite should adsorb *p*-xylene followed by etylbenzene, *o*-xylene, and *m*-xylene. From Figures 4.55 to 4.72, the results from the single component experiment, *KY* zeolite adsorbs preferentially *p*-xylene followed by etylbenzene, *m*-xylene, and *o*-xylene. The inconsistency was observed between *m*-xylene and *o*-xylene. The results from the pulse test, however, are consistent with the prediction. Moreover, the selectivity of *p*-xylene over *m*-xylene and *o*-xylene from the experimental data, in Table 4.1 to 4.6, is close to each other. The adsorption experiment was carried out on the single component basis. Unlike the adsorption experiment, the pulse test was a multi-component adsorption. The discrepancy may be due to the effect from the presence of several components at the same time. Yet, these phenomena are still unexplainable. Further study should be made in order to understand these complications.

Table 4.1 Selectivity from the single component experiment of *p*-xylene on *KY* zeolite LOI=1.2%

Selectivity	Temperature (°C)		
	40	65	90
PX/OX	6.5845	5.5048	4.9029
PX/MX	6.1252	5.0436	4.5554
PX/EB	3.3351	3.4525	3.0510

Table 4.2 Selectivity from the single component experiment of *p*-xylene on *KY* zeolite LOI=2.4%

Selectivity	Temperature (°C)		
	40	65	90
PX/OX	5.3769	5.0601	5.0857
PX/MX	5.2980	5.1200	5.0508
PX/EB	2.7741	2.6633	2.2719

Table 4.3 Selectivity from the single component experiment of *p*-xylene on *KY* zeolite LOI=4.4%

Selectivity	Temperature (°C)		
	40	65	90
PX/OX	4.6919	4.7671	3.5710
PX/MX	4.5988	3.8729	3.2020
PX/EB	2.3062	2.3648	1.9811

Table 4.4 Selectivity from the single component experiment of *p*-xylene on *KBaX* zeolite LOI=1.2%

Selectivity	Temperature (°C)		
	40	65	90
PX/OX	4.4774	3.4024	2.7101
PX/MX	3.9465	3.3439	2.5781
PX/EB	2.7408	2.0178	1.8145

Table 4.5 Selectivity from the single component experiment of *p*-xylene on *KBaX* zeolite LOI=2.5%

Selectivity	Temperature (°C)		
	40	65	90
PX/OX	3.5167	3.1789	2.6673
PX/MX	3.3172	3.1100	2.6397
PX/EB	1.8001	1.7024	1.6033

Table 4.6 Selectivity from the single component experiment of *p*-xylene on *KBaX* zeolite LOI=4.5%

Selectivity	Temperature (°C)		
	40	65	90
PX/OX	2.9757	2.5965	2.0899
PX/MX	2.8879	2.5278	1.9498
PX/EB	1.8389	1.6514	1.4115

Table 4.7 Selectivity from the pulse test of *p*-xylene on *KY* zeolite LOI=1.2%

Selectivity	Temperature (°C)		
	40	**65**	**90**
PX/OX	6.3557	5.9697	4.1840
PX/MX	7.1920	5.3983	4.7056
PX/EB	3.0870	2.6540	2.2732

Table 4.8 Selectivity from the pulse test of *p*-xylene on *KY* zeolite LOI=2.4%

Selectivity	Temperature (°C)		
	40	**65**	**90**
PX/OX	7.1269	5.4885	4.4120
PX/MX	7.7643	5.8577	4.8131
PX/EB	2.9200	2.5695	2.2790

Table 4.9 Selectivity from the pulse test of *p*-xylene on *KY* zeolite LOI=4.4%

Selectivity	Temperature (°C)		
	40	**65**	**90**
PX/OX	5.0194	4.1136	3.3352
PX/MX	5.6800	4.5472	3.7006
PX/EB	2.2023	1.9900	1.7755

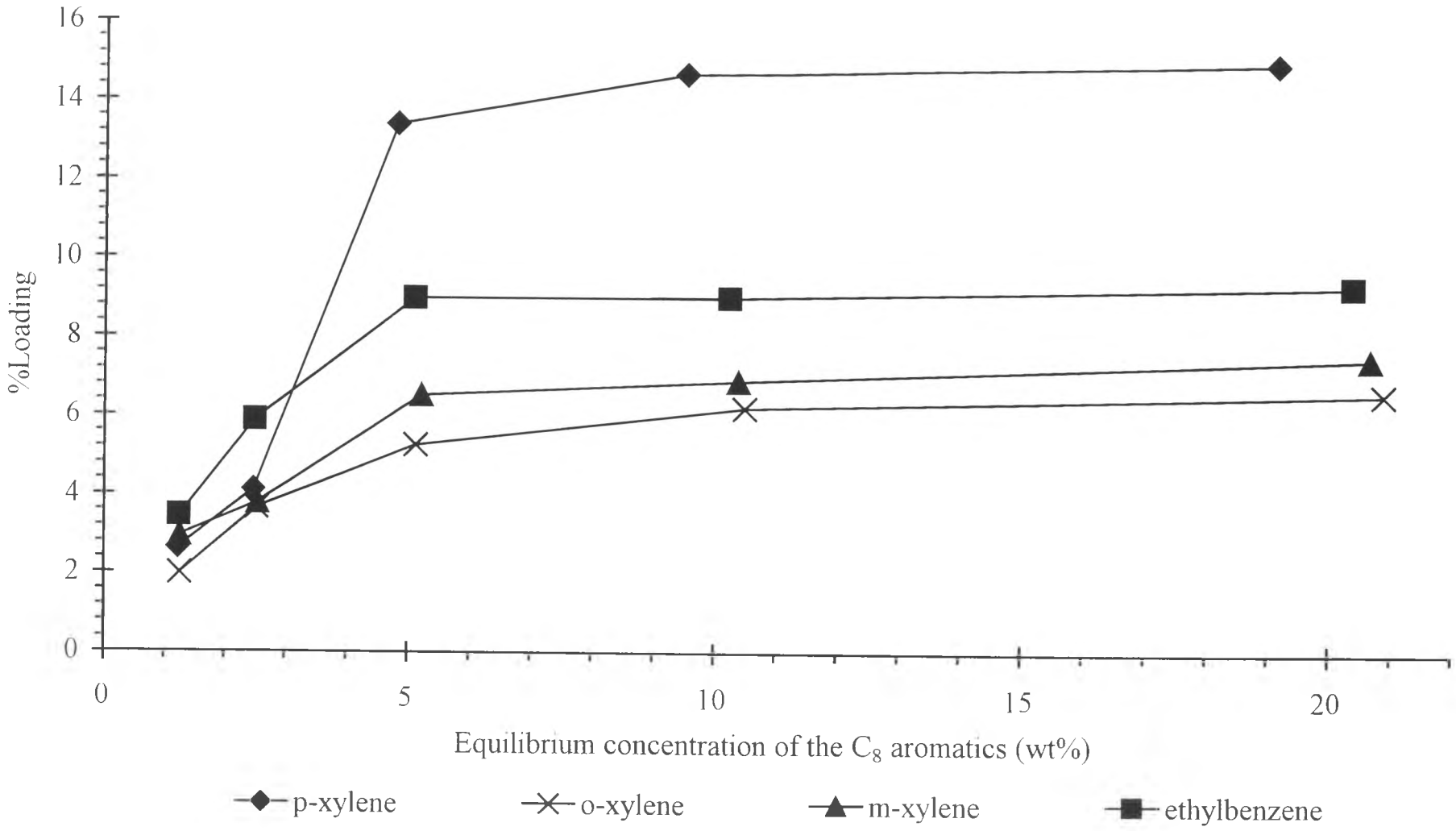

Figure 4.1 Adsorption of the C_8 aromatics on the *KY* zeolite, LOI=1.2% at 40 °C

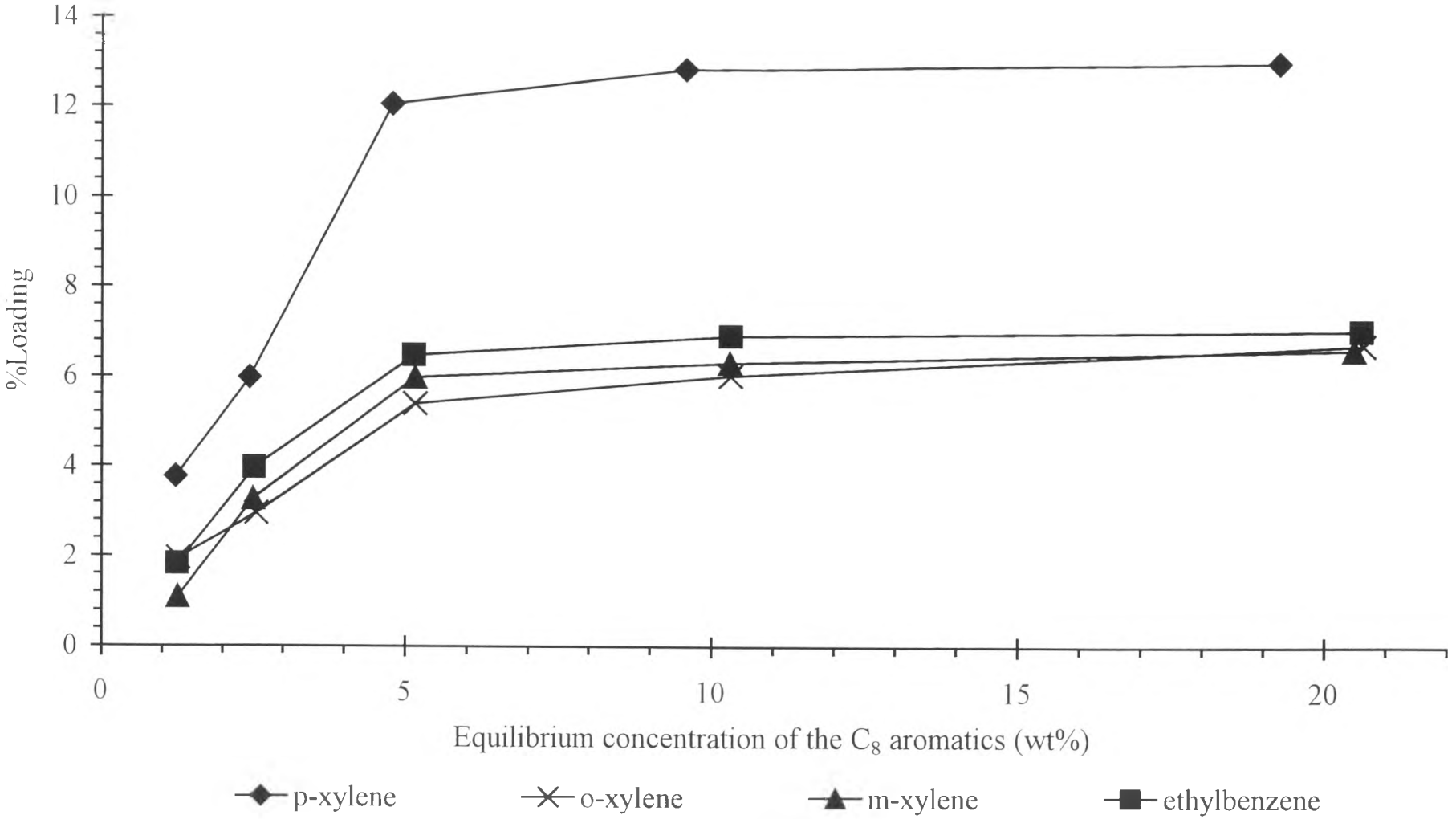

Figure 4.2 Adsorption of the C_8 aromatics on the *KY* zeolite, LOI=1.2% at 65 °C

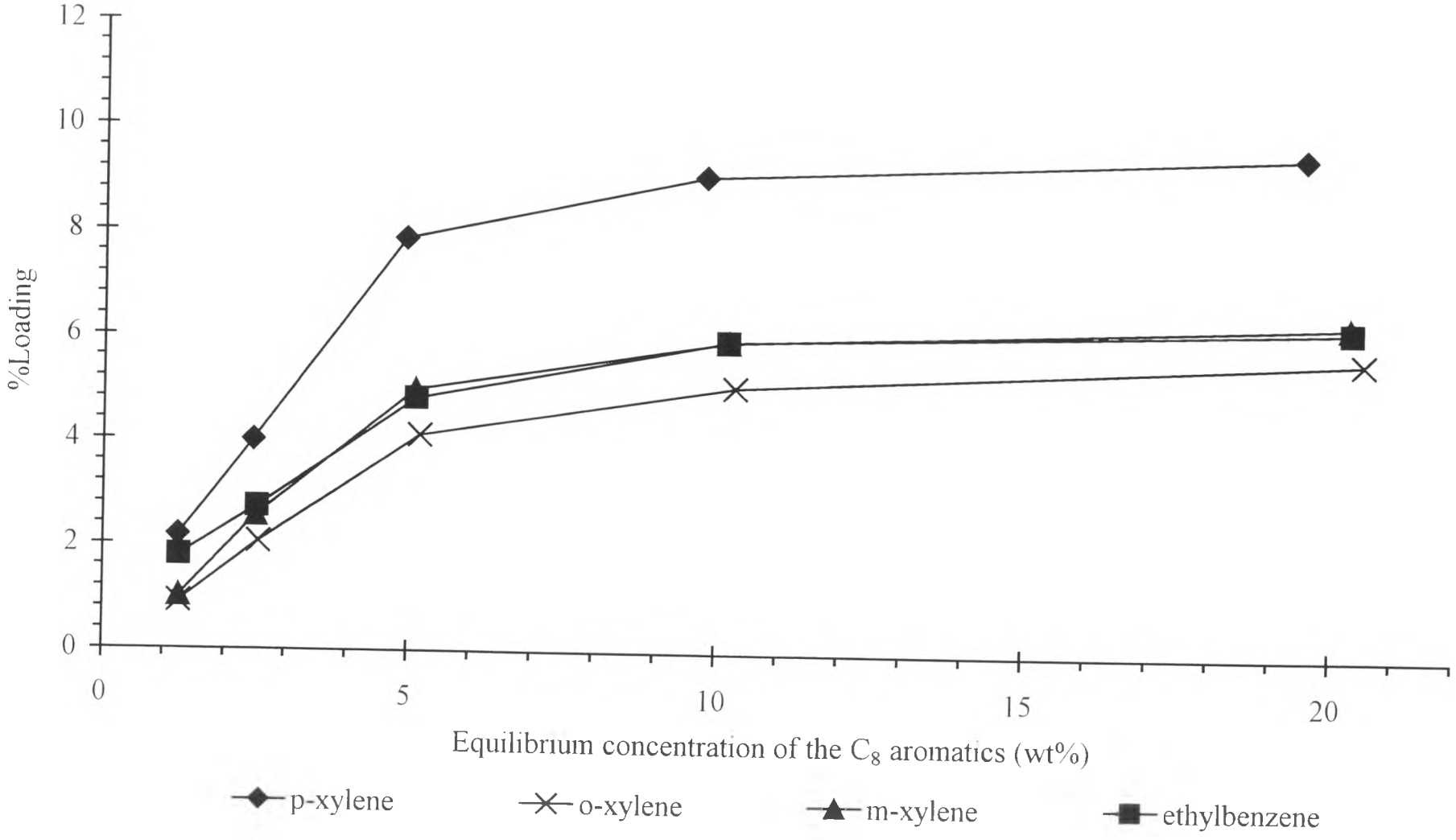

Figure 4.3 Adsorption of the C_8 aromatics on the *KY* zeolite, LOI=1.2% at 90 °C

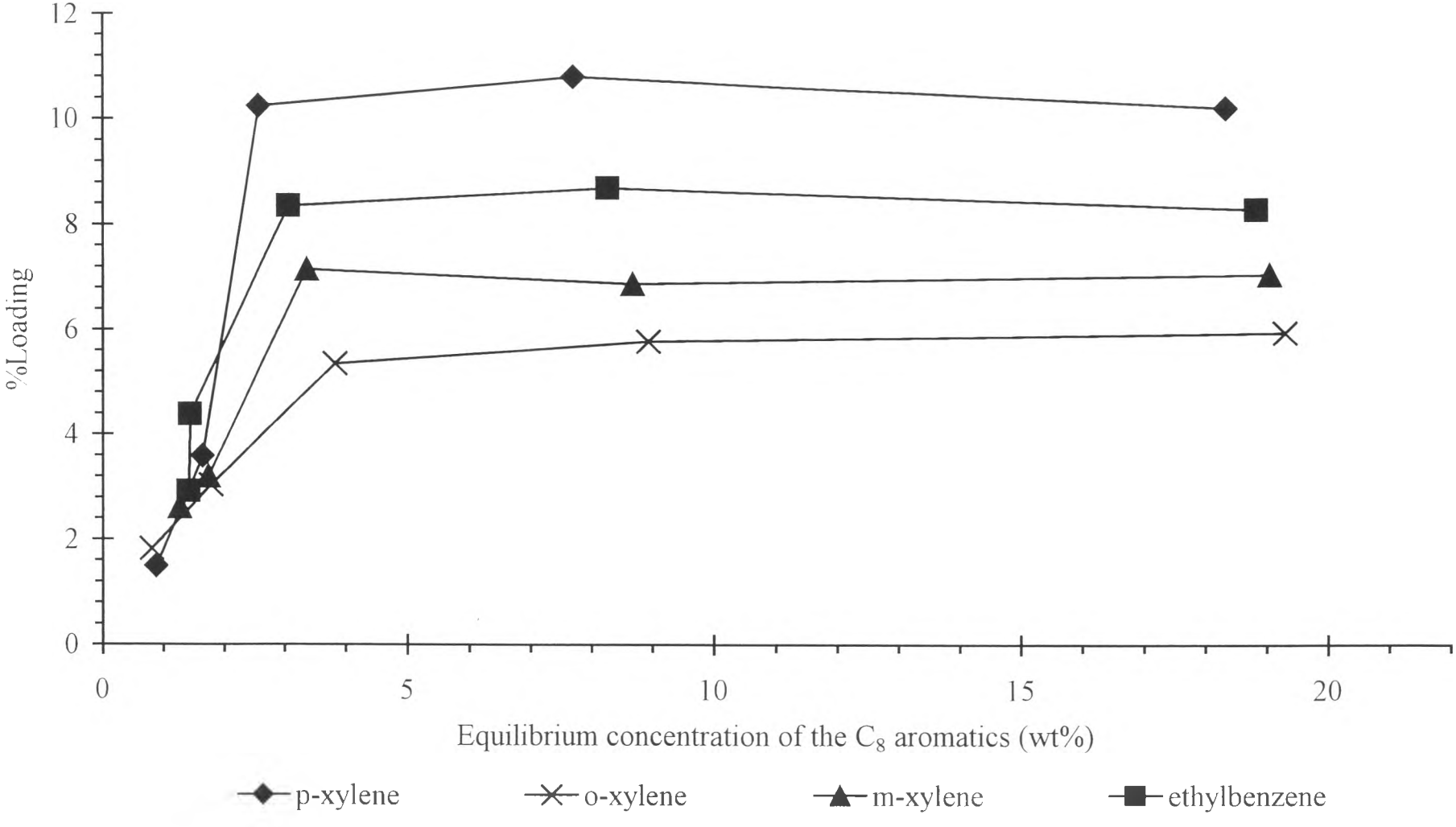

Figure 4.4 Adsorption of the C_8 aromatics on the *KY* zeolite, LOI=2.4% at 40 °C

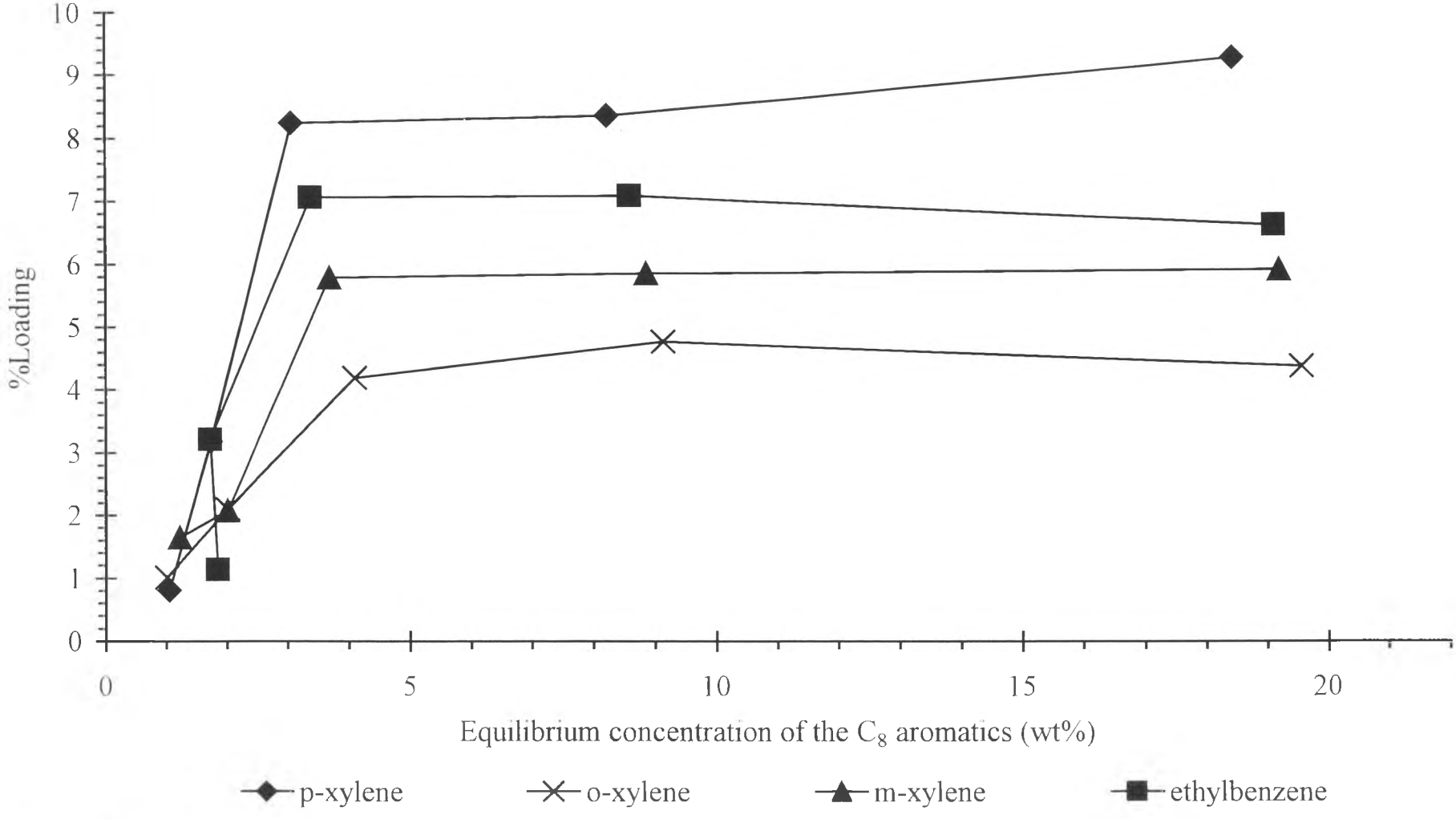

Figure 4.5 Adsorption of the C_8 aromatics on the *KY* zeolite, LOI=2.4% at 65 °C

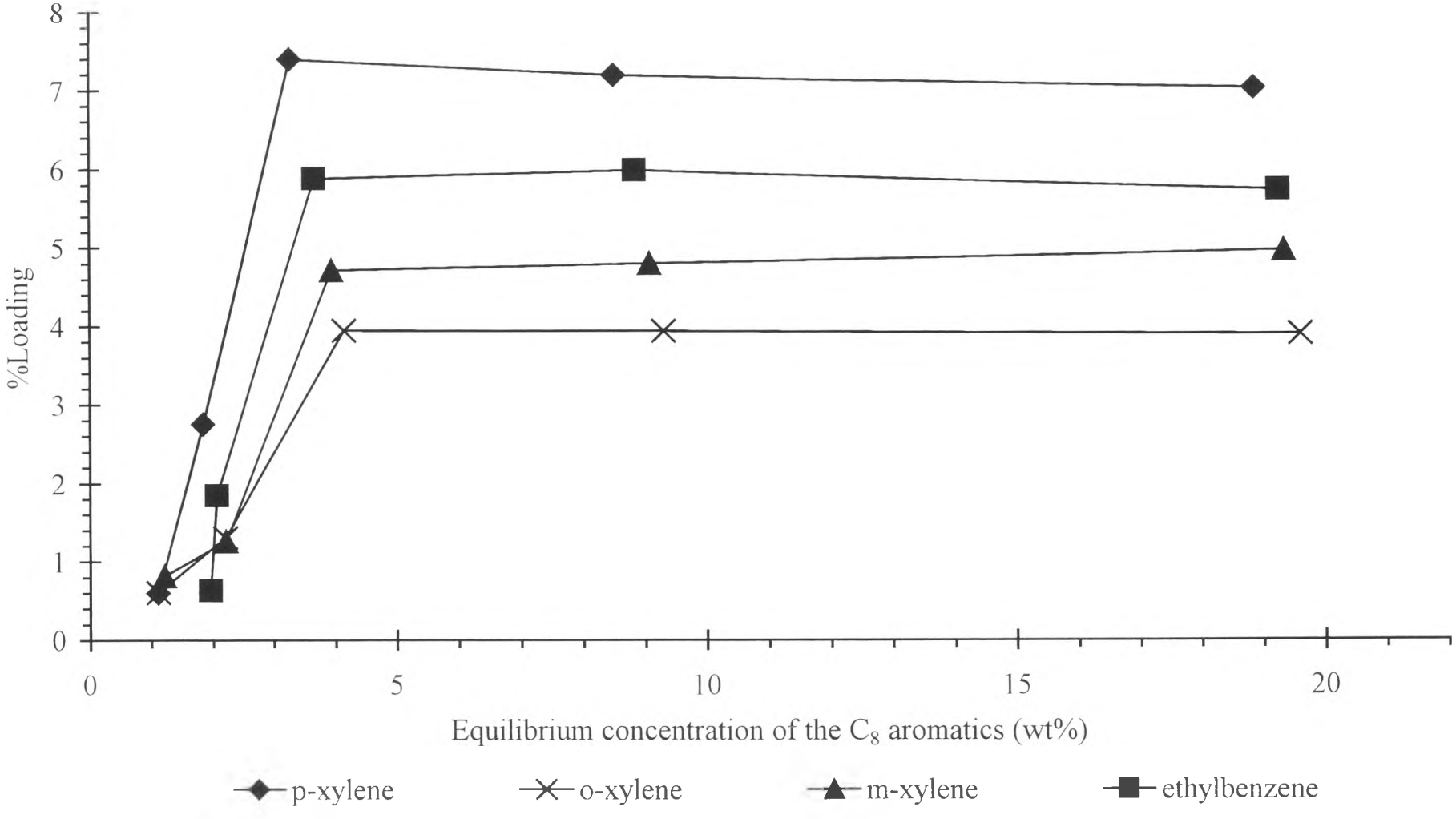

Figure 4.6 Adsorption of the C_8 aromatics on the *KY* zeolite, LOI=2.4% at 90 °C

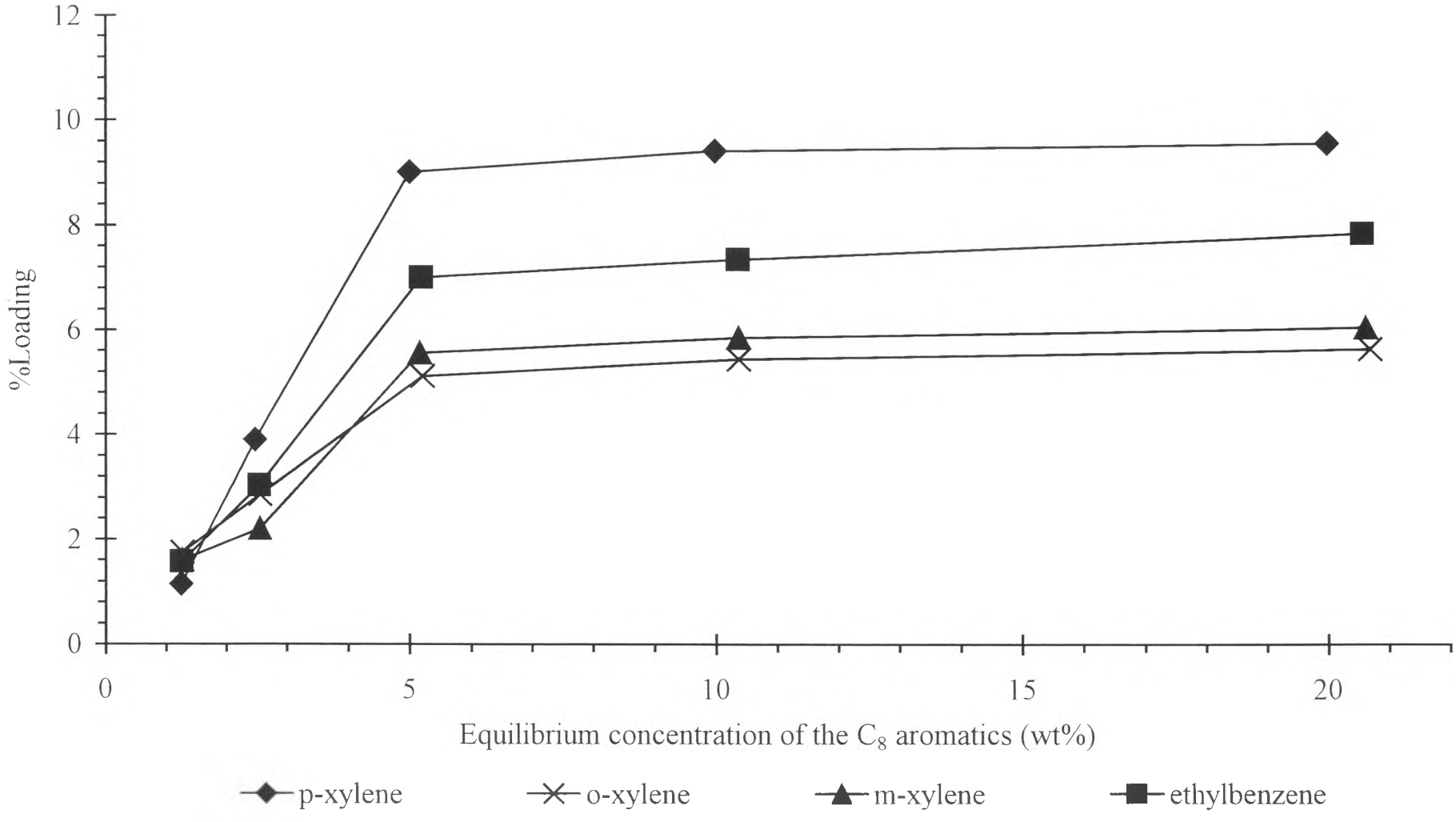

Figure 4.7 Adsorption of the C_8 aromatics on the *KY* zeolite, LOI=4.4% at 40 °C

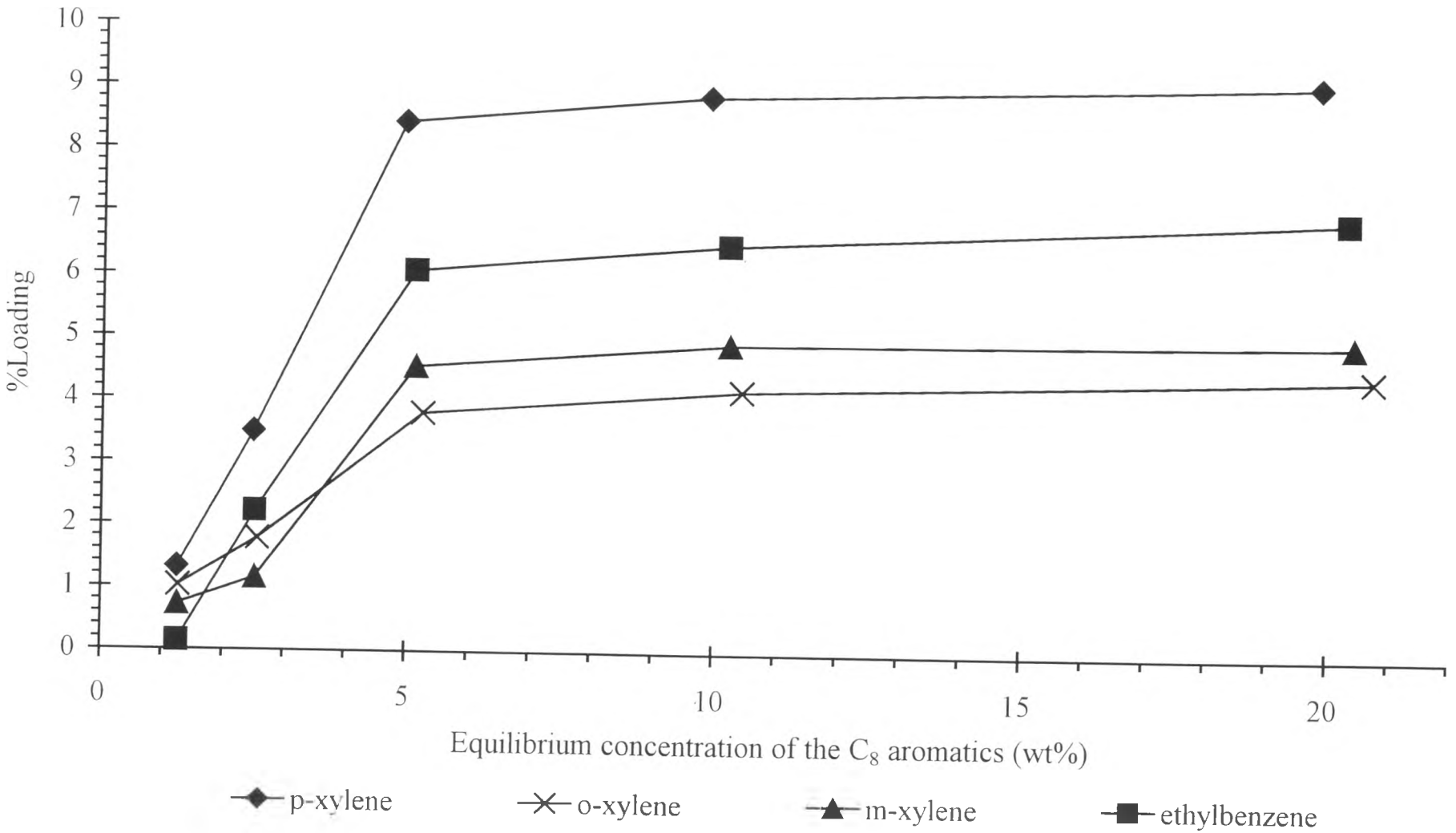

Figure 4.8 Adsorption of the C_8 aromatics on the *KY* zeolite, LOI=4.4% at 65 °C

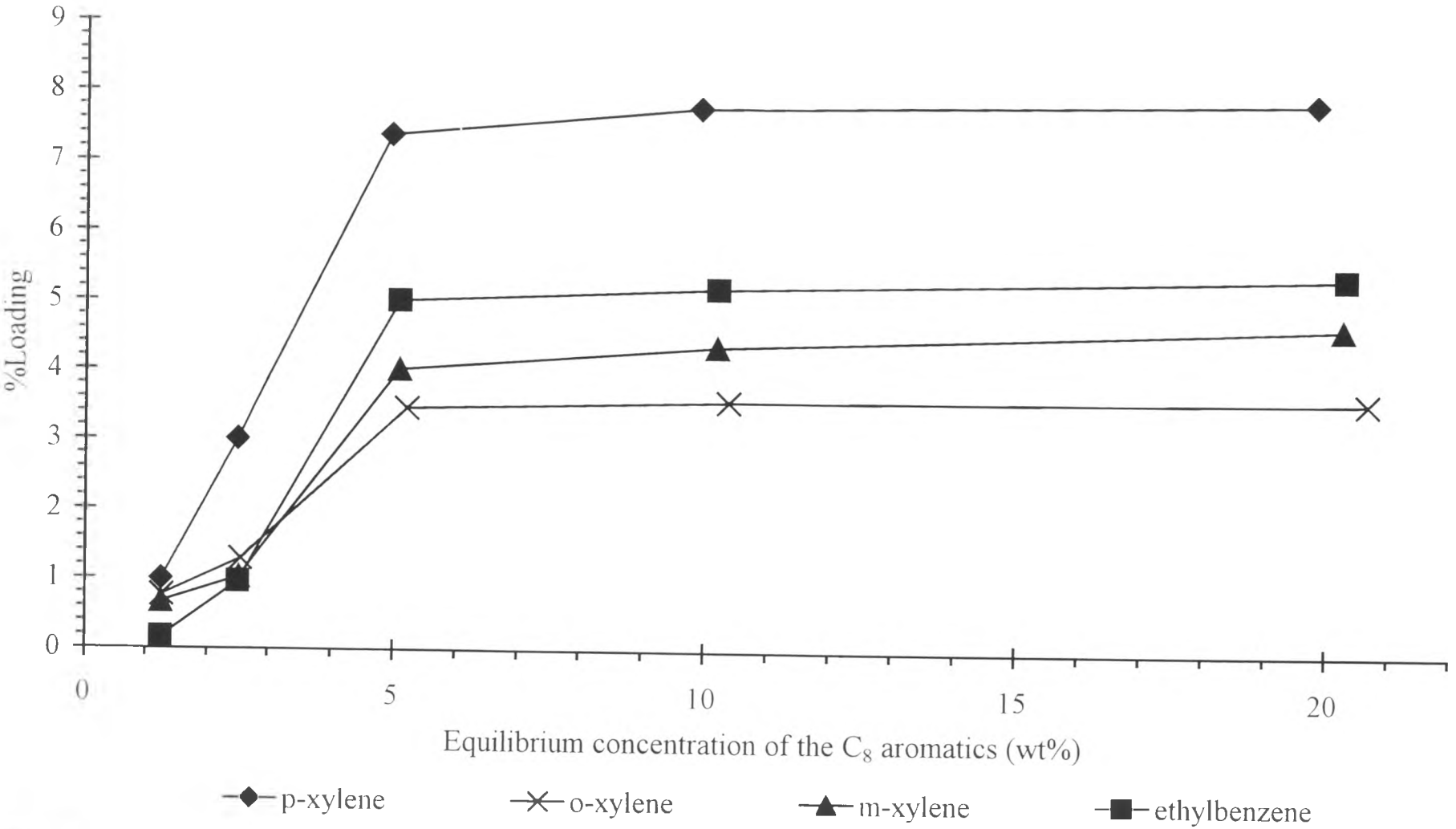

Figure 4.9 Adsorption of the C_8 aromatics on the *KY* zeolite, LOI=4.4% at 90 °C

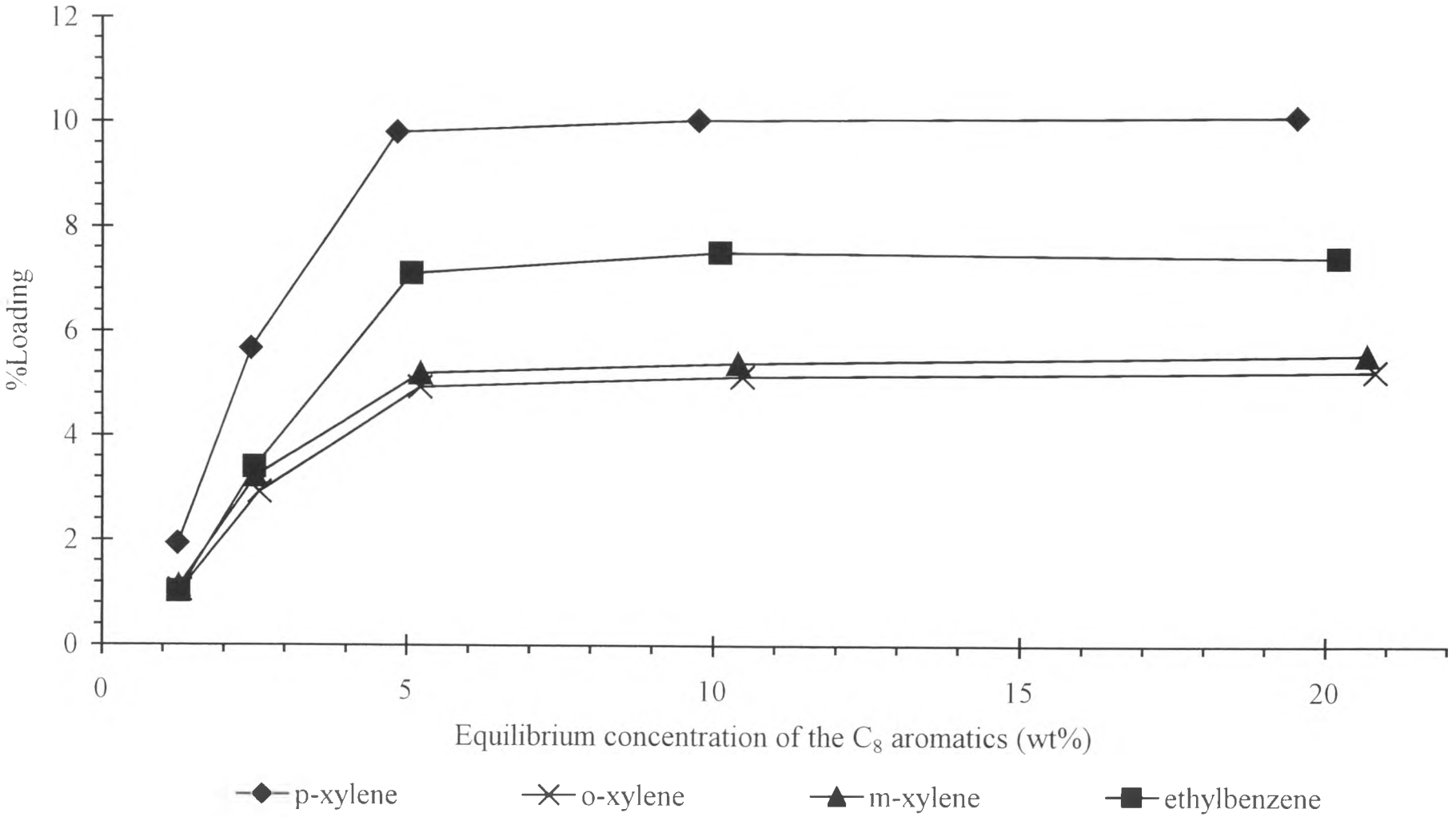

Figure 4.10 Adsorption of the C_8 aromatics on the *KBaX* zeolite, LOI=1.2% at 40 °C

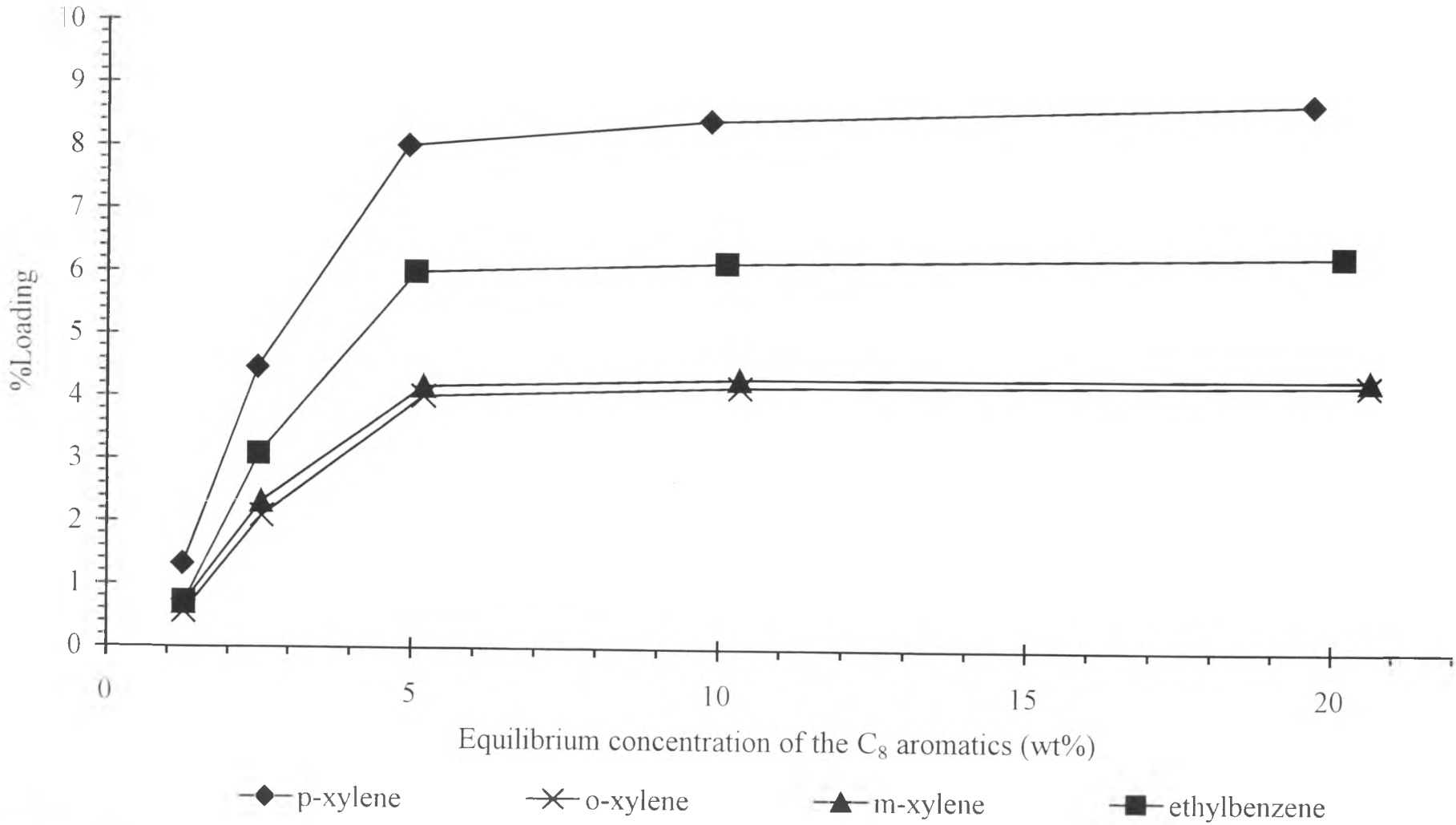

Figure 4.11 Adsorption of the C_8 aromatics on the *KBaX* zeolite, LOI=1.2% at 65 °C

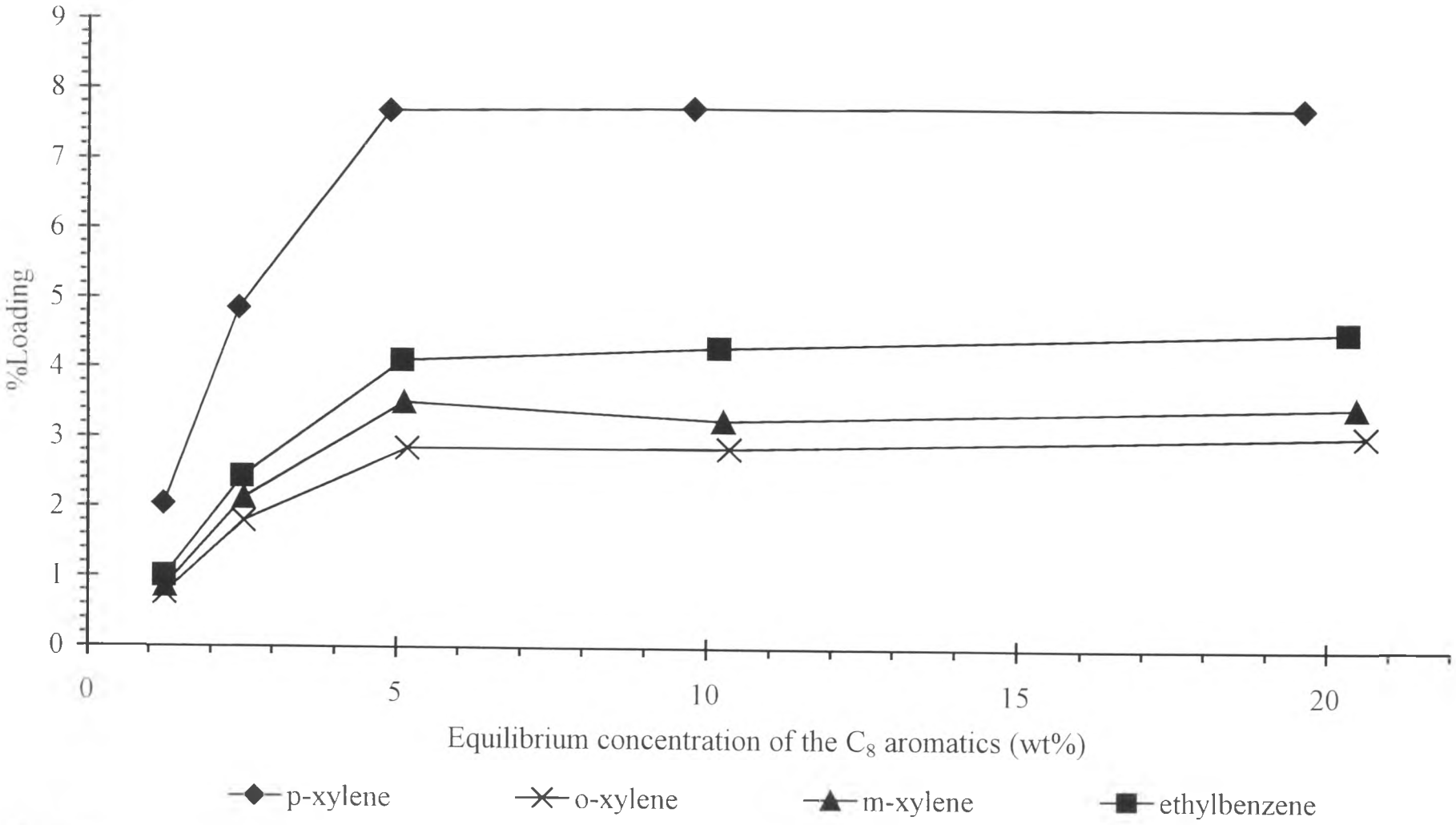

Figure 4.12 Adsorption of the C_8 aromatics on the *KBaX* zeolite, LOI=1.2% at 90 °C

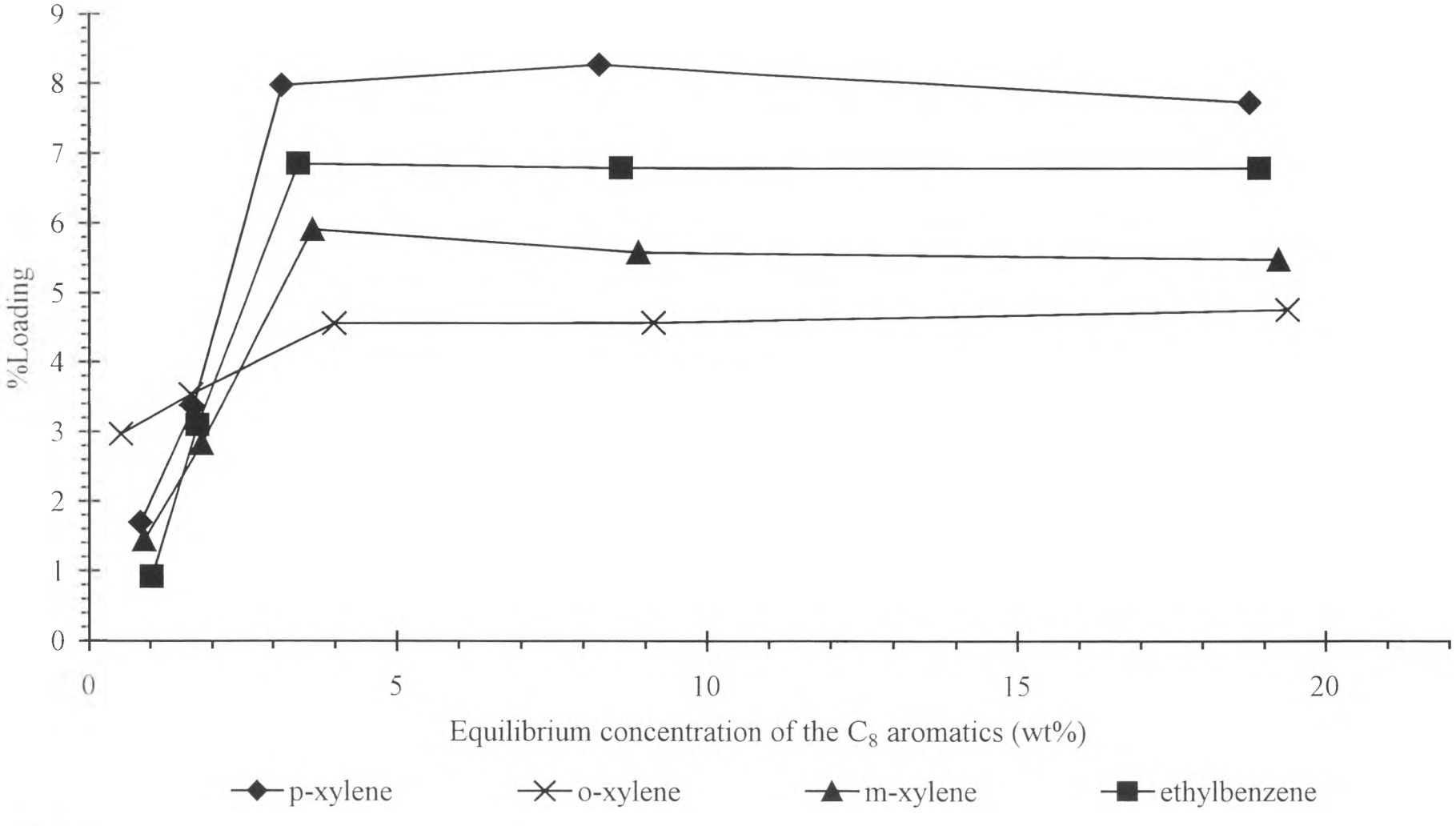

Figure 4.13 Adsorption of the C_8 aromatics on the *KBaX* zeolite, LOI=2.5% at 40 °C

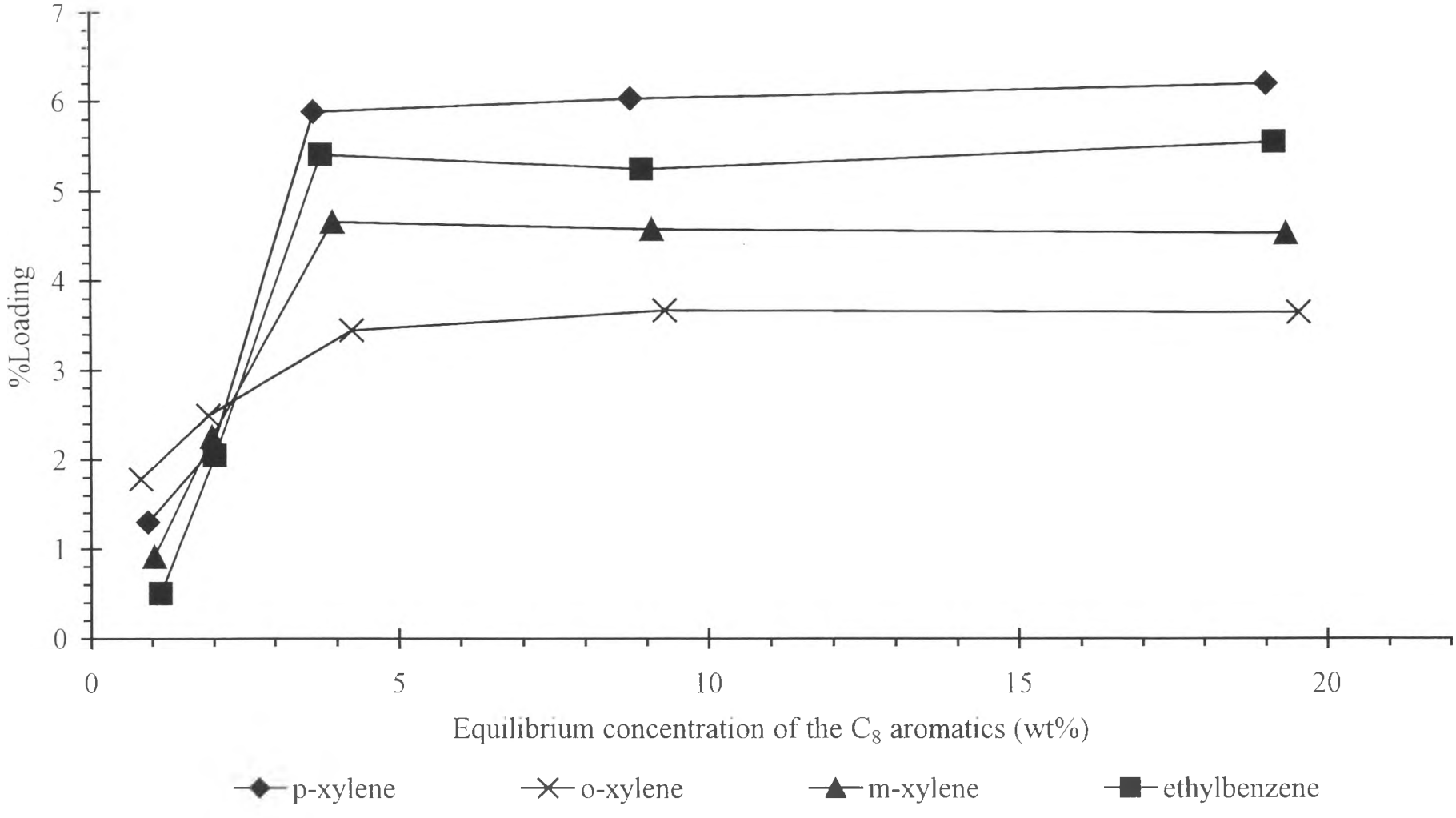

Figure 4.14 Adsorption of the C_8 aromatics on the *KBaX* zeolite, LOI=2.5% at 65 °C

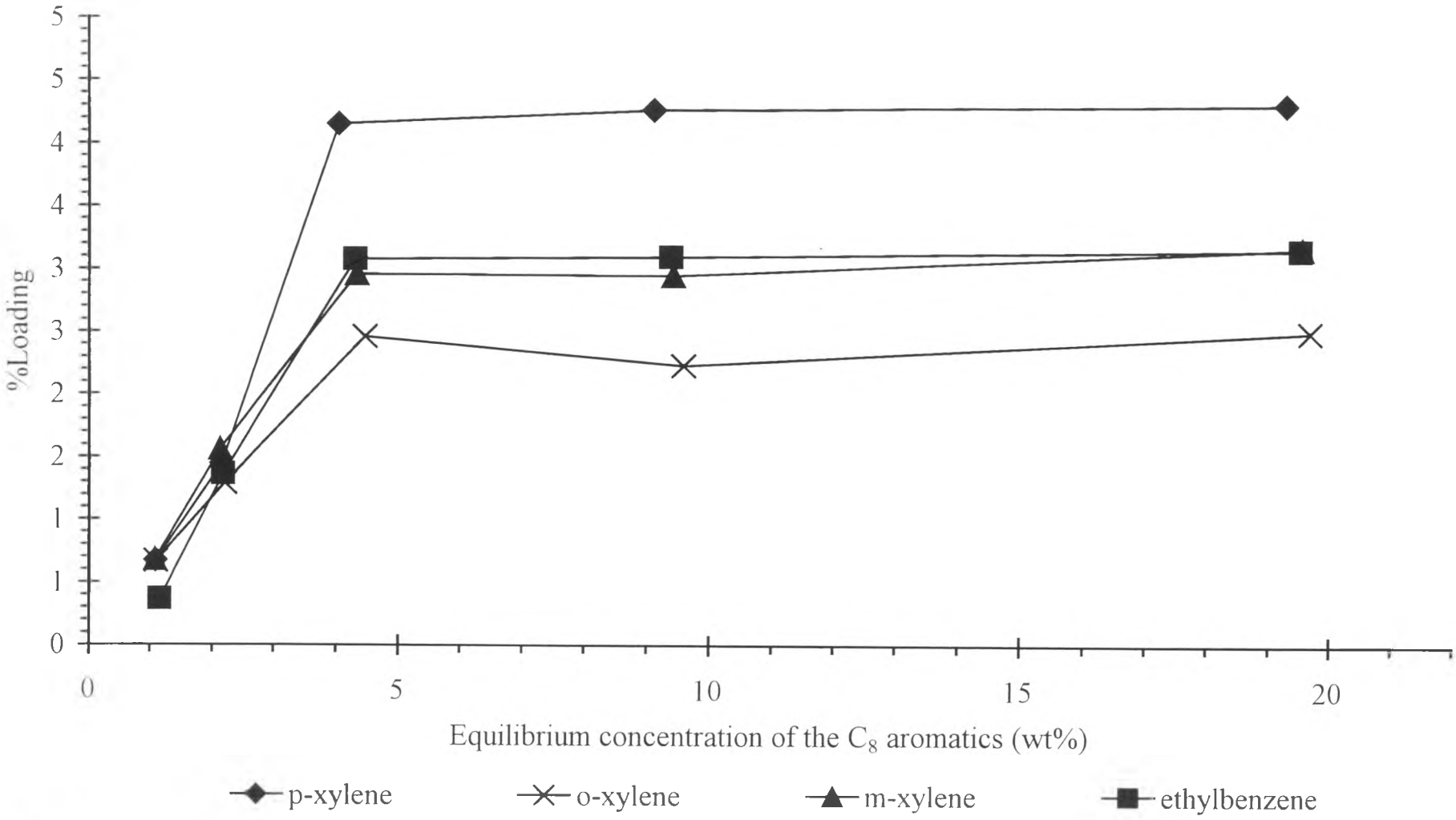

Figure 4.15 Adsorption of the C_8 aromatics on the *KBaX* zeolite, LOI=2.5% at 90 °C

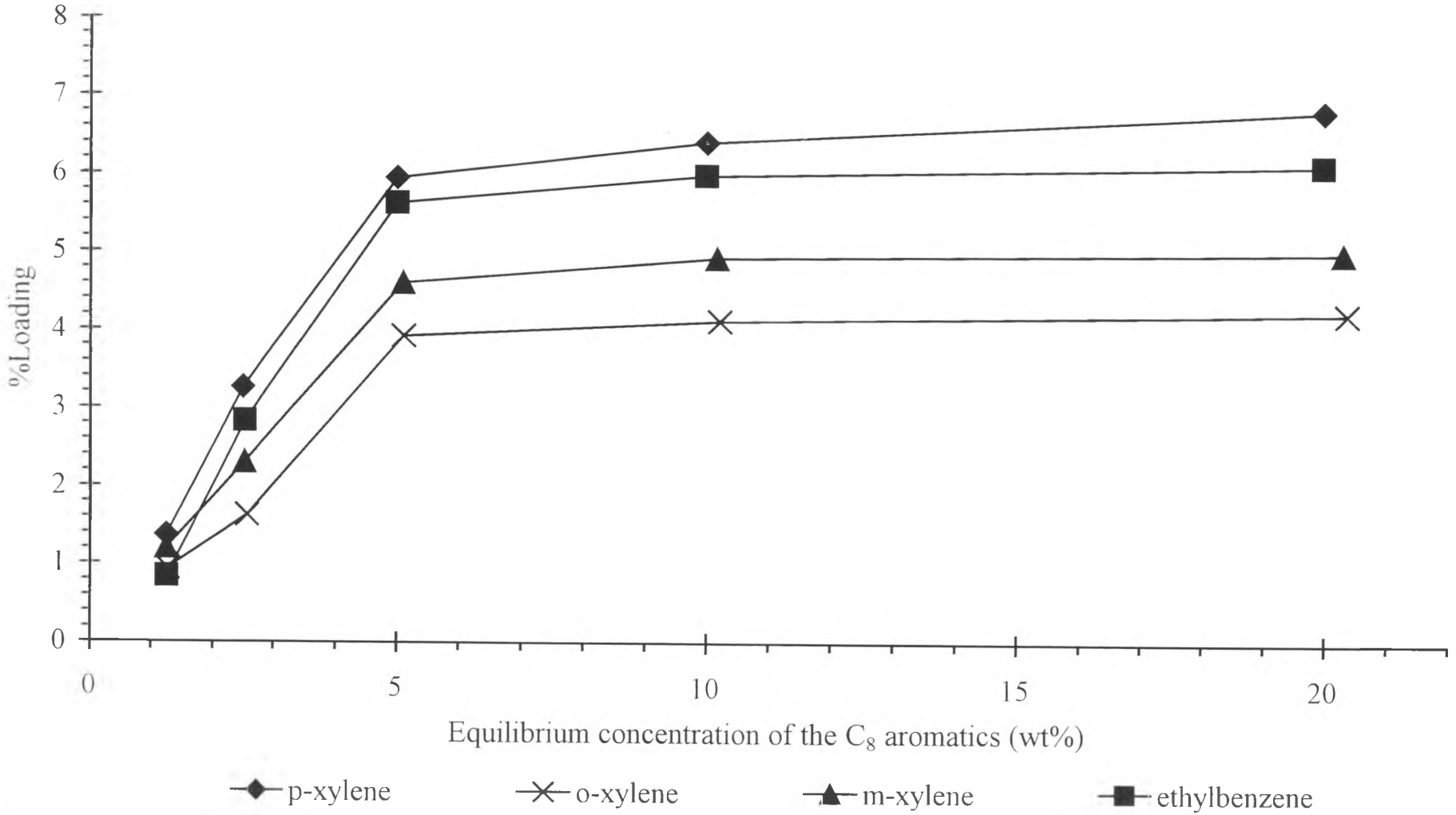

Figure 4.16 Adsorption of the C_8 aromatics on the *KBaX* zeolite, LOI=4.5% at 40 °C

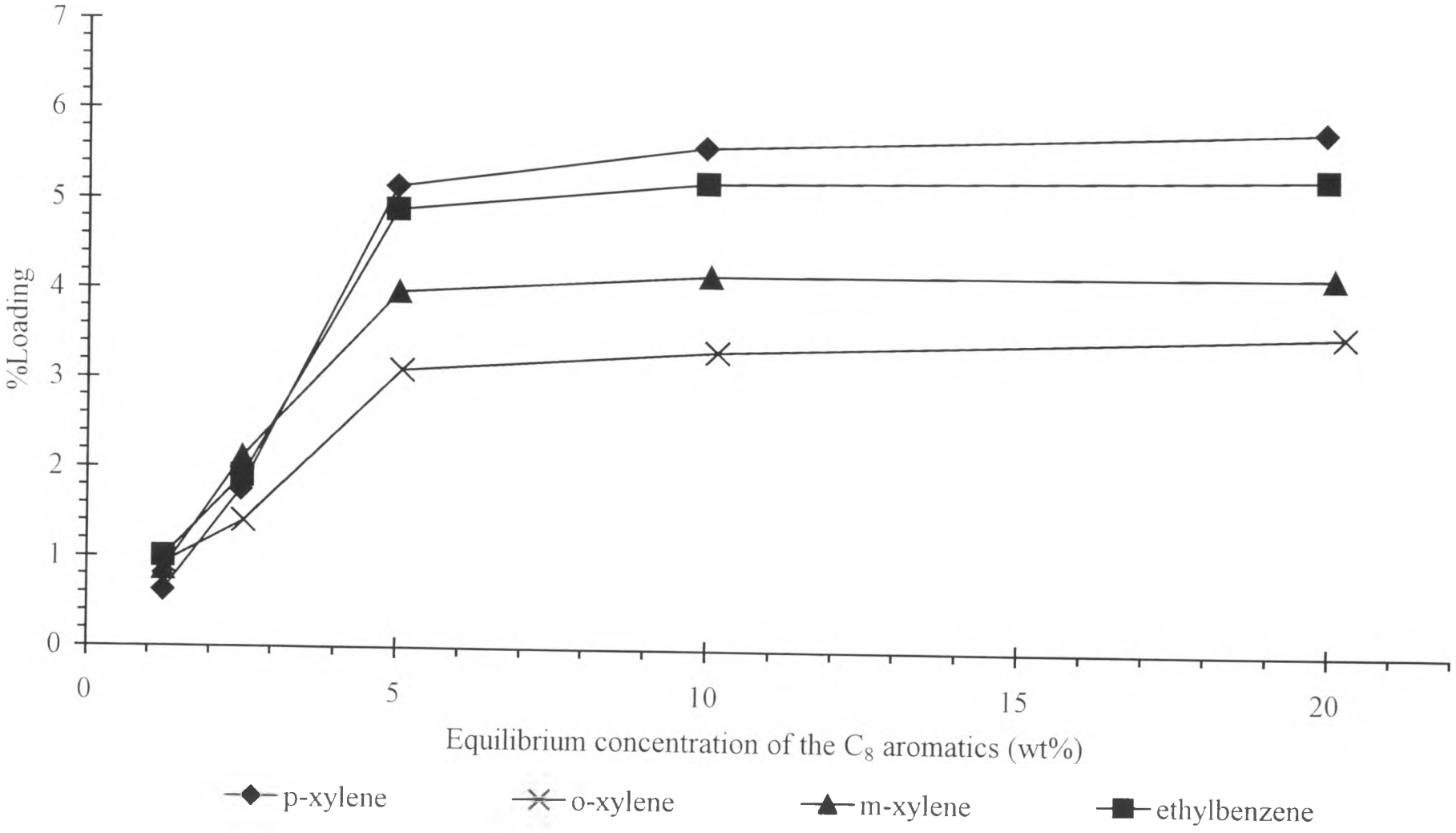

Figure 4.17 Adsorption of the C_8 aromatics on the *KBaX* zeolite, LOI=4.5% at 65 °C

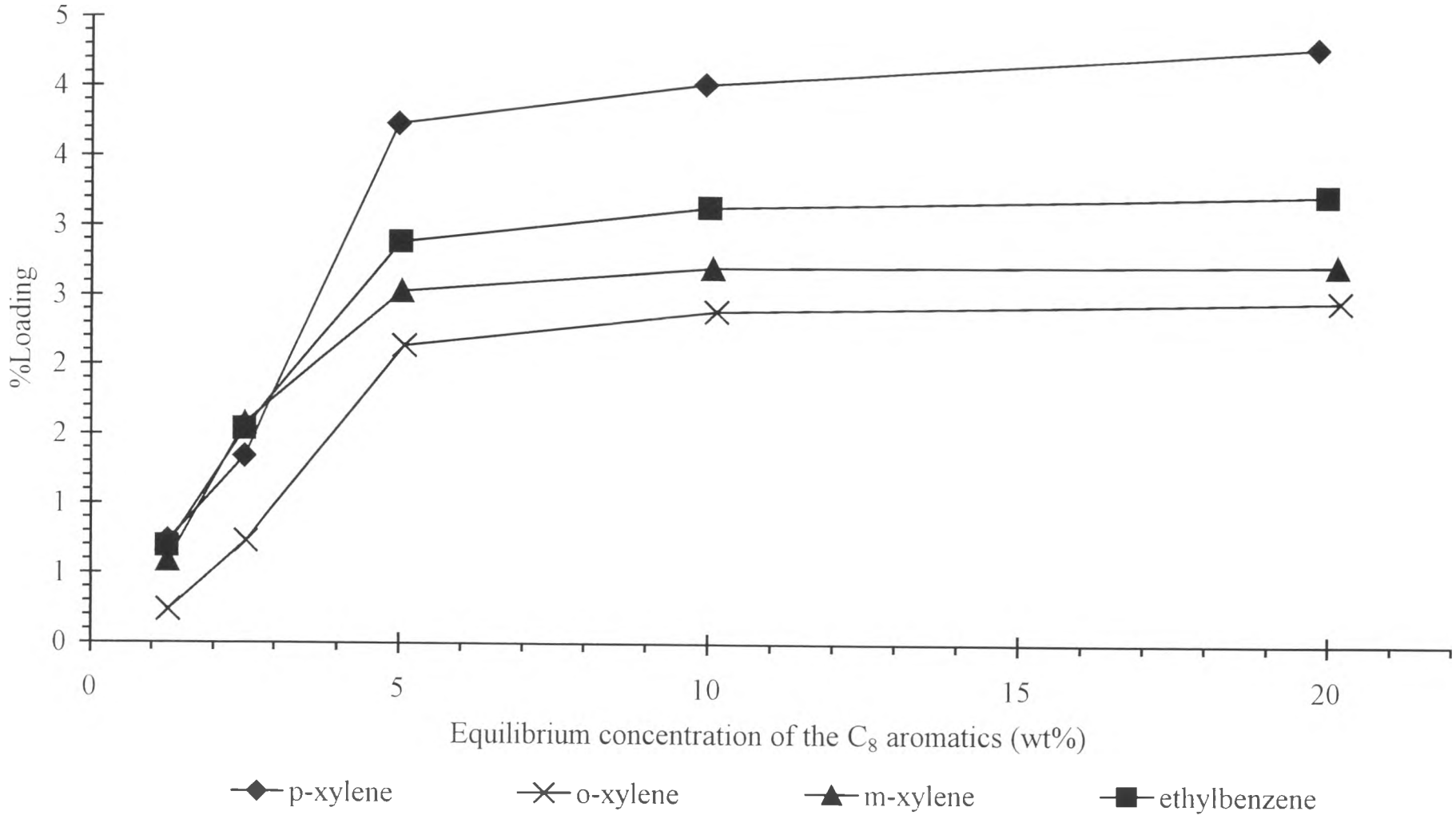

Figure 4.18 Adsorption of the C_8 aromatics on the *KBaX* zeolite, LOI=4.5% at 90 °C

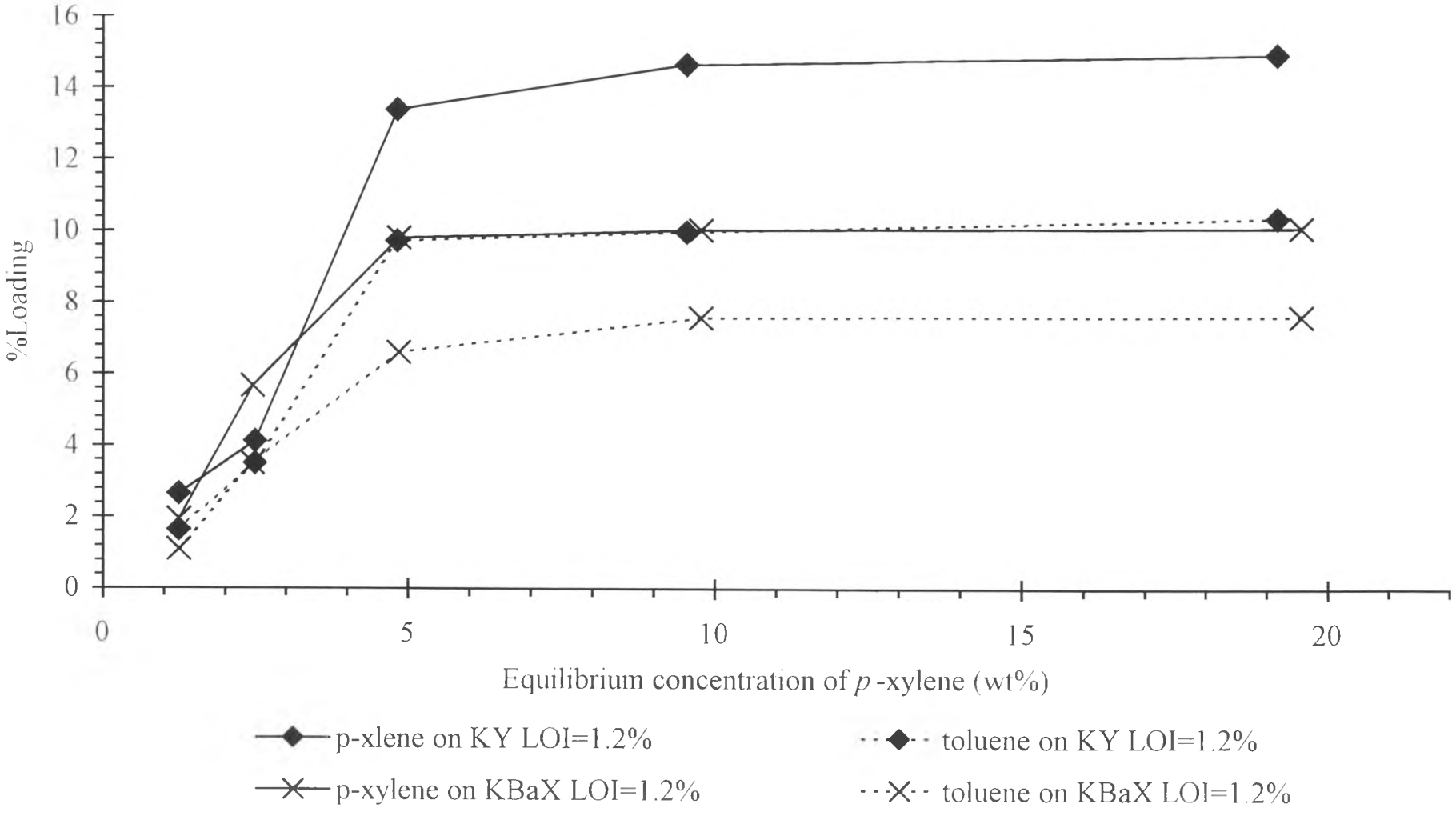

Figure 4.19 Adsorption of *p*-xylene and toluene on *KY* and *KBaX* zeolites at 40 °C

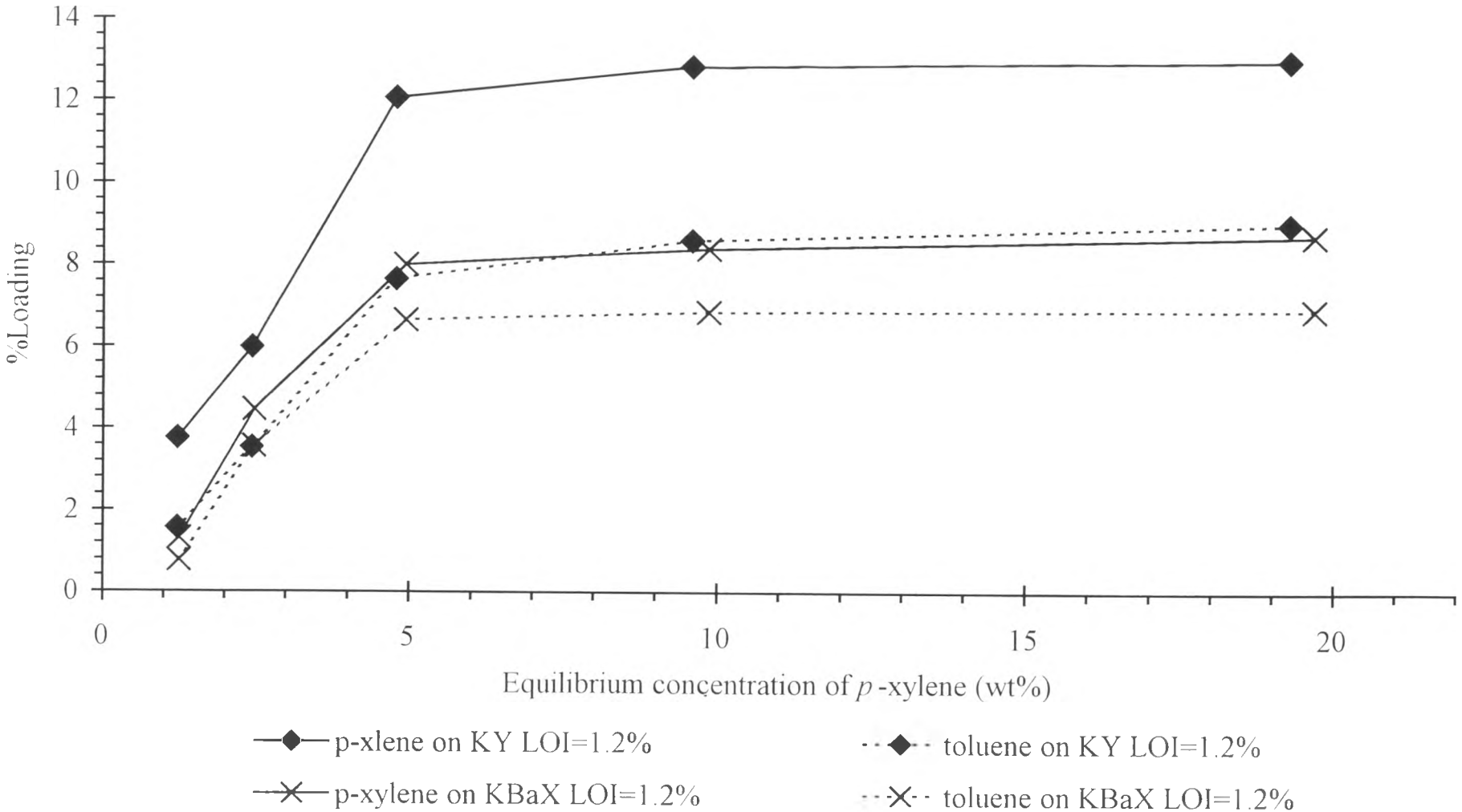

Figure 4.20 Adsorption of *p*-xylene and toluene on *KY* and *KBaX* zeolites at 65 °C

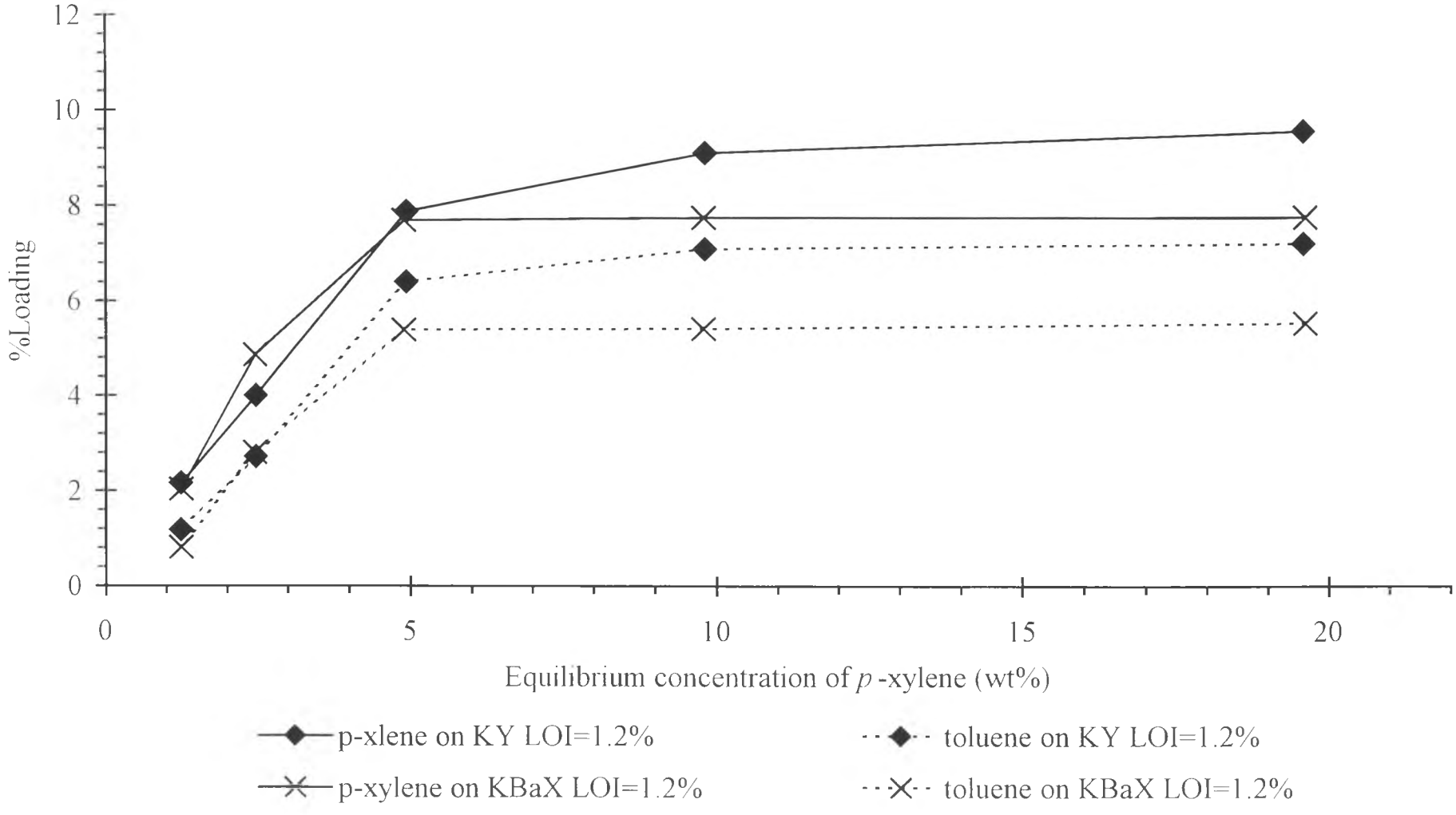

Figure 4.21 Adsorption of *p*-xylene and toluene on *KY* and *KBaX* zeolites at 90 °C

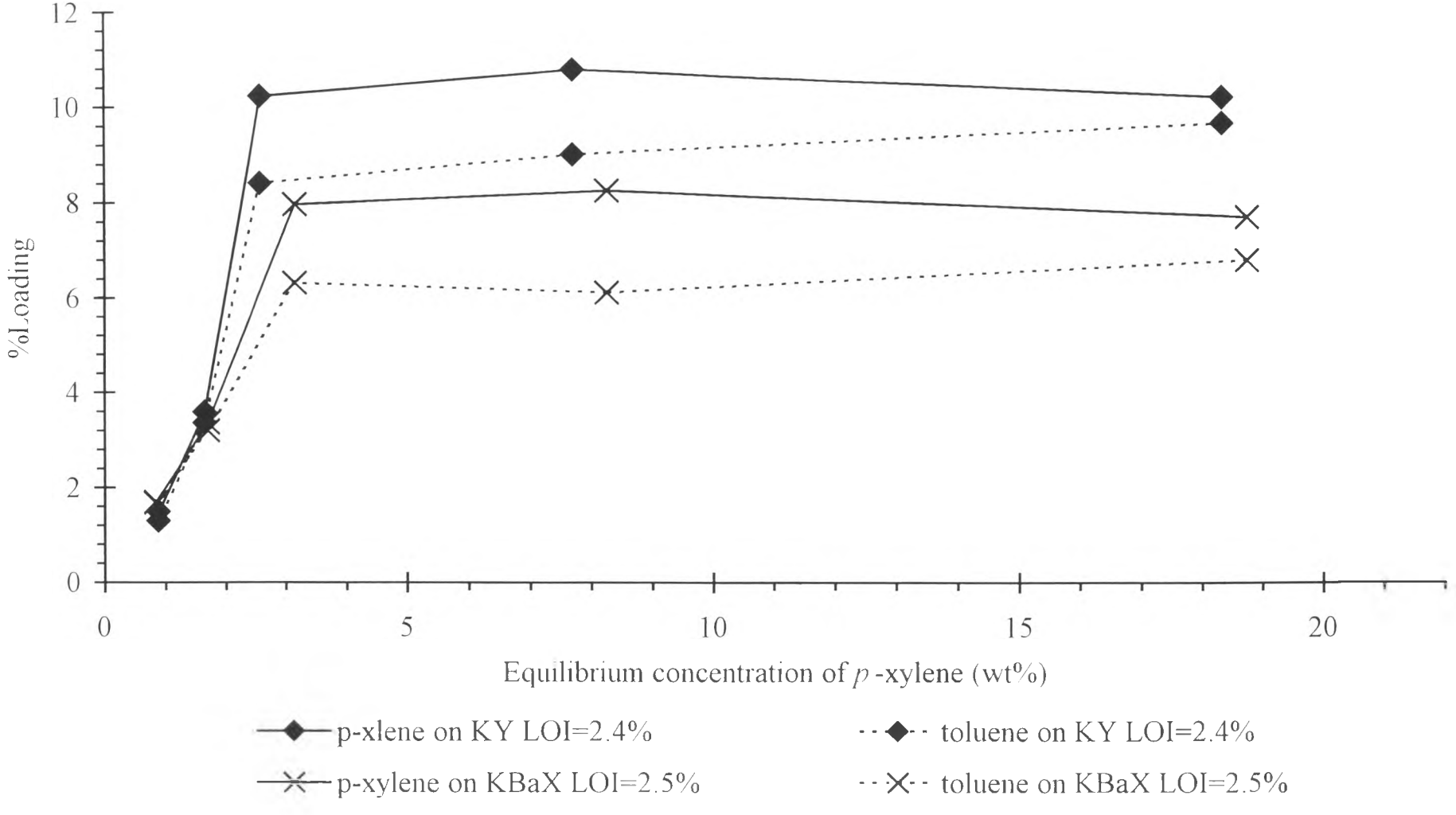

Figure 4.22 Adsorption of *p*-xylene and toluene on *KY* and *KBaX* zeolites at 40 °C

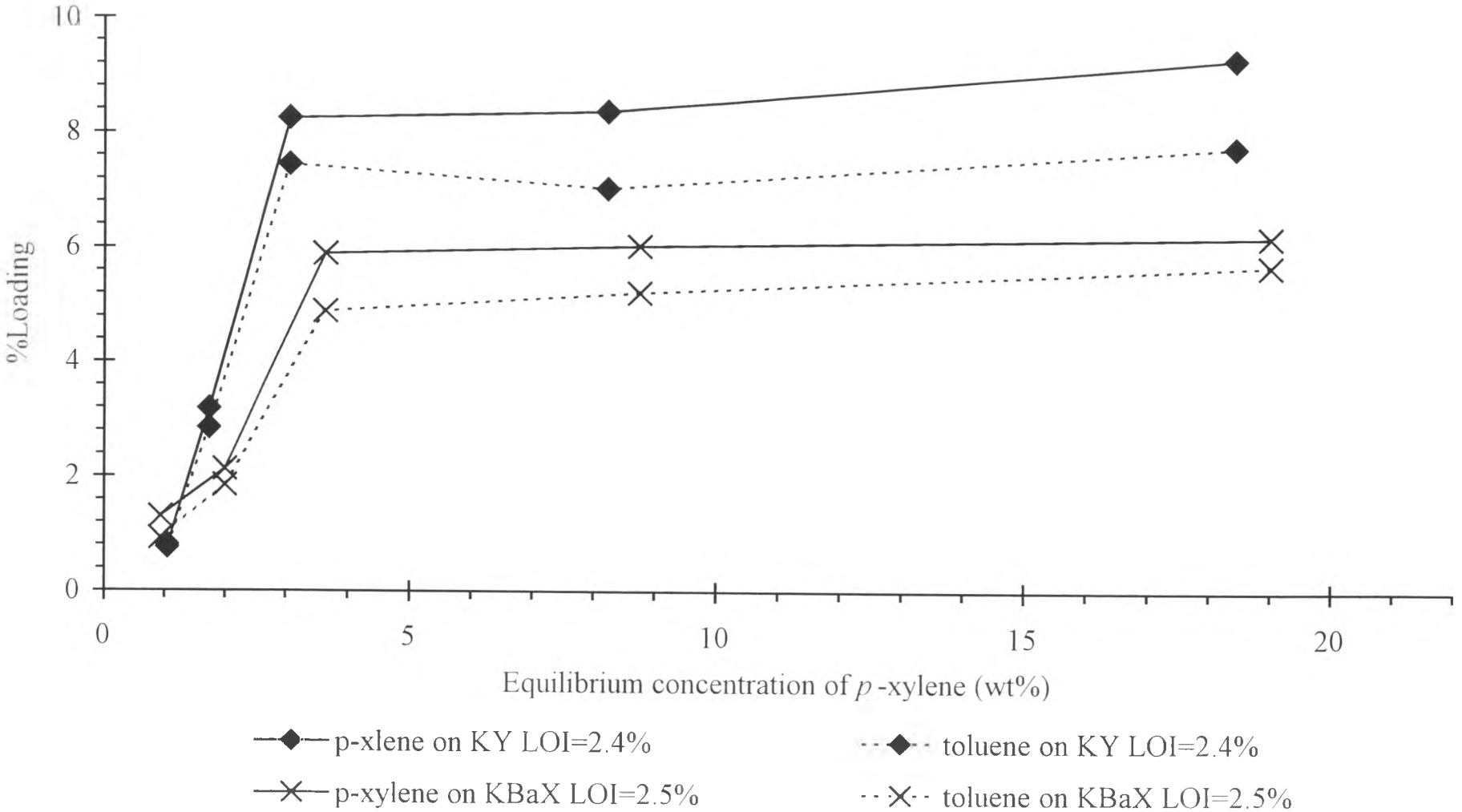

Figure 4.23 Adsorption of *p* -xylene and toluene on *KY* and *KBaX* zeolites at 65 °C

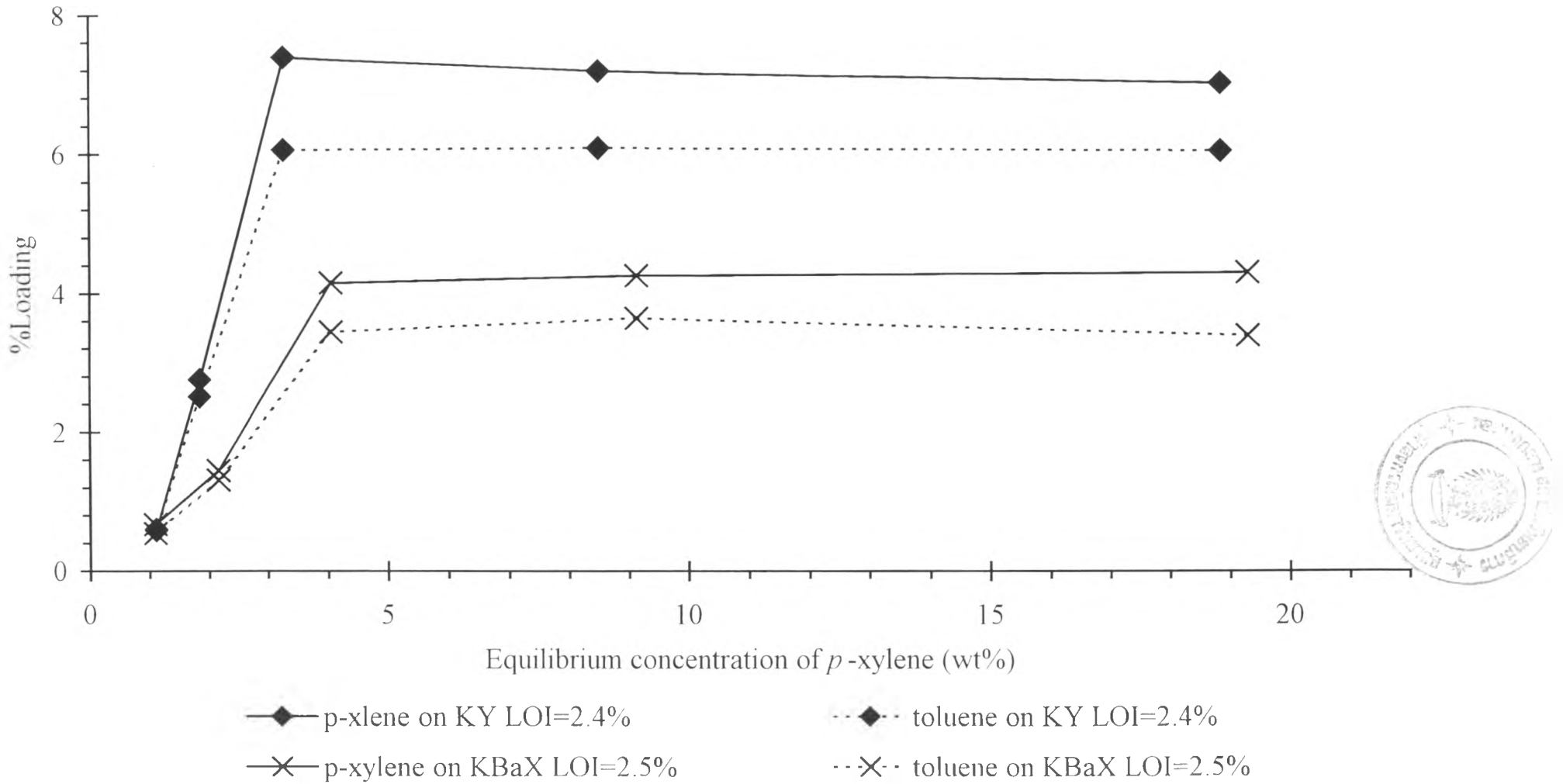

Figure 4.24 Adsorption of *p* -xylene and toluene on *KY* and *KBaX* zeolites at 90 °C

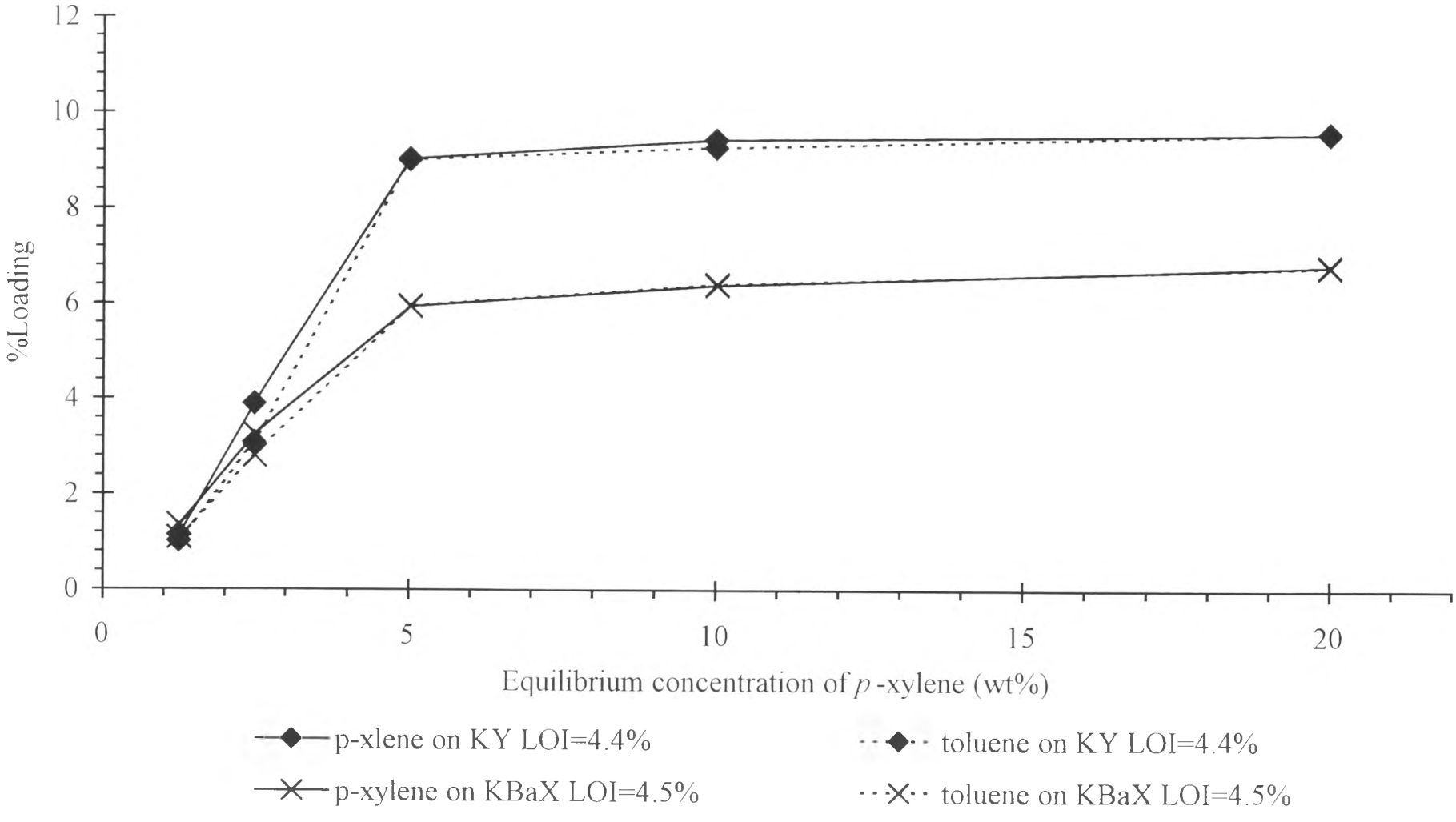

Figure 4.25 Adsorption of *p* -xylene and toluene on *KY* and *KBaX* zeolites at 40 °C

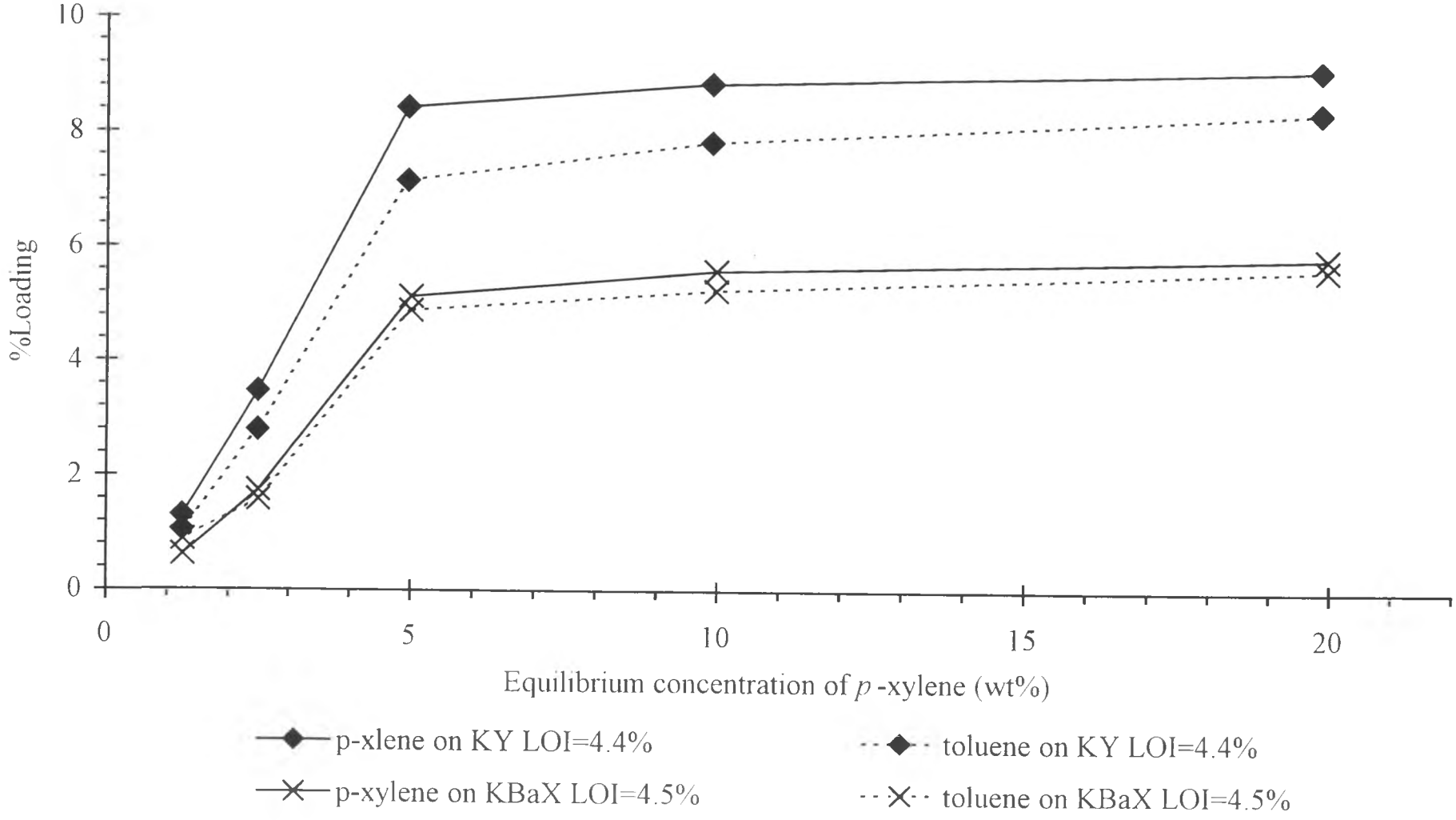

Figure 4.26 Adsorption of *p* -xylene and toluene on *KY* and *KBaX* zeolites at 65 °C

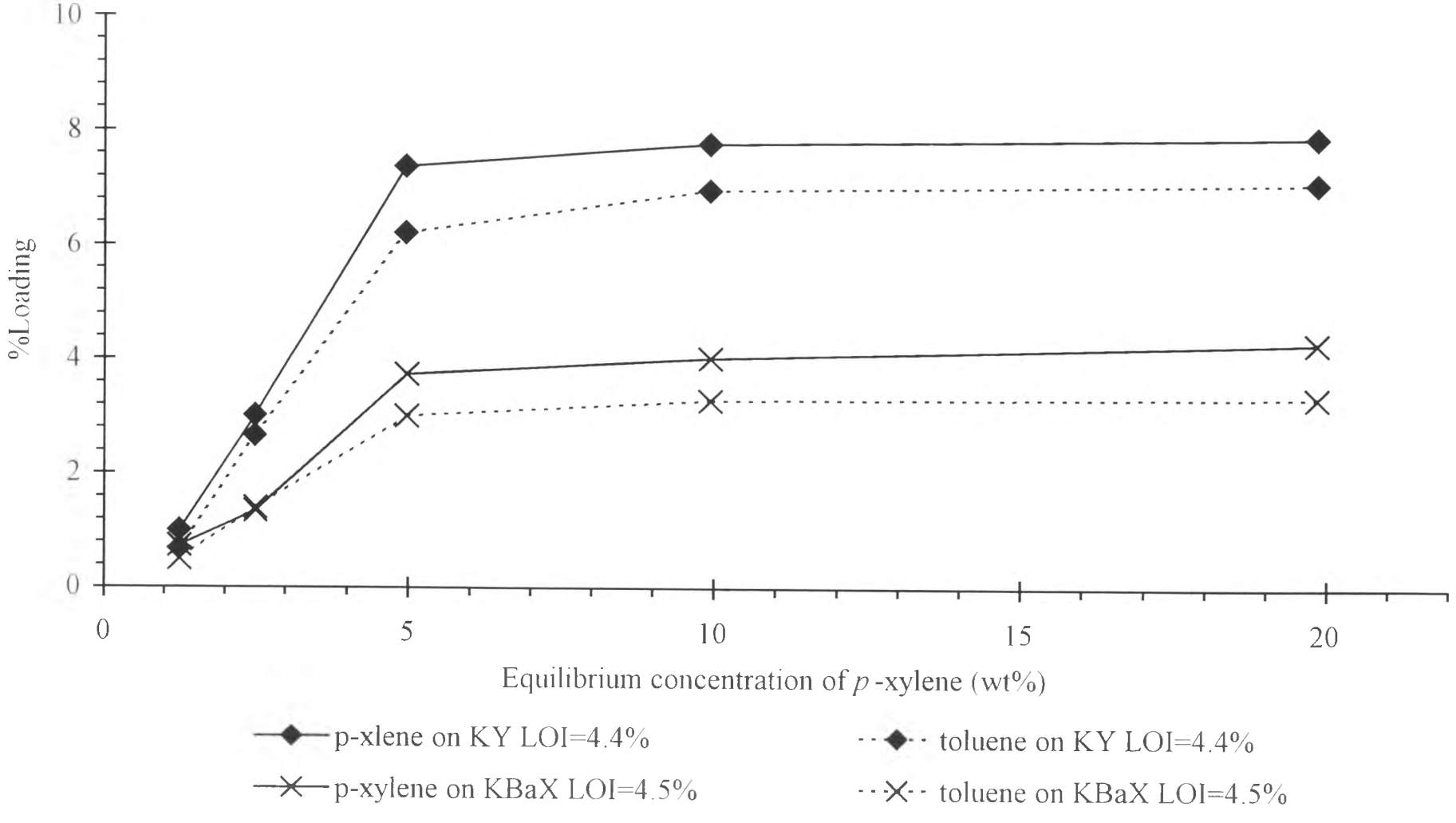

Figure 4.27 Adsorption of *p* -xylene and toluene on *KY* and *KBaX* zeolites at 90 °C

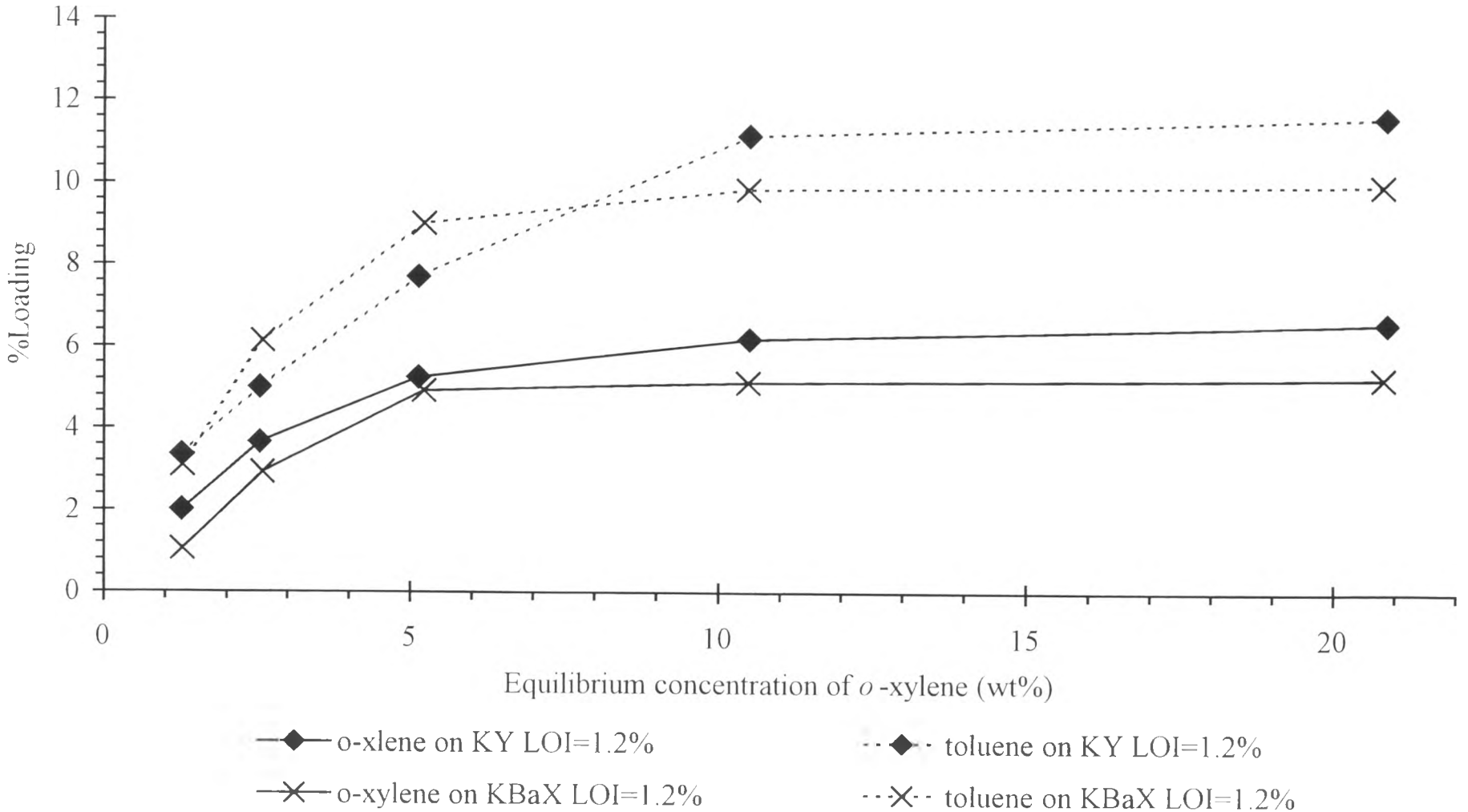

Figure 4.28 Adsorption of *o* -xylene and toluene on *KY* and *KBaX* zeolites LOI=1.2% at 40 °C

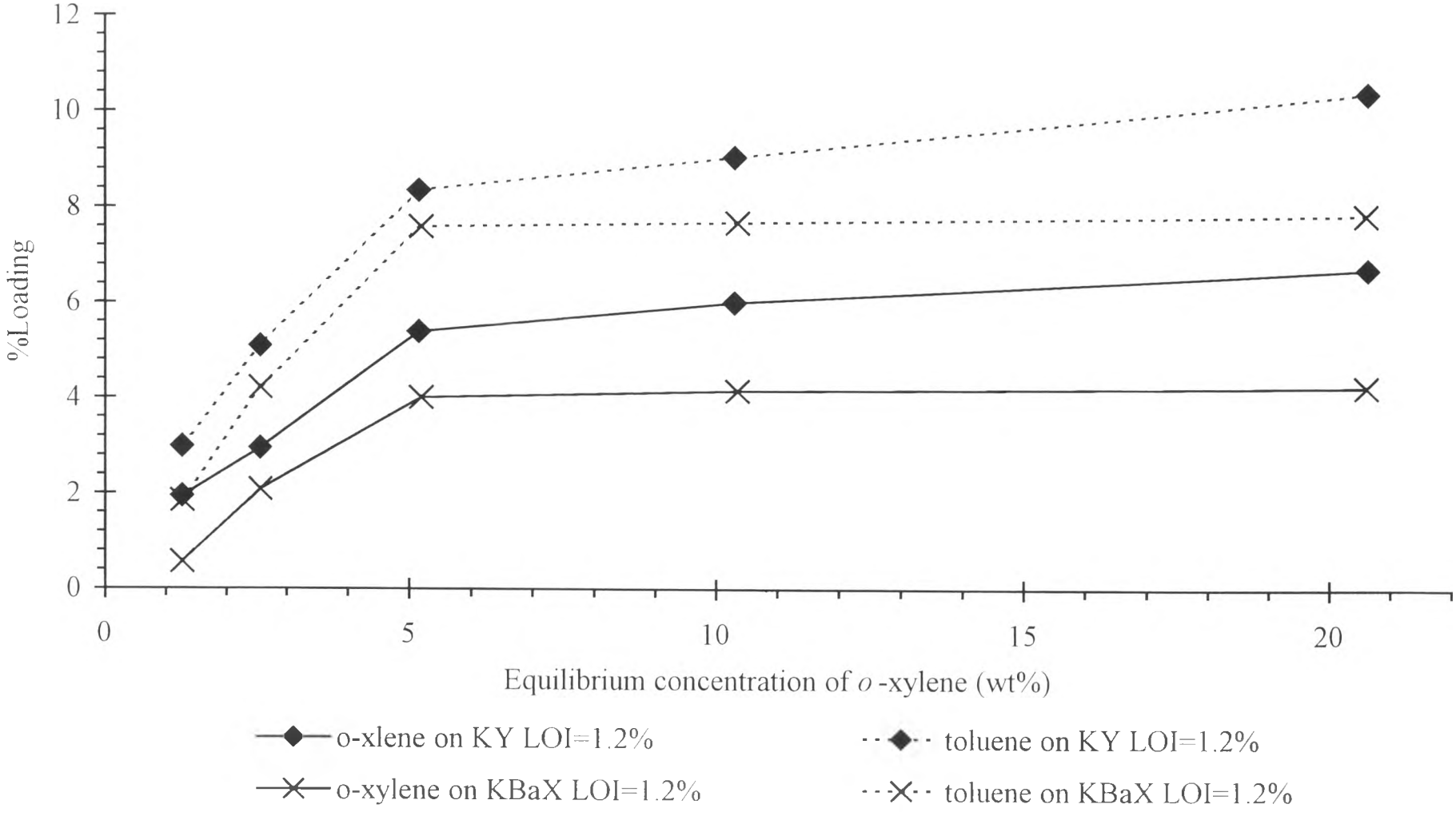

Figure 4.29 Adsorption of *o* -xylene and toluene on *KY* and *KBaX* zeolites LOI=1.2% at 65 °C

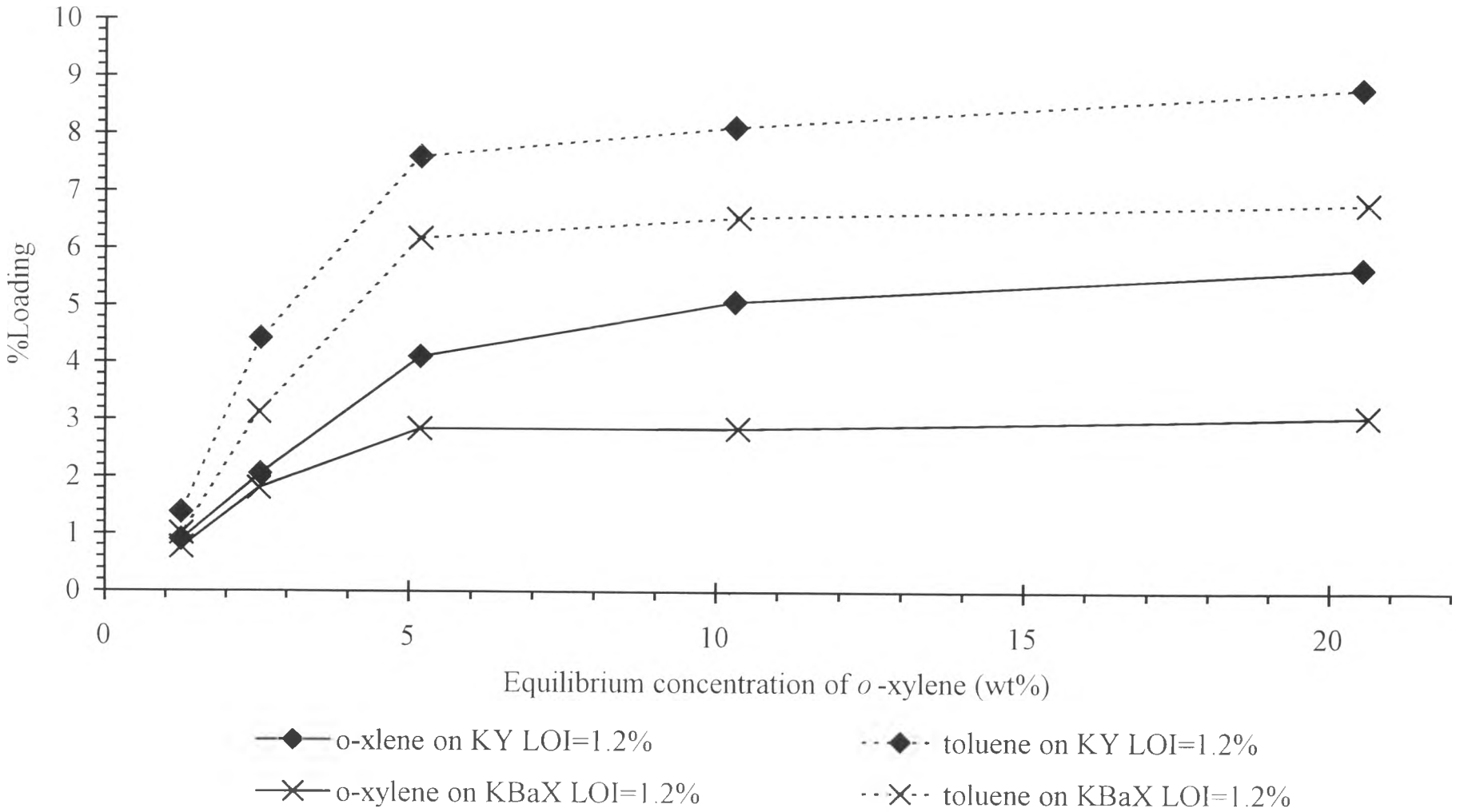

Figure 4.30 Adsorption of *o* -xylene and toluene on *KY* and *KBaX* zeolites LOI=1.2% at 90 °C

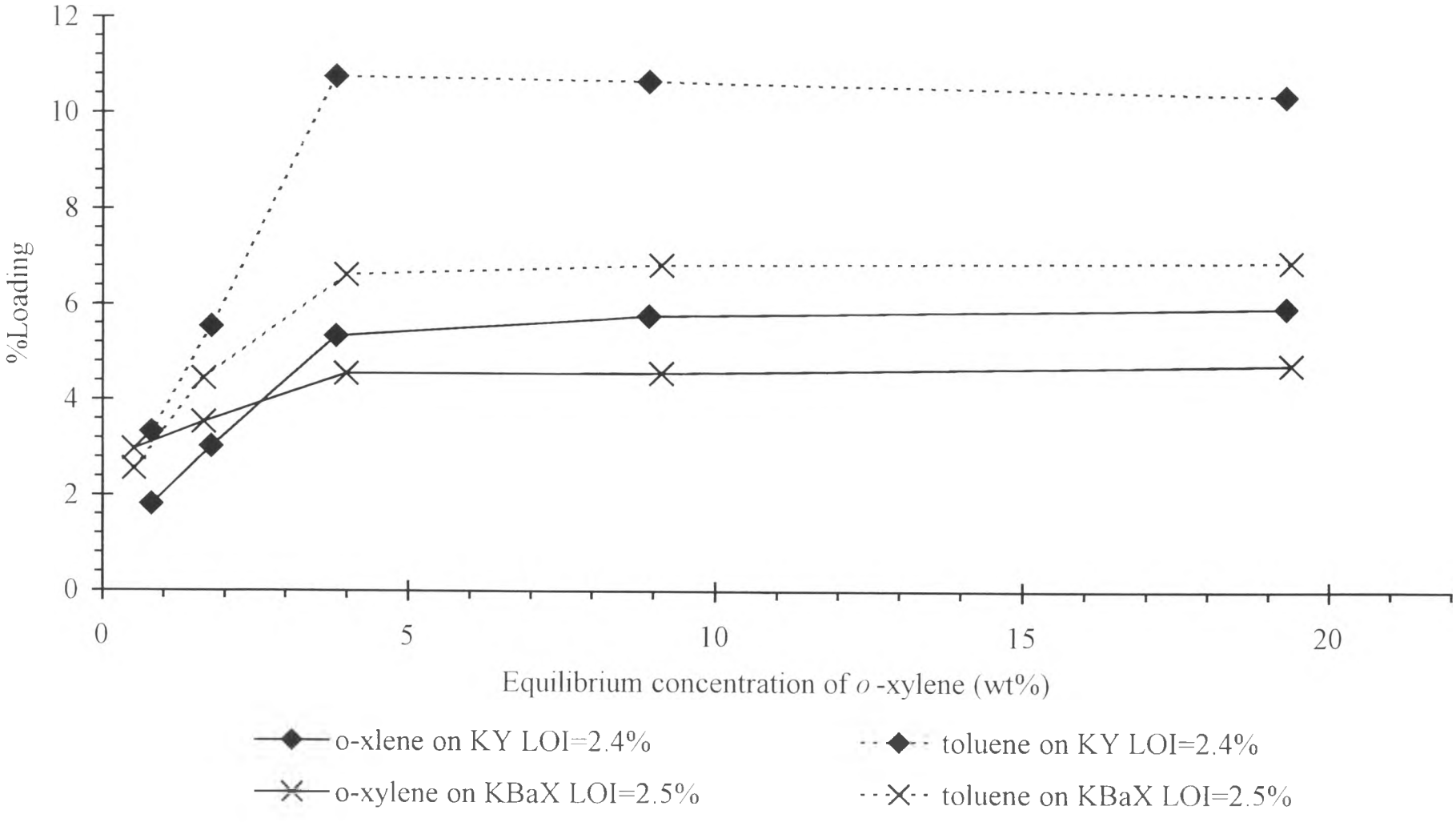

Figure 4.31 Adsorption of *o* -xylene and toluene on *KY* and *KBaX* zeolites LOI=2.5% at 40 °C

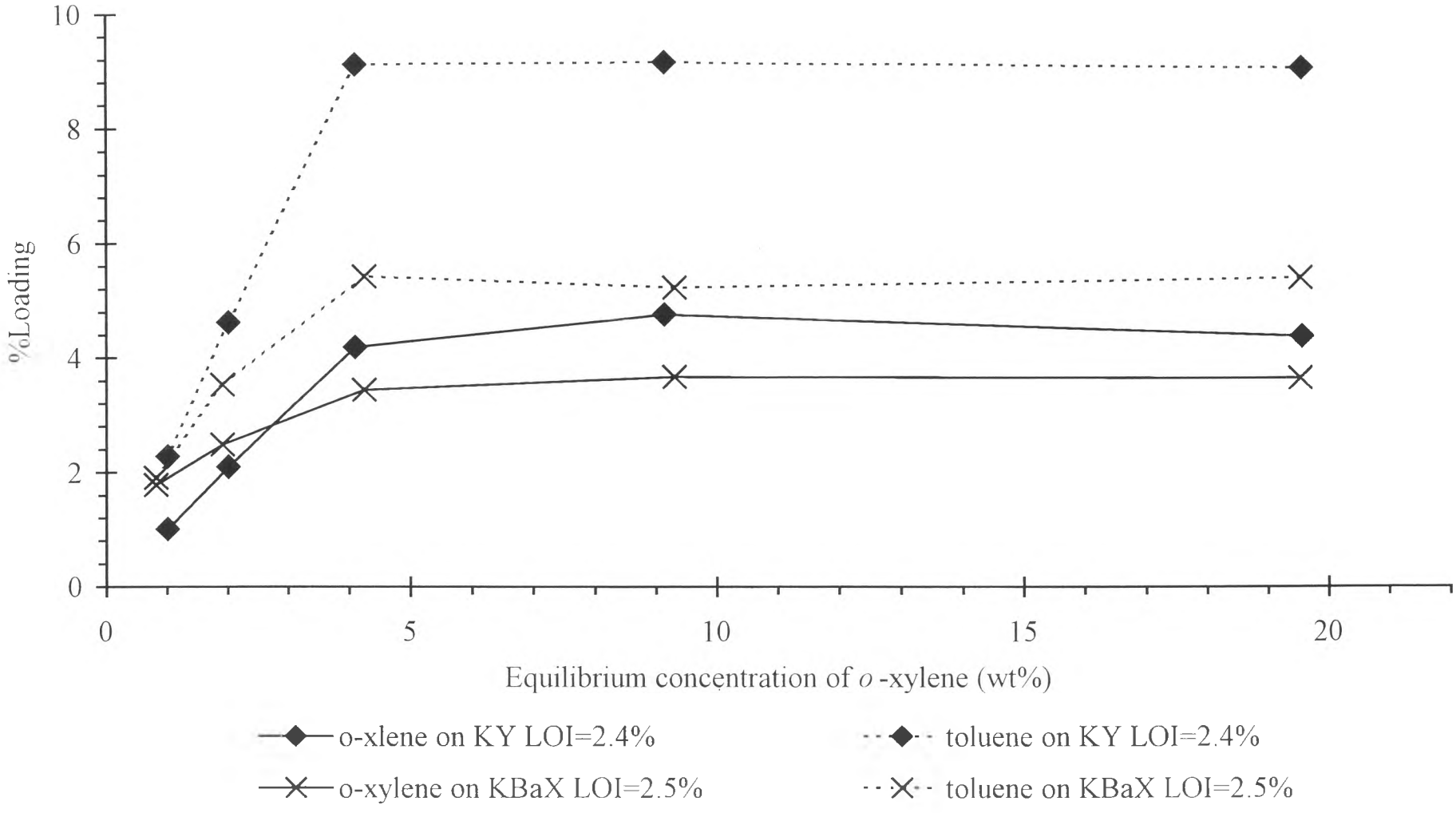

Figure 4.32 Adsorption of *o* -xylene and toluene on *KY* and *KBaX* zeolites LOI=2.5% at 65 °C

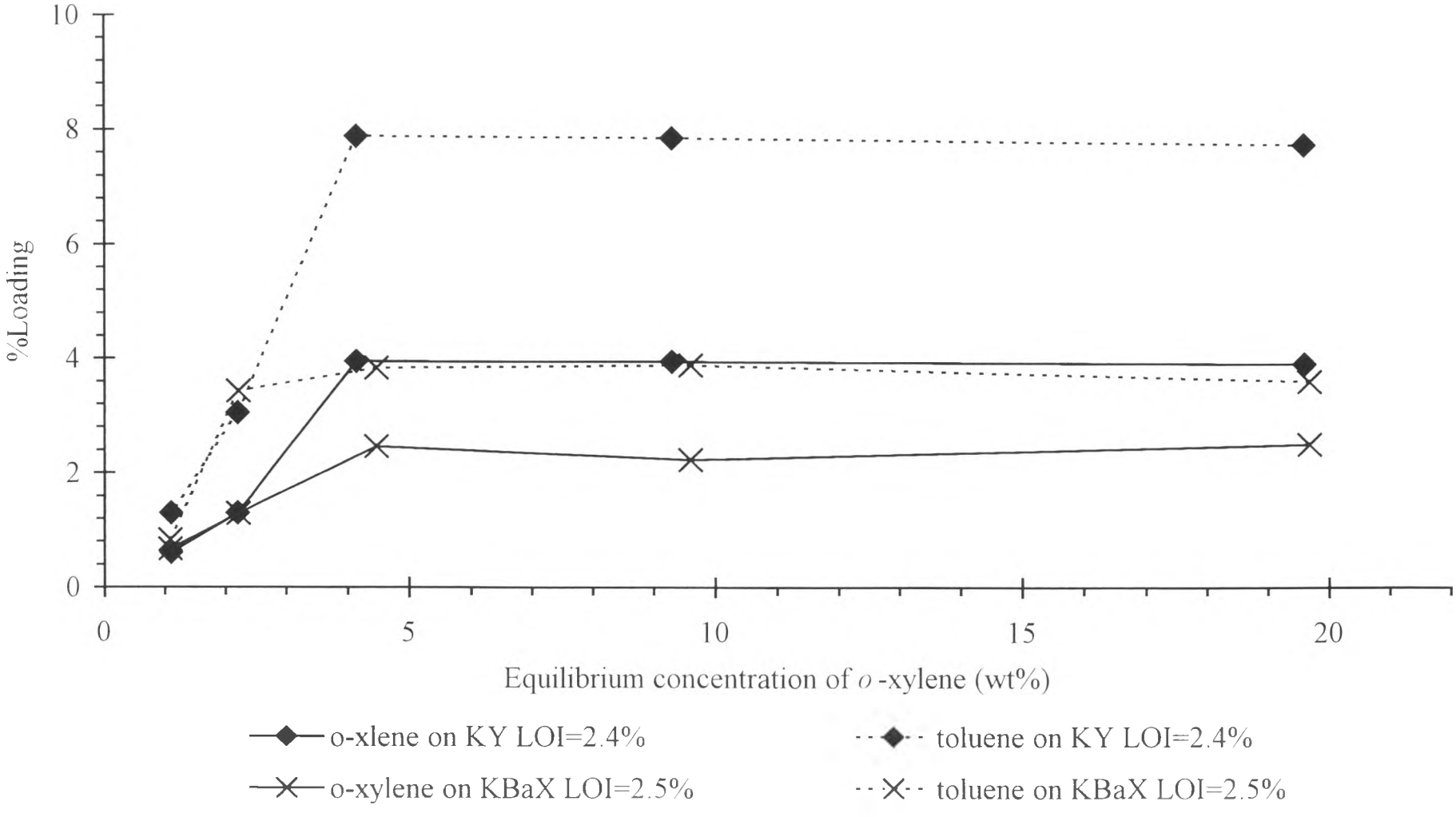

Figure 4.33 Adsorption of *o* -xylene and toluene on *KY* and *KBaX* zeolites LOI=2.5% at 90 °C

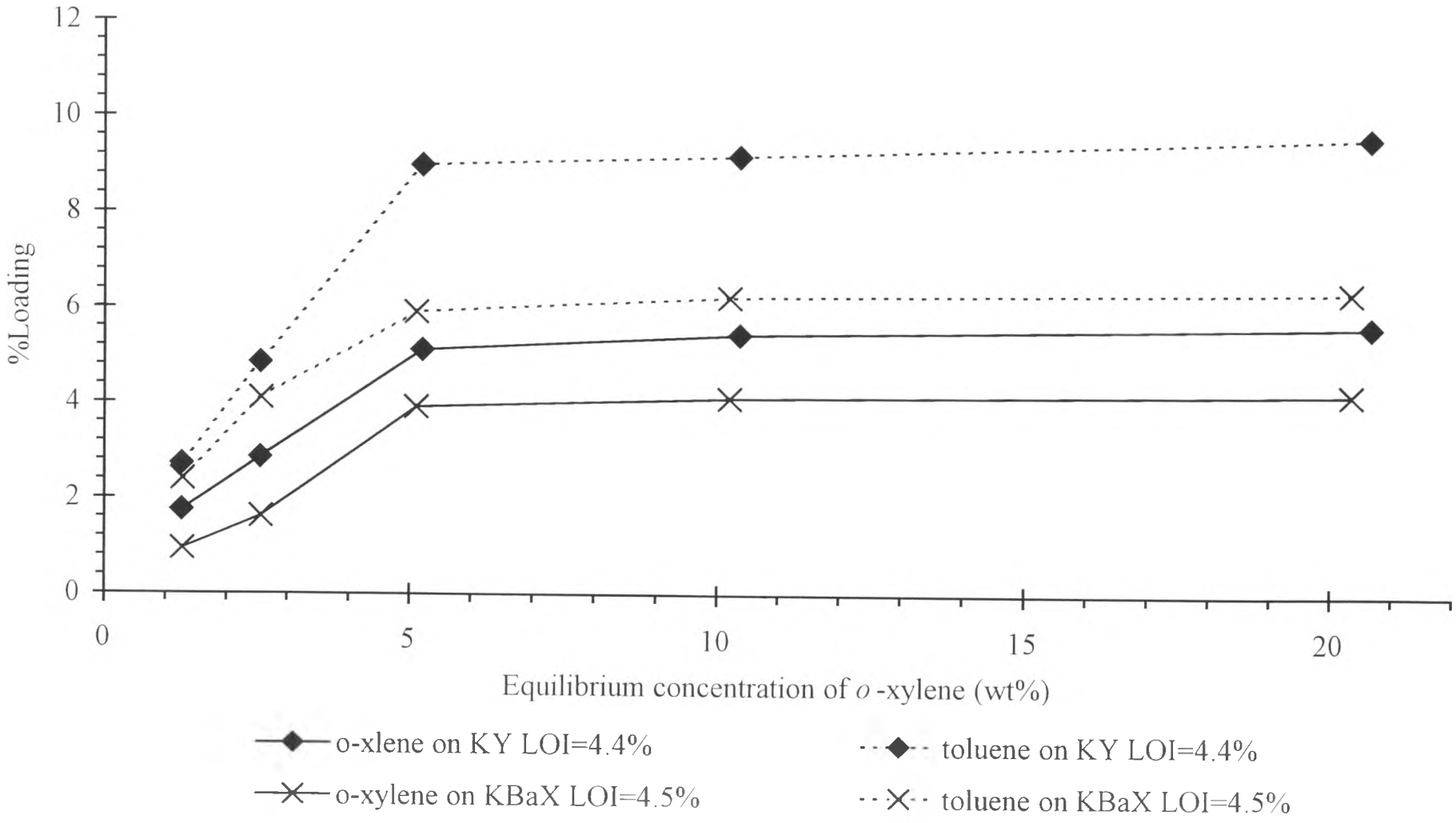

Figure 4.34 Adsorption of *o* -xylene and toluene on *KY* and *KBaX* zeolites LOI=4.5% at 40 °C

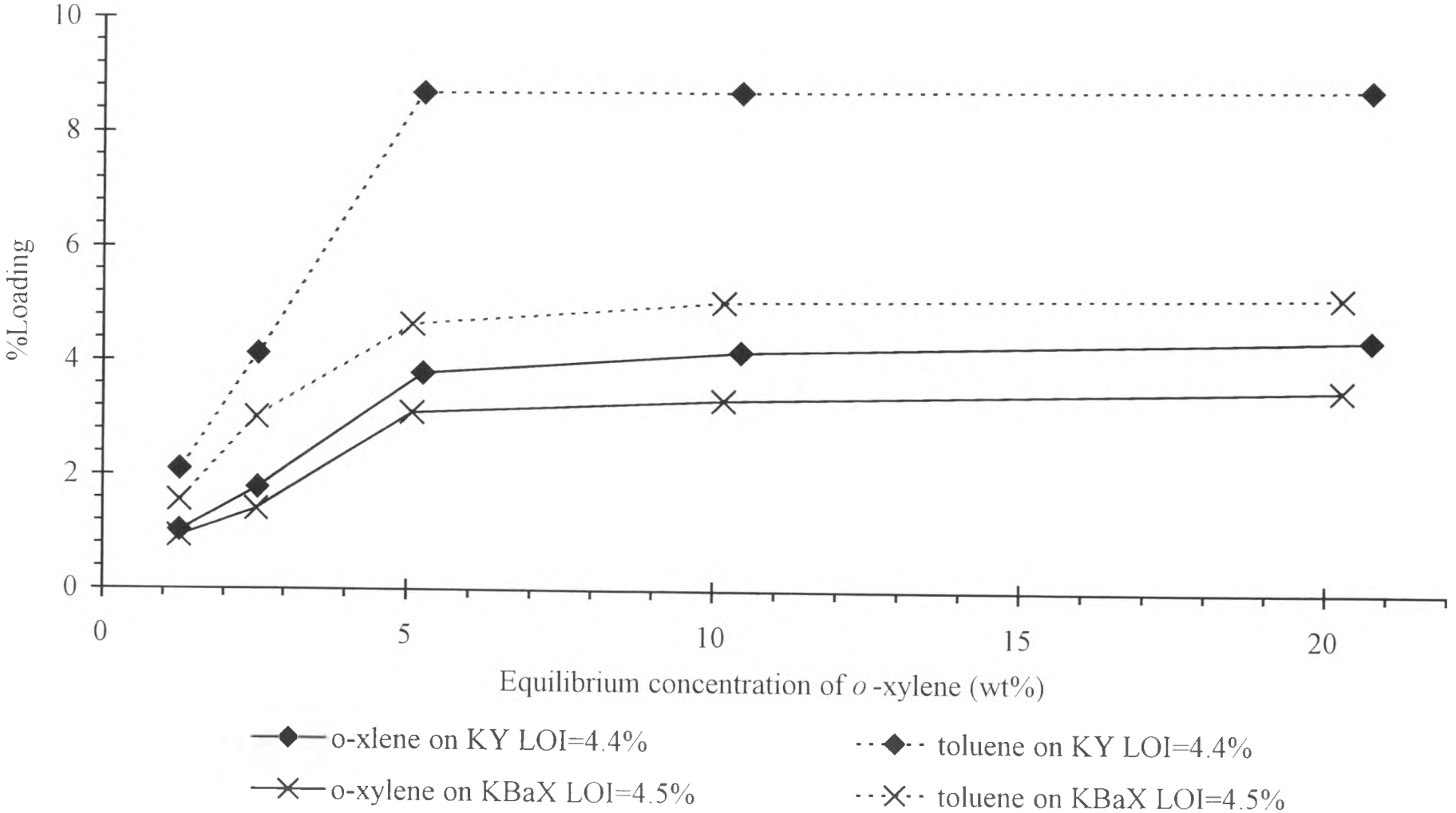

Figure 4.35 Adsorption of *o* -xylene and toluene on *KY* and *KBaX* zeolites LOI=4.5% at 65 °C

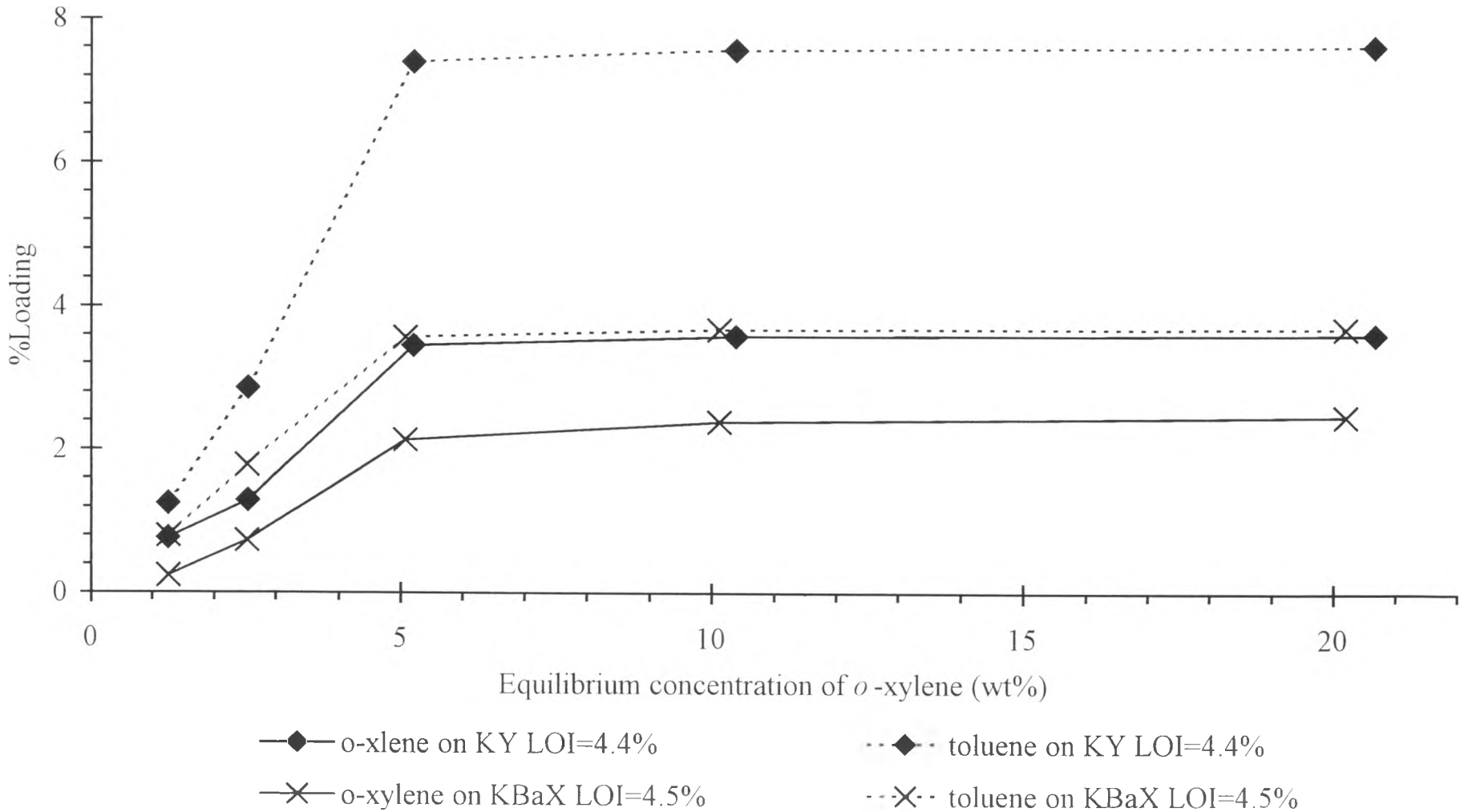

Figure 4.36 Adsorption of *o* -xylene and toluene on *KY* and *KBaX* zeolites LOI=4.5% at 90 °C

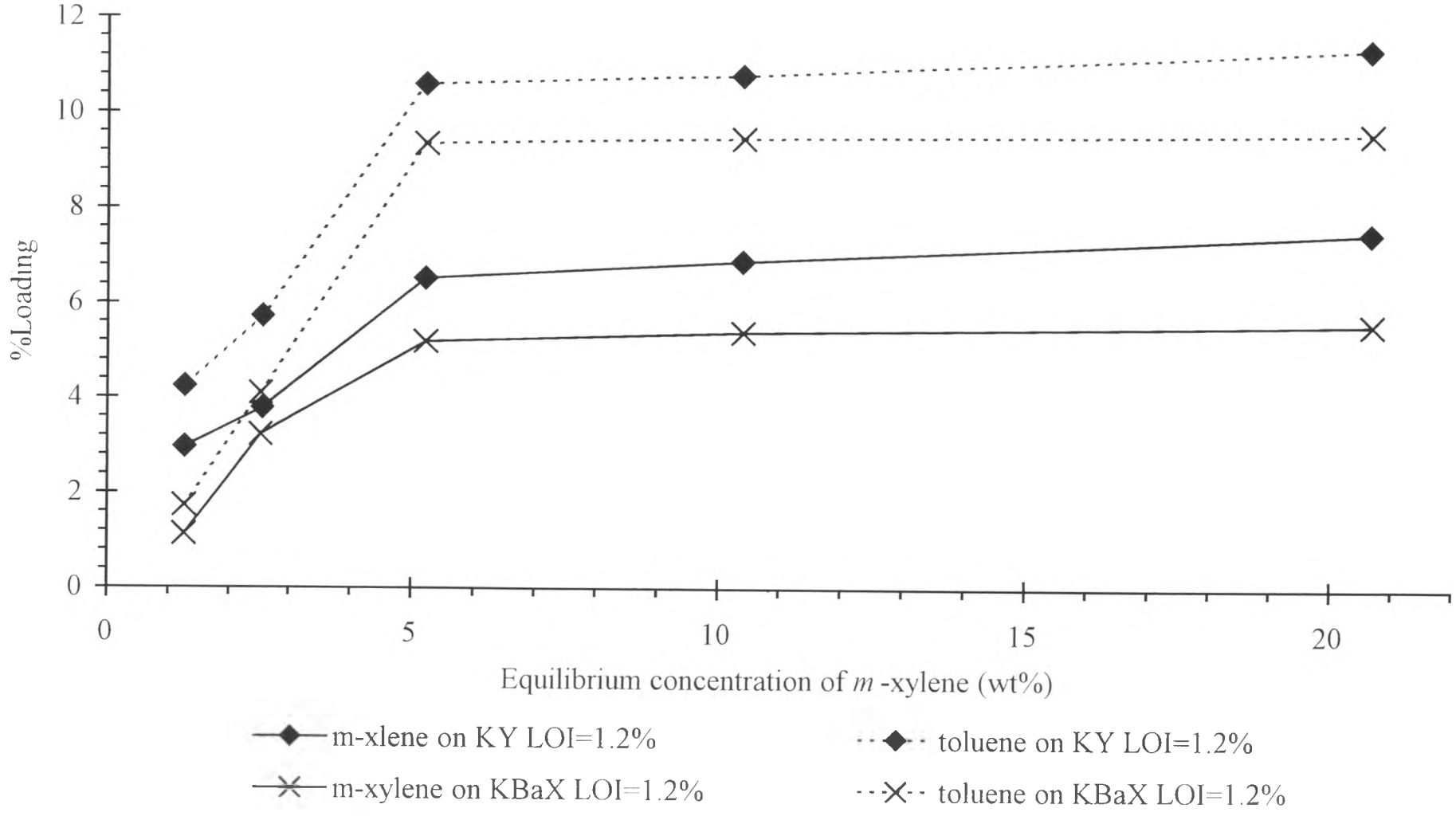

Figure 4.37 Adsorption of *m* -xylene and toluene on *KY* and *KBaX* zeolites LOI=1.2% at 40 °C

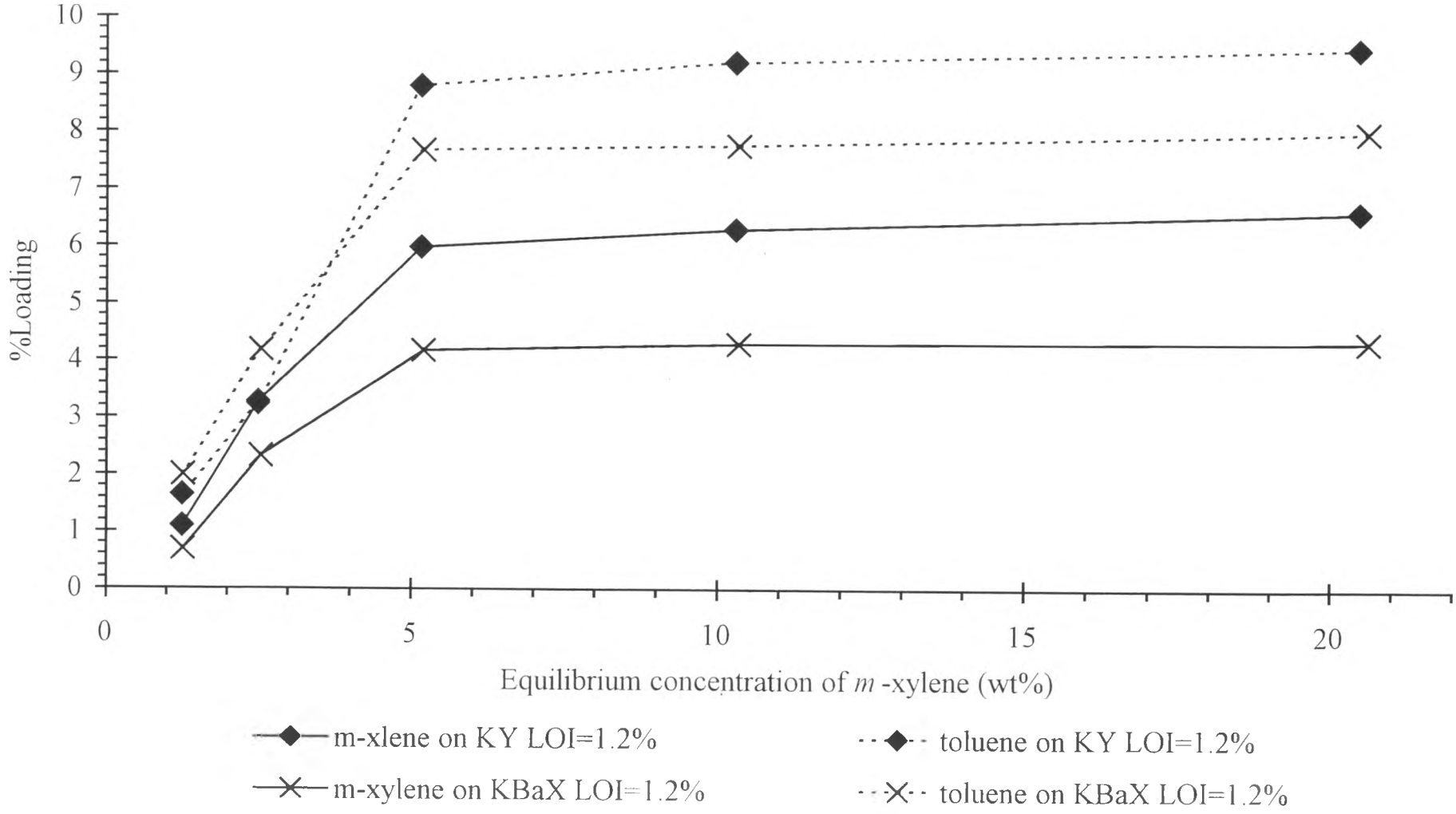

Figure 4.38 Adsorption of *m* -xylene and toluene on *KY* and *KBaX* zeolites LOI=1.2% at 65 °C

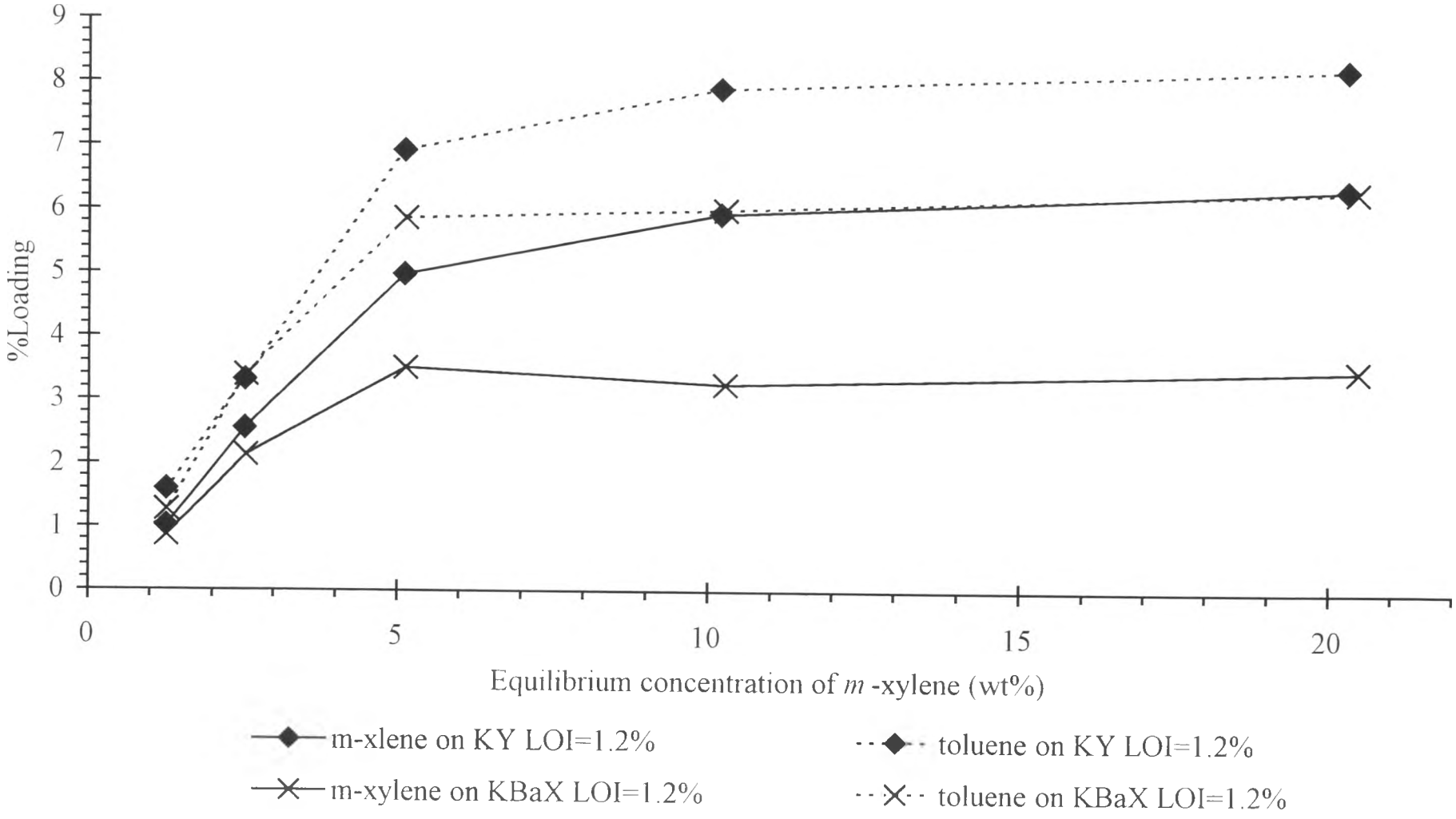

Figure 4.39 Adsorption of *m* -xylene and toluene on *KY* and *KBaX* zeolites LOI=1.2% at 90 °C

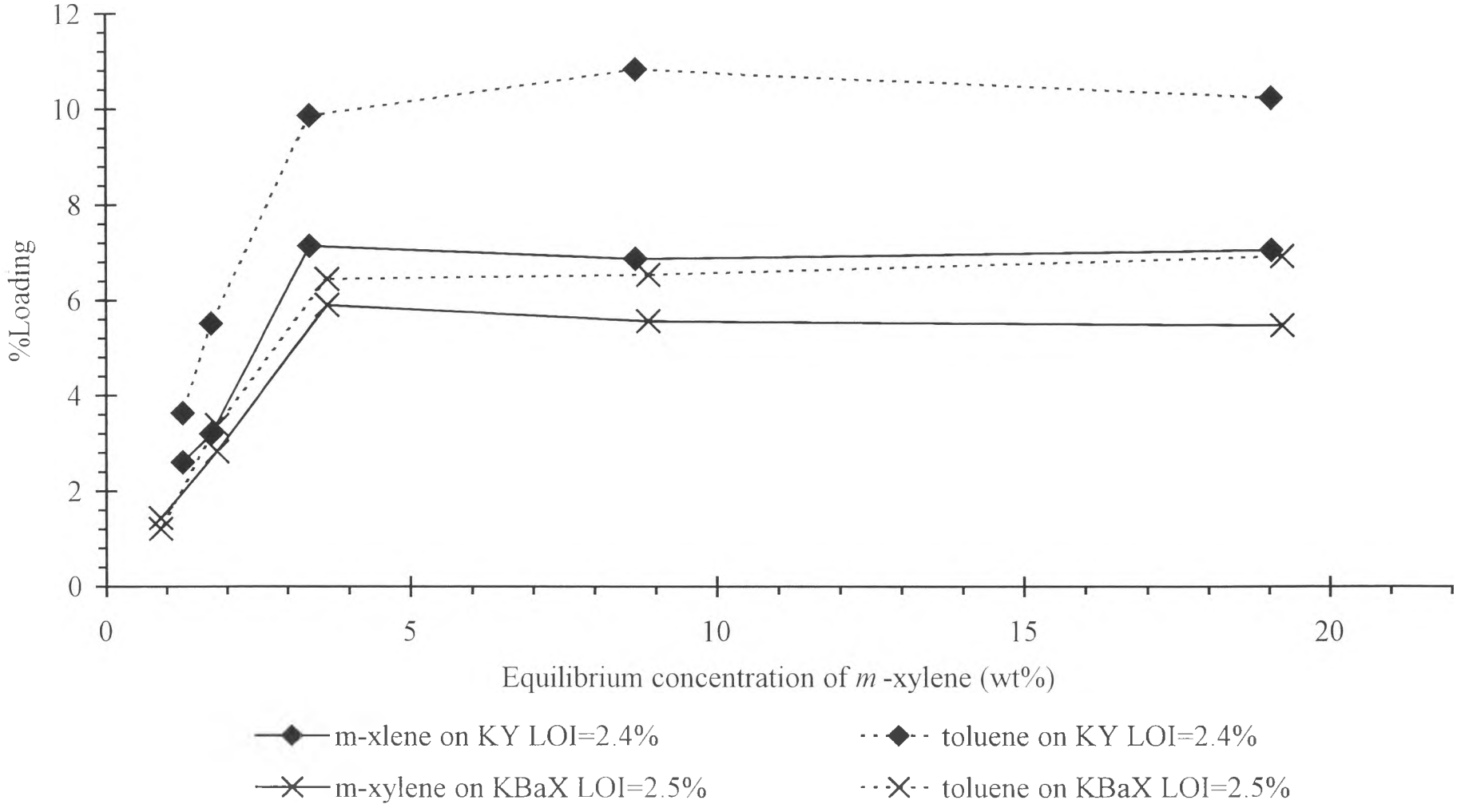

Figure 4.40 Adsorption of *m* -xylene and toluene on *KY* and *KBaX* zeolites LOI=2.5% at 40 °C

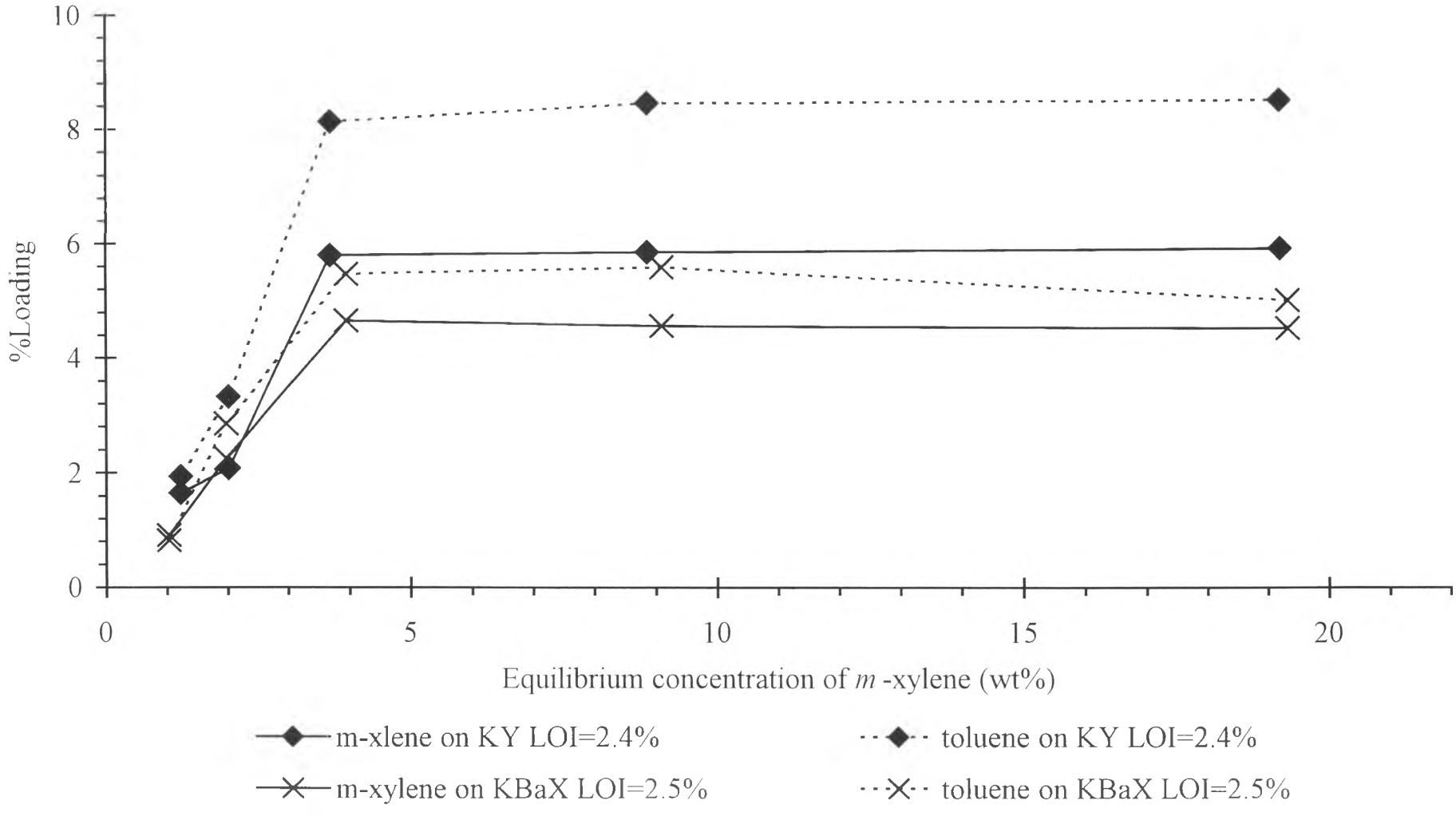

Figure 4.41 Adsorption of *m* -xylene and toluene on *KY* and *KBaX* zeolites LOI=2.5% at 65 °C

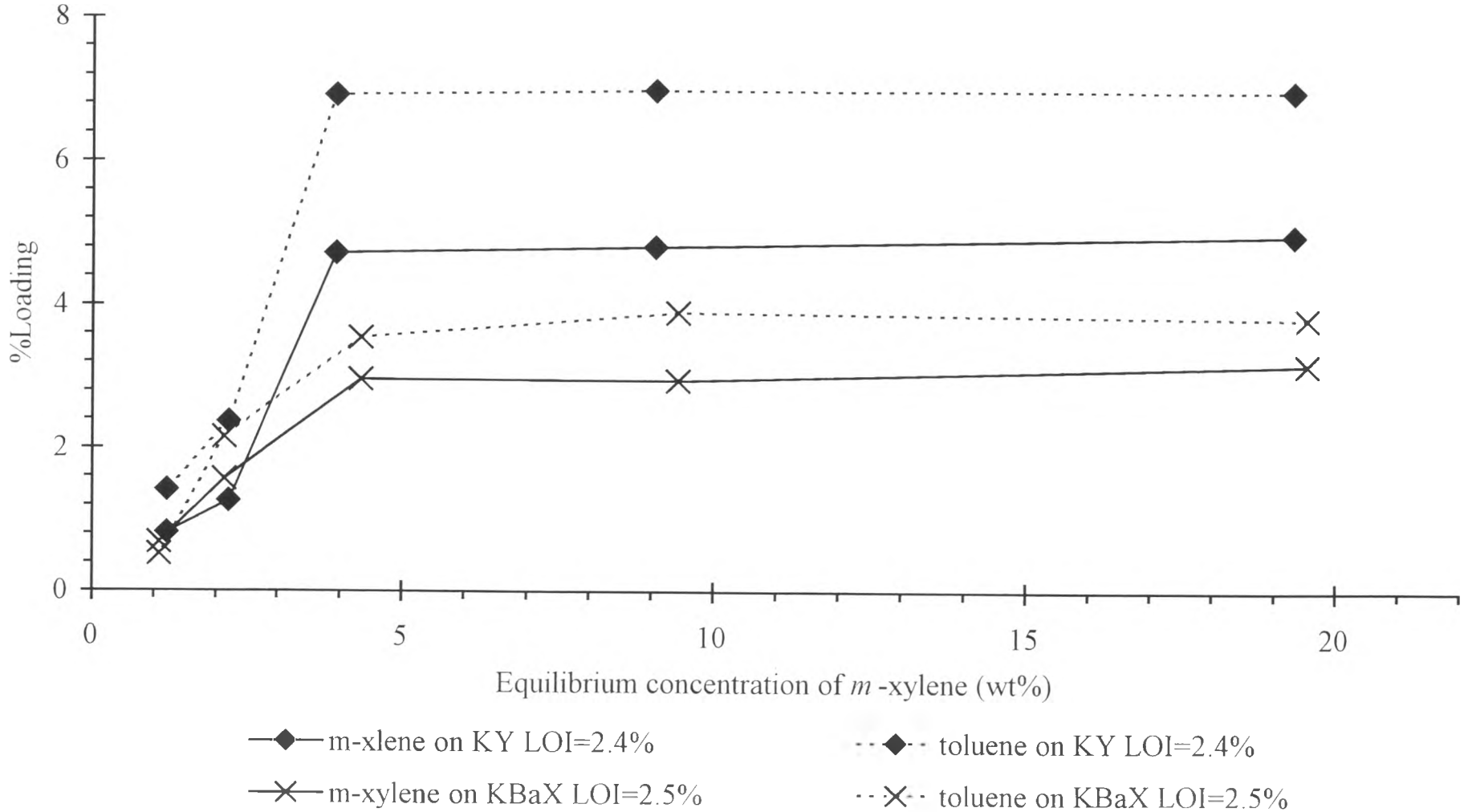

Figure 4.42 Adsorption of *m* -xylene and toluene on *KY* and *KBaX* zeolites LOI=2.5% at 90 °C

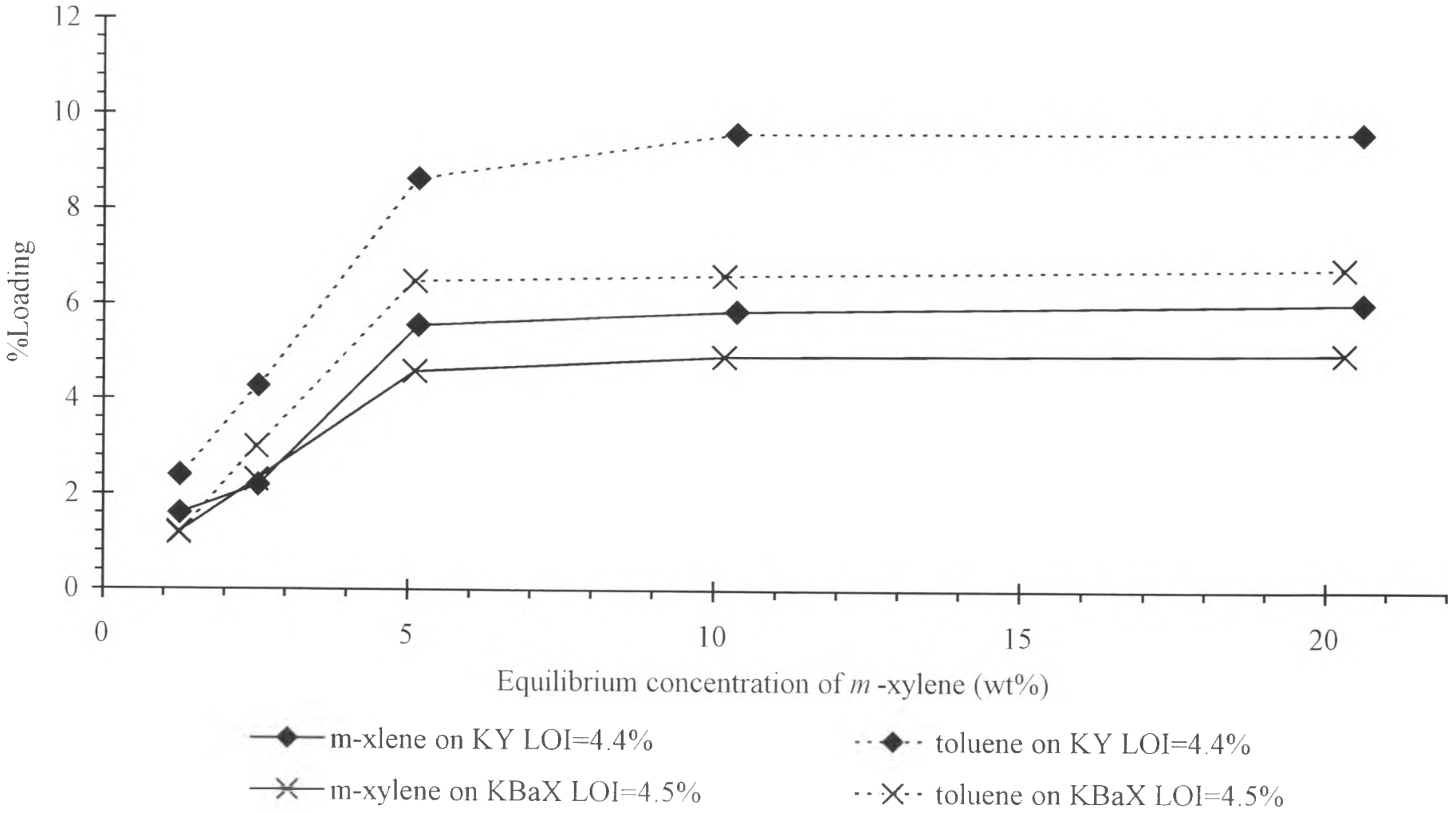

Figure 4.43 Adsorption of *m* -xylene and toluene on *KY* and *KBaX* zeolites LOI=4.5% at 40 °C

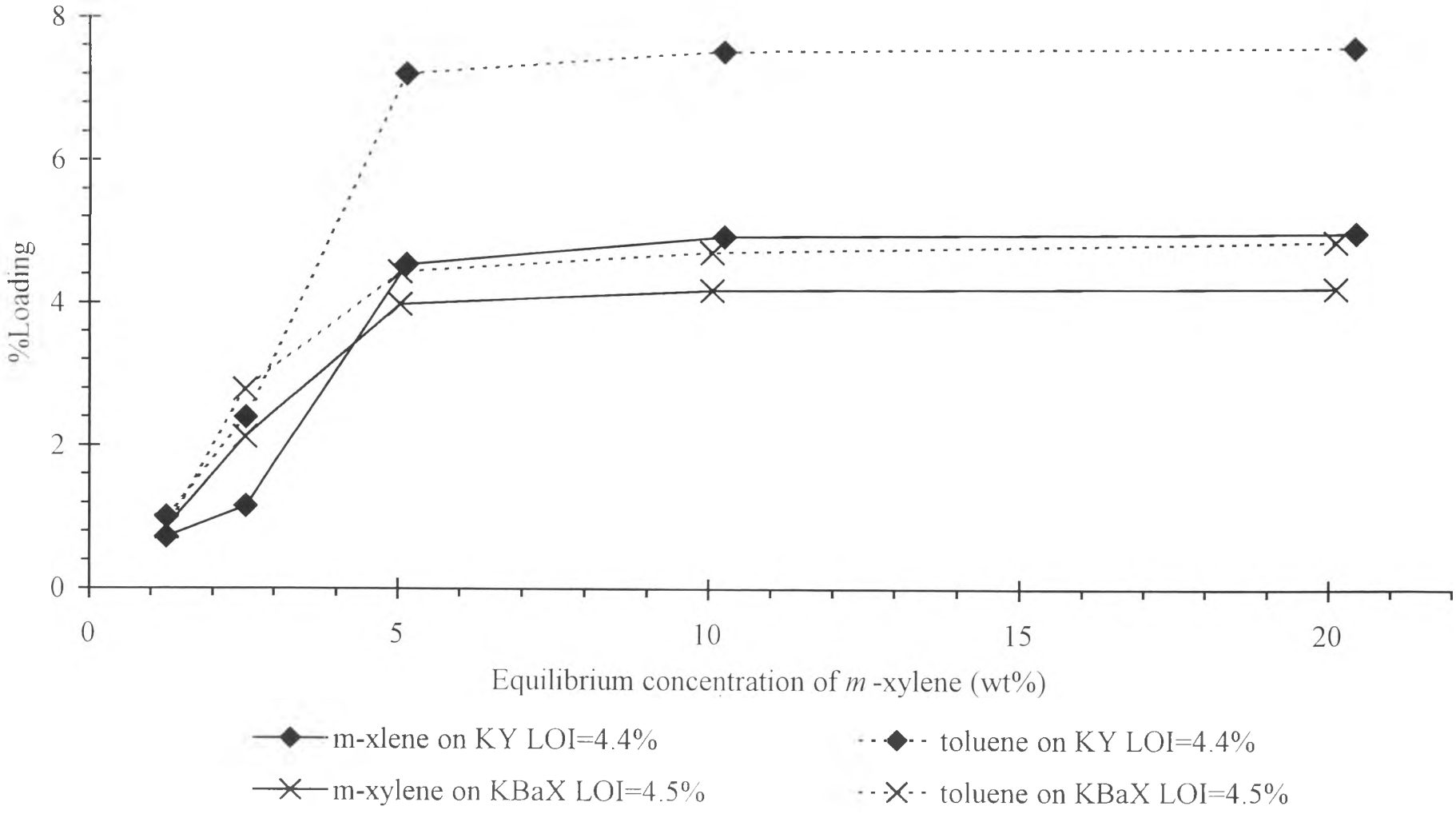

Figure 4.44 Adsorption of *m* -xylene and toluene on *KY* and *KBaX* zeolites LOI=4.5% at 65 °C

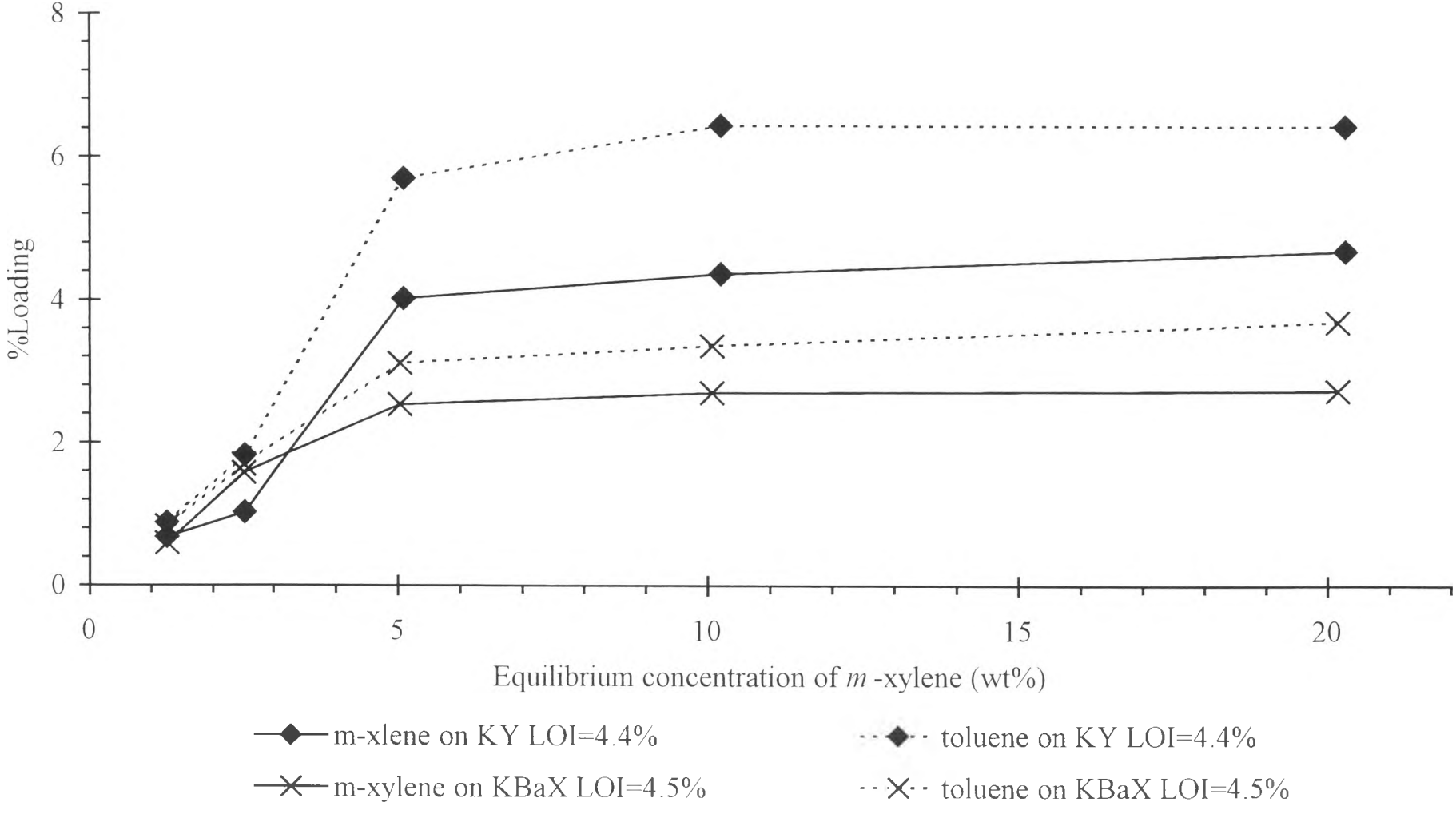

Figure 4.45 Adsorption of *m* -xylene and toluene on *KY* and *KBaX* zeolites LOI=4.5% at 90 °C

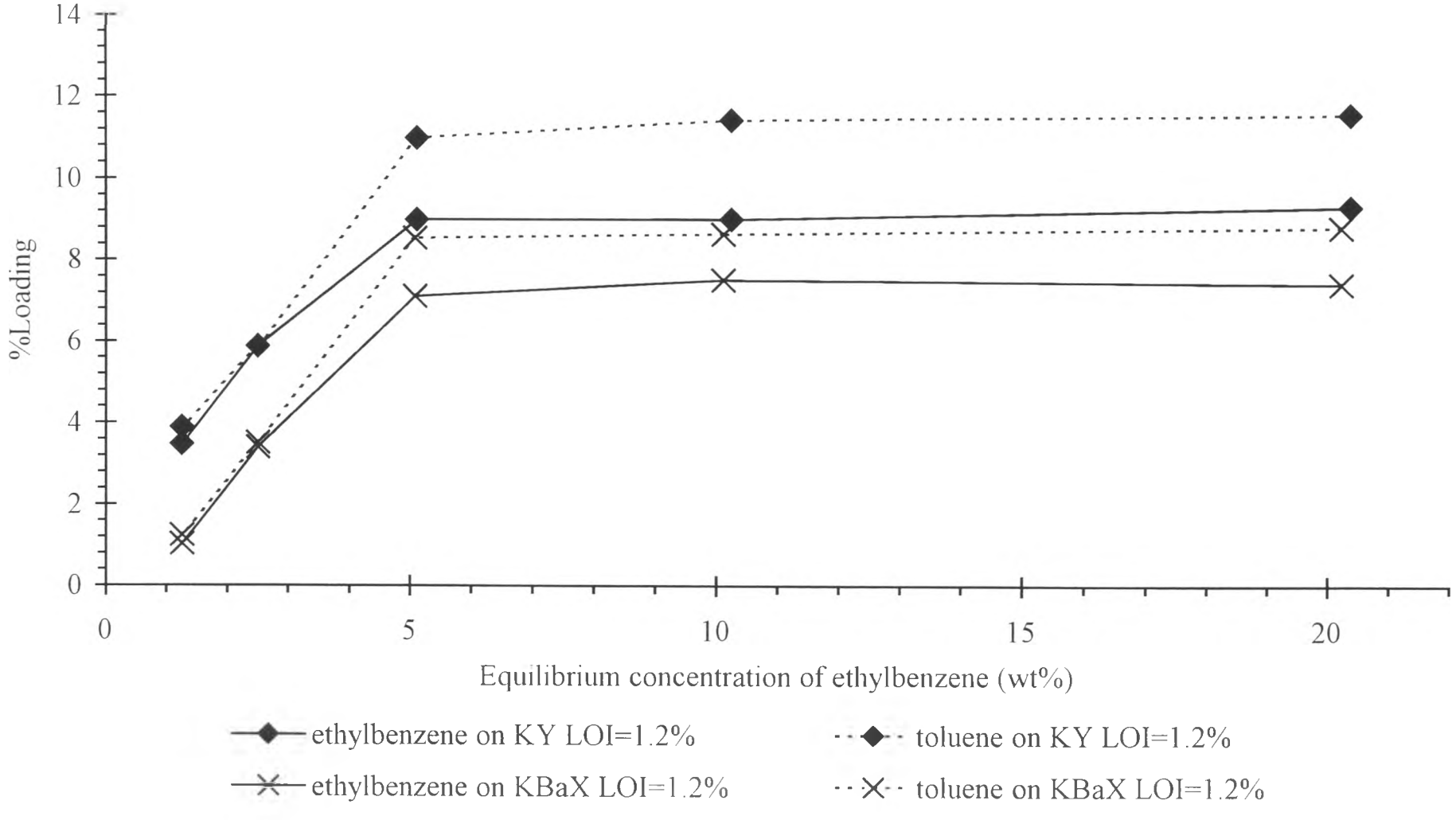

Figure 4.46 Adsorption of etylbenzene and toluene on *KY* and *KBaX* zeolites at 40 °C

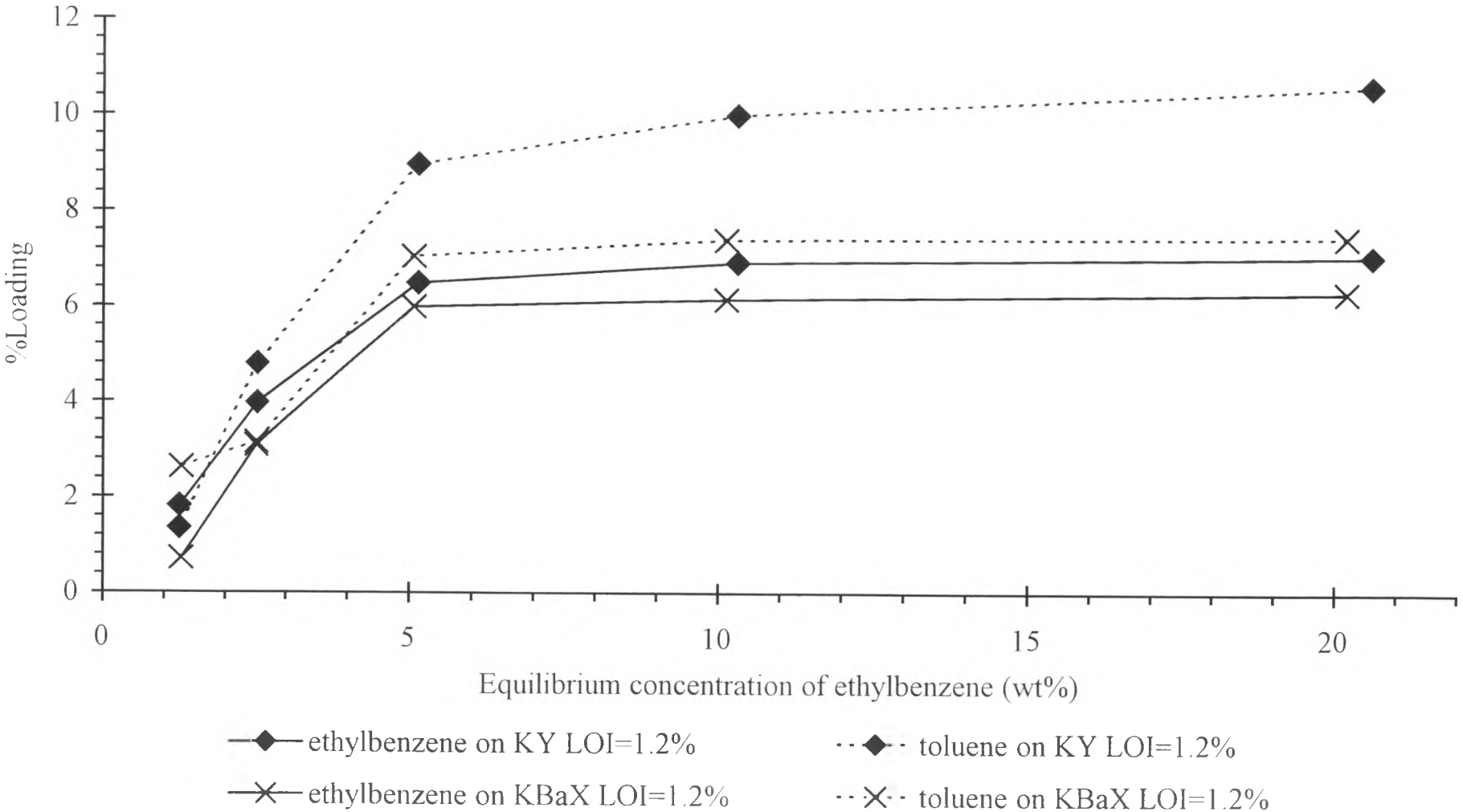

Figure 4.47 Adsorption of etylbenzene and toluene on *KY* and *KBaX* zeolites at 65 °C

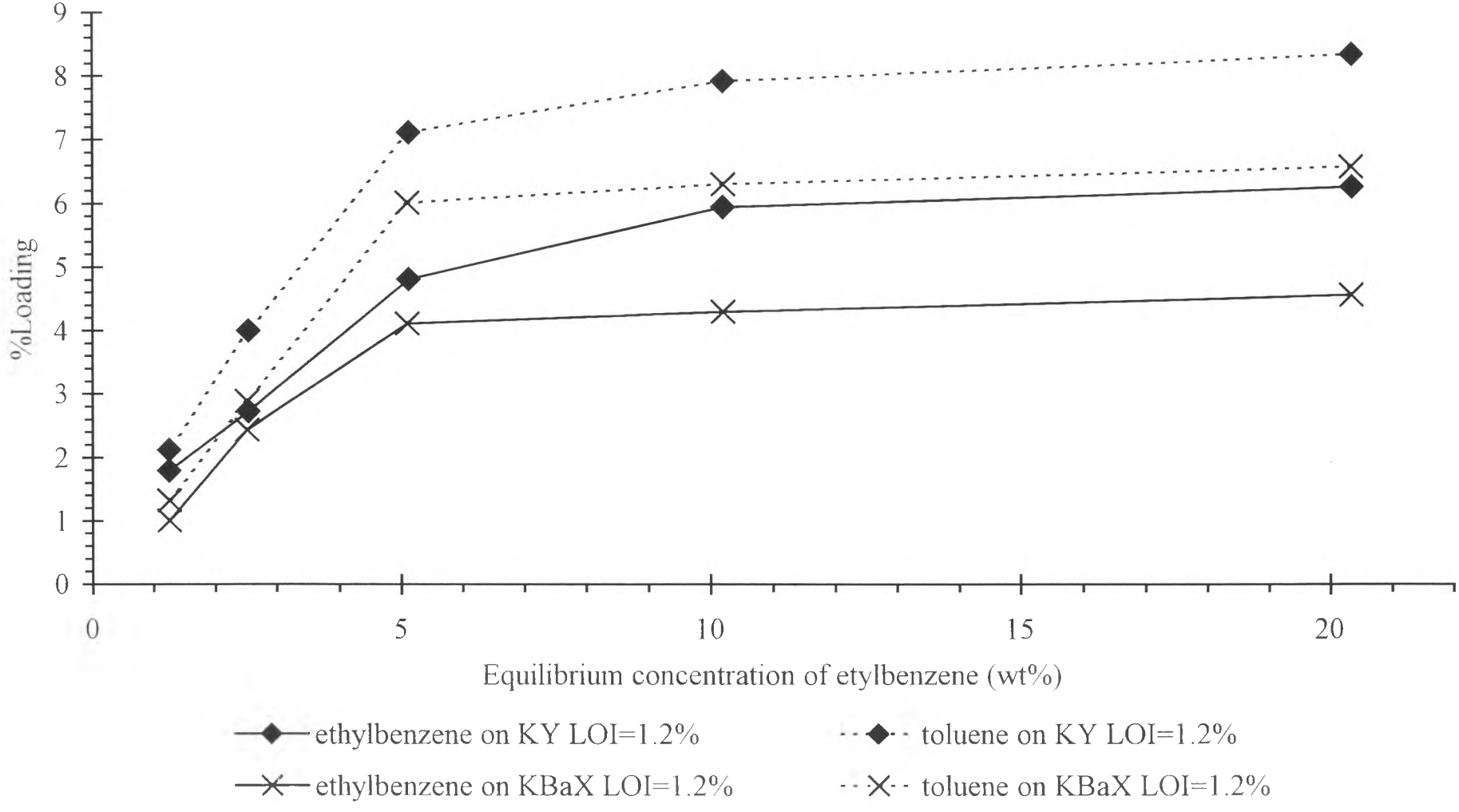

Figure 4.48 Adsorption of etylbenzene and toluene on *KY* and *KBaX* zeolites at 90 °C

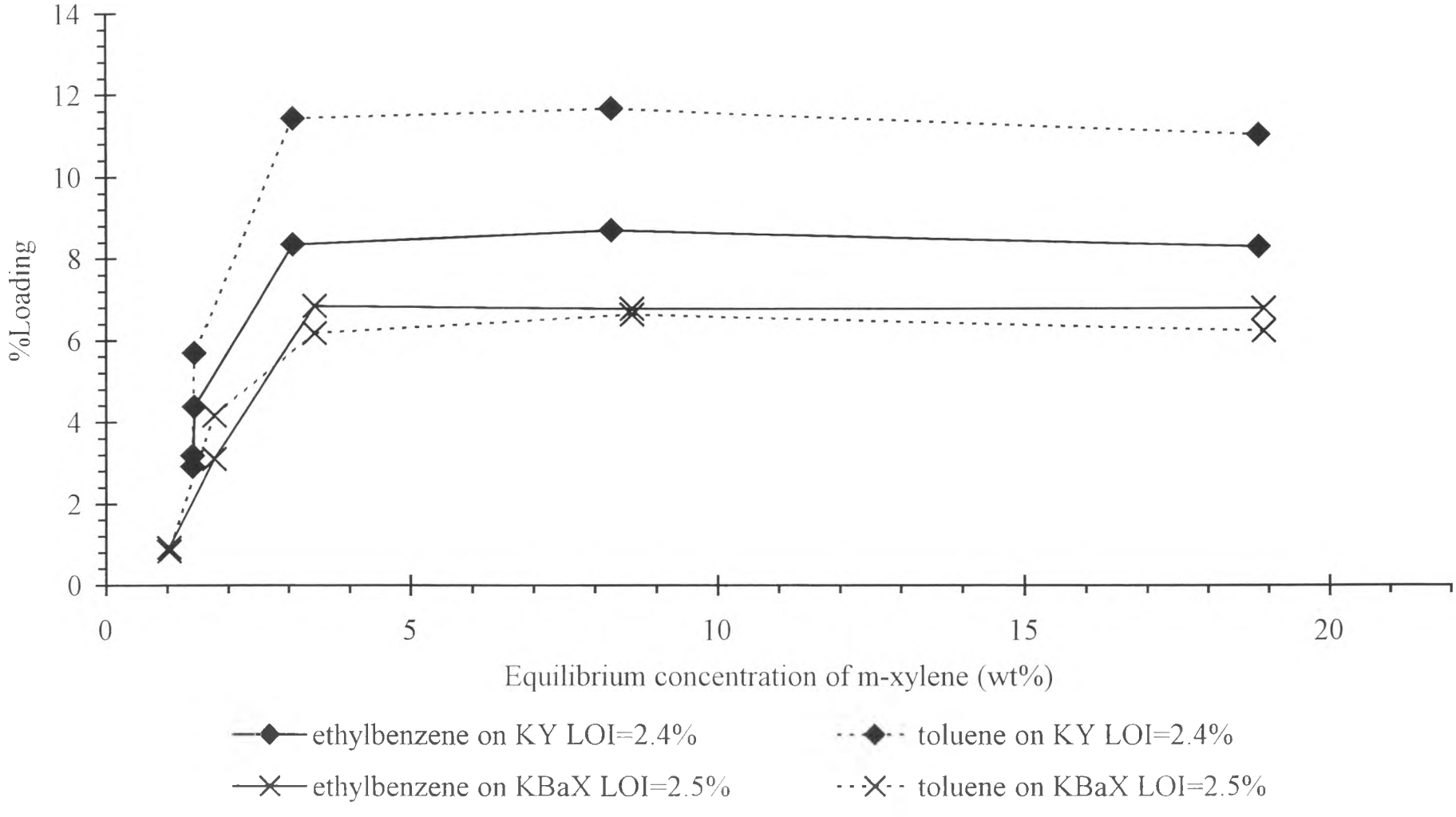

Figure 4.49 Adsorption of etylbenzene and toluene on *KY* and *KBaX* zeolites at 40 °C

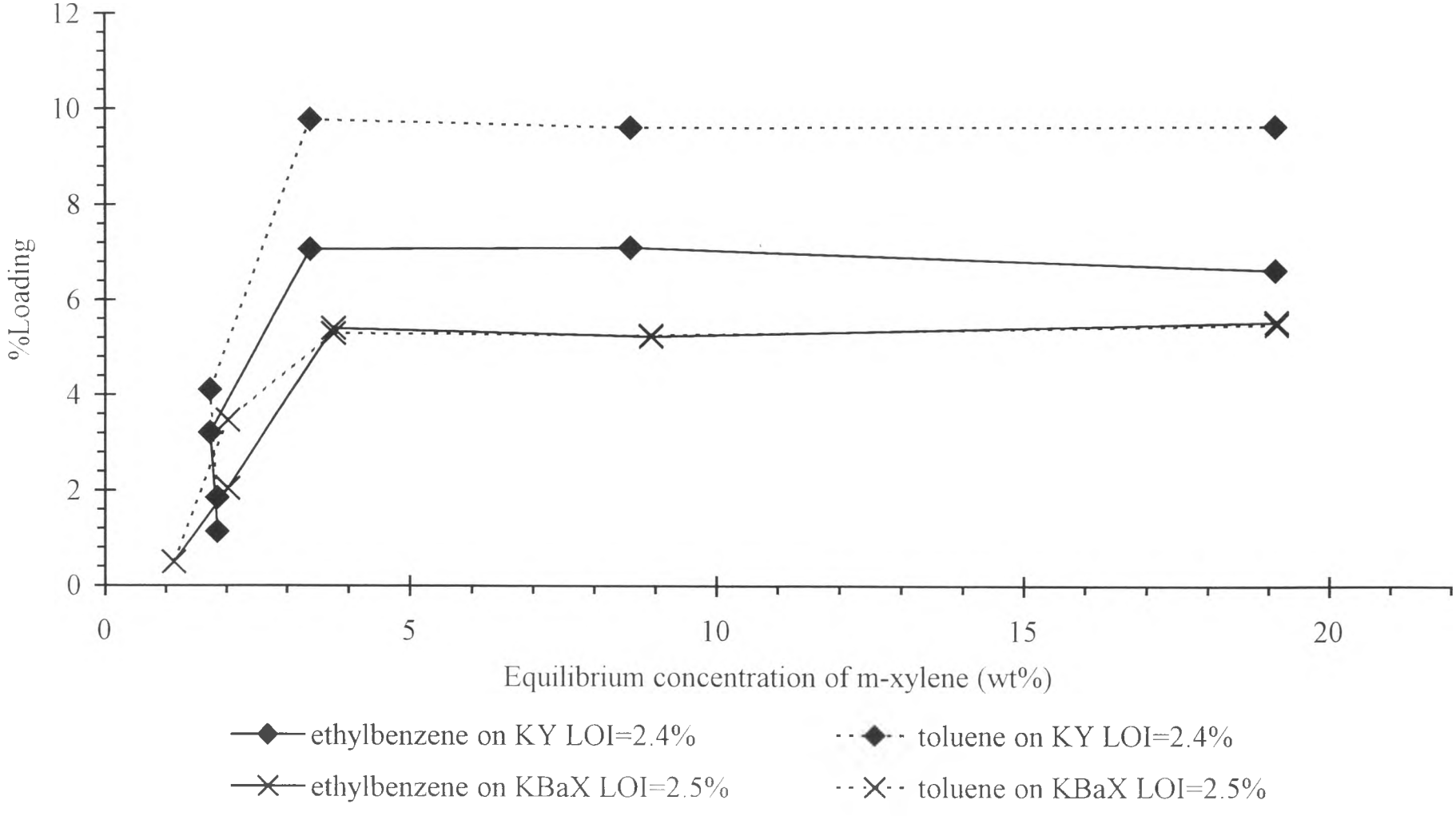

Figure 4.50 Adsorption of etylbenzene and toluene on *KY* and *KBaX* zeolites at 65 °C

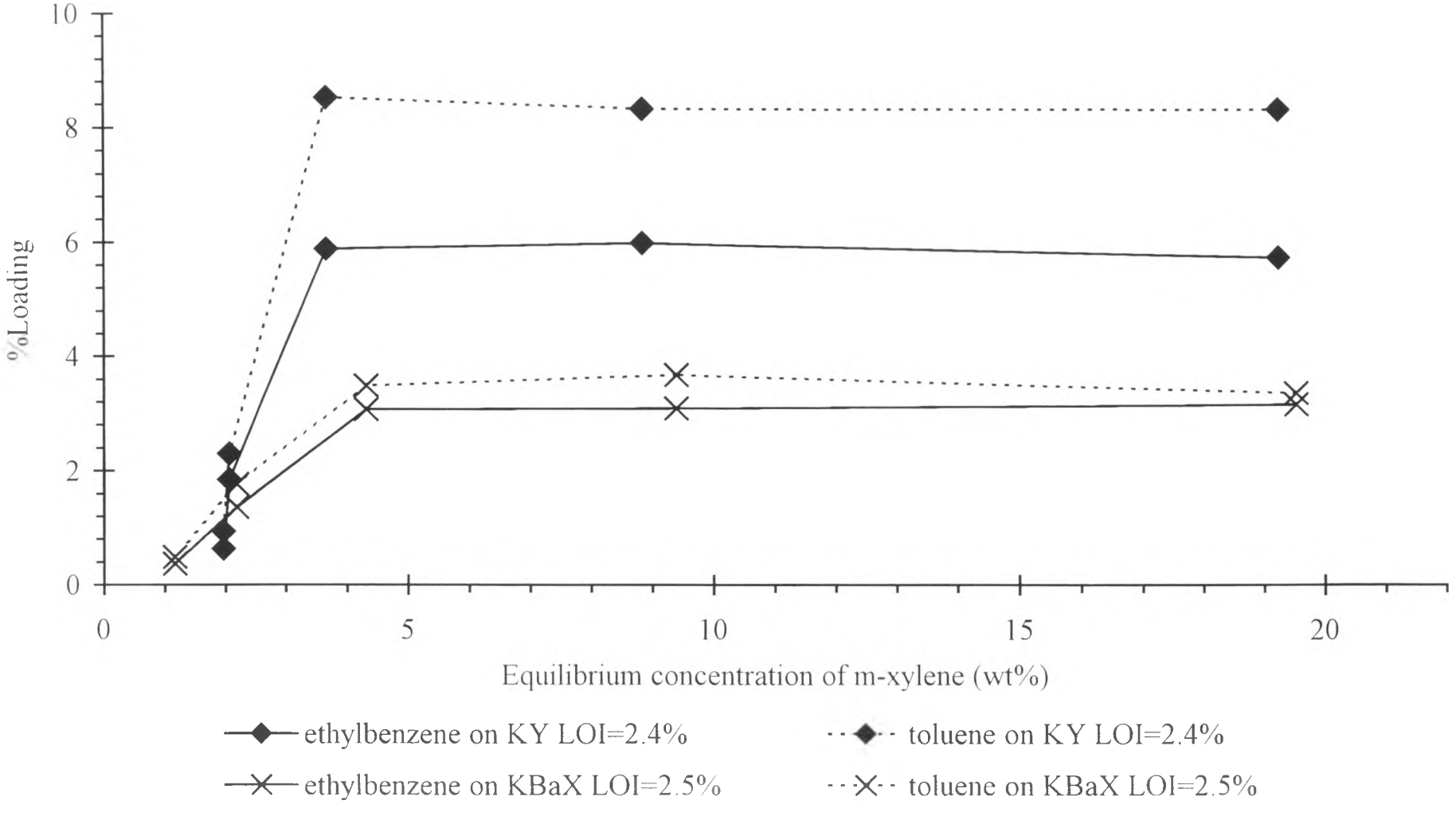

Figure 4.51 Adsorption of etylbenzene and toluene on *KY* and *KBaX* zeolites at 90 °C

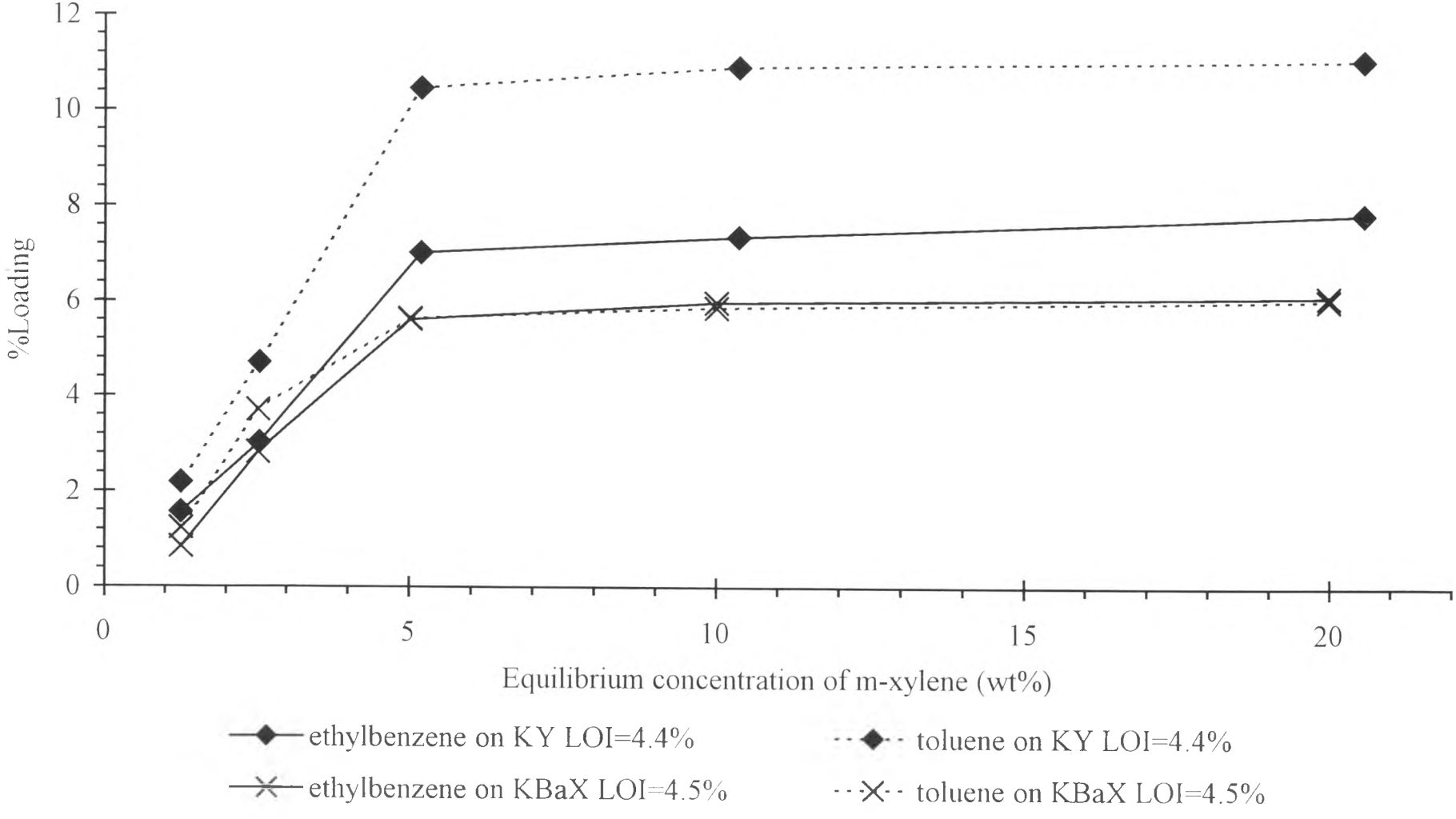

Figure 4.52 Adsorption of etylbenzene and toluene on *KY* and *KBaX* zeolites at 40 °C

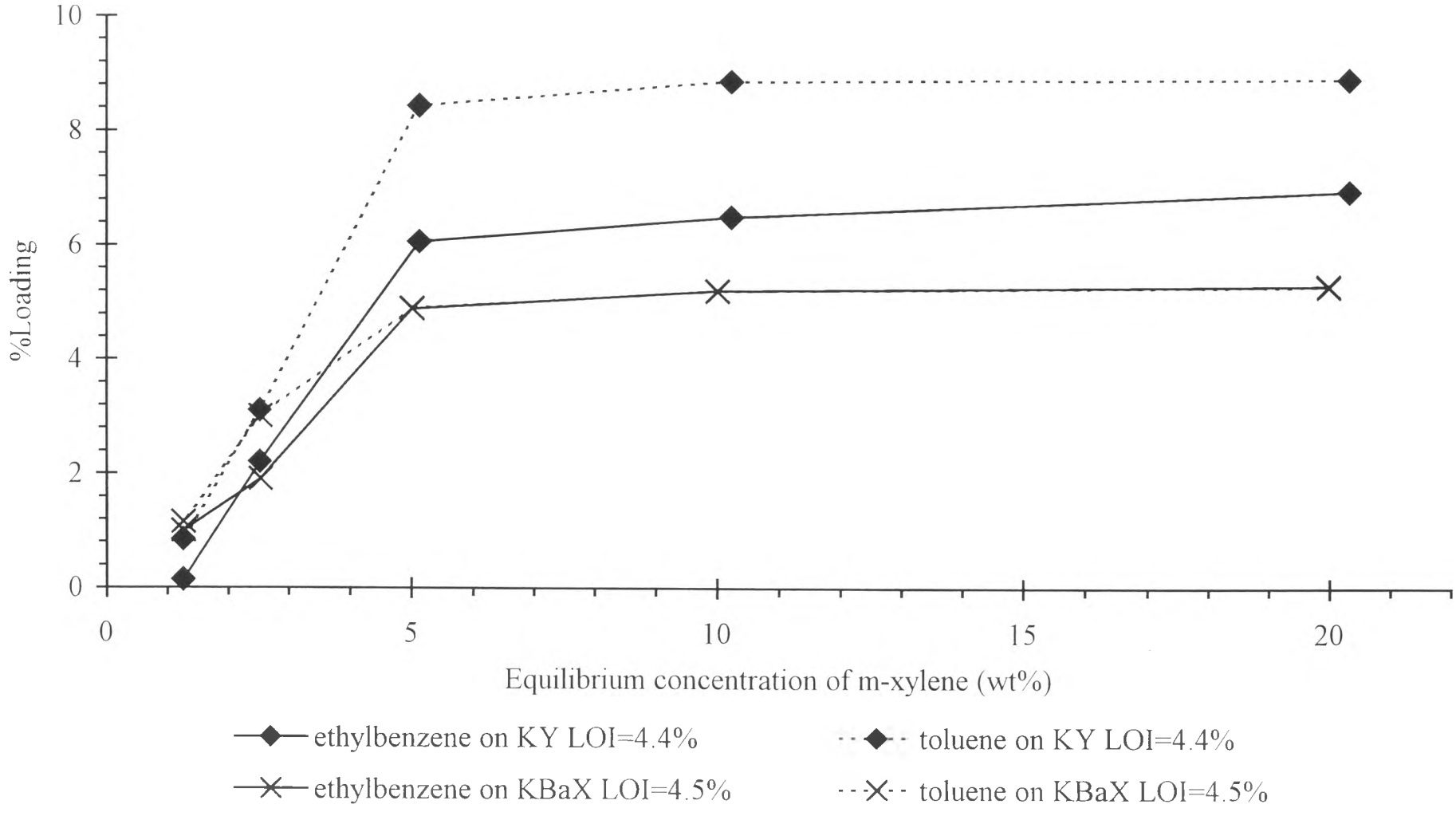

Figure 4.53 Adsorption of etylbenzene and toluene on *KY* and *KBaX* zeolites at 65 °C

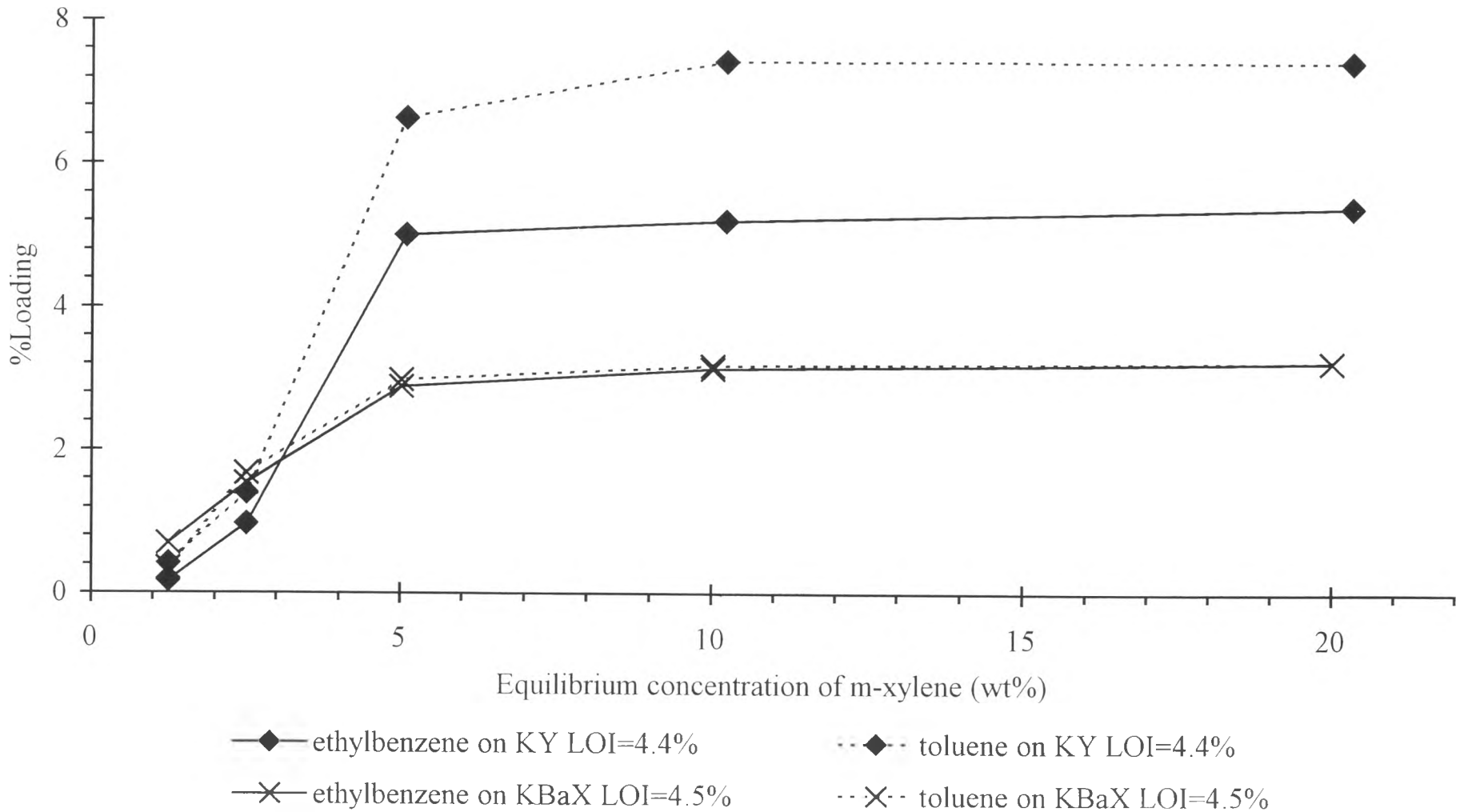

Figure 4.54 Adsorption of etylbenzene and toluene on *KY* and *KBaX* zeolites at 90 °C

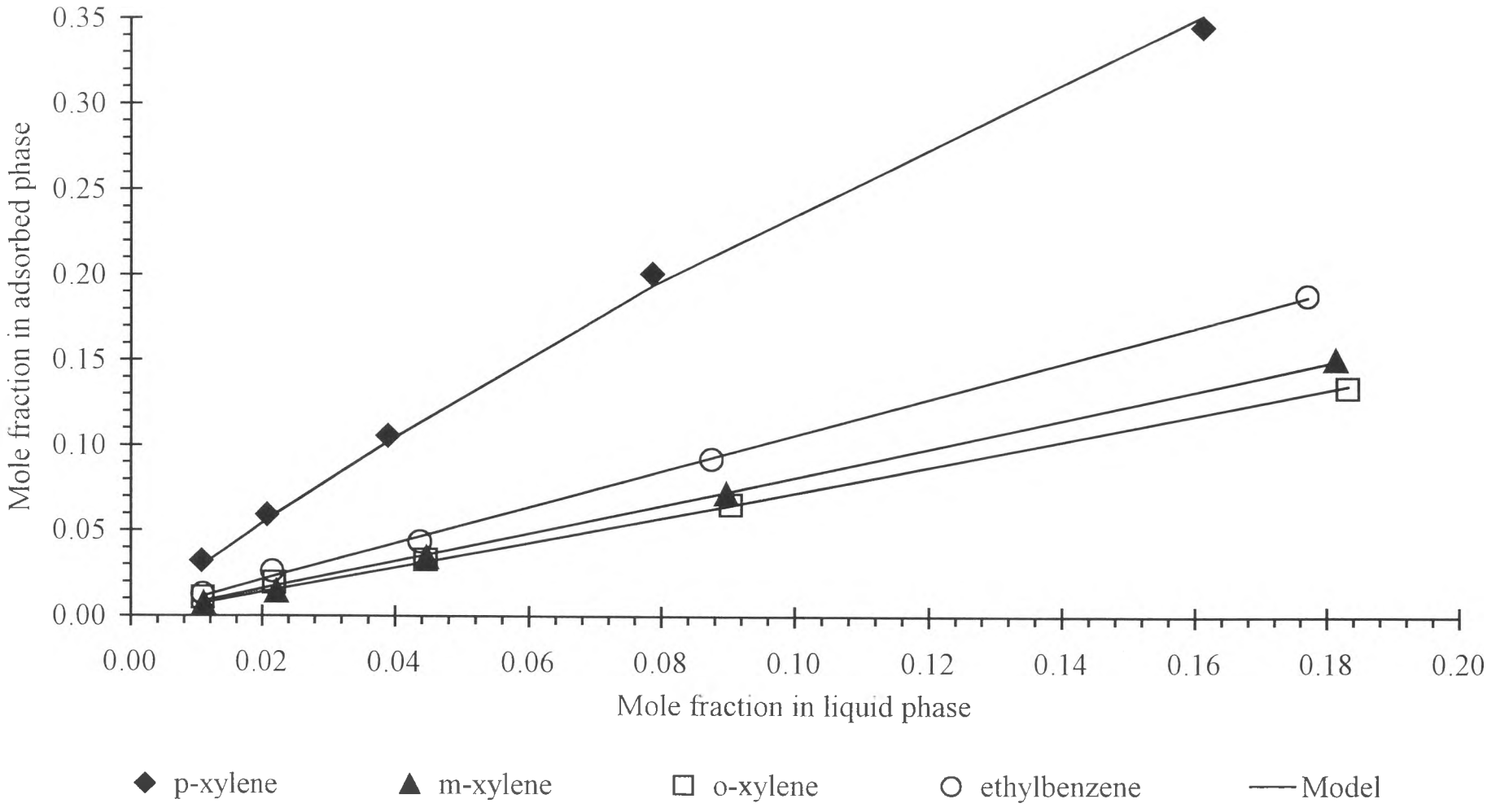

Figure 4.55 Adsorption of the C_8 aromatics on the *KY* zeolite, LOI=1.2% at 40 °C

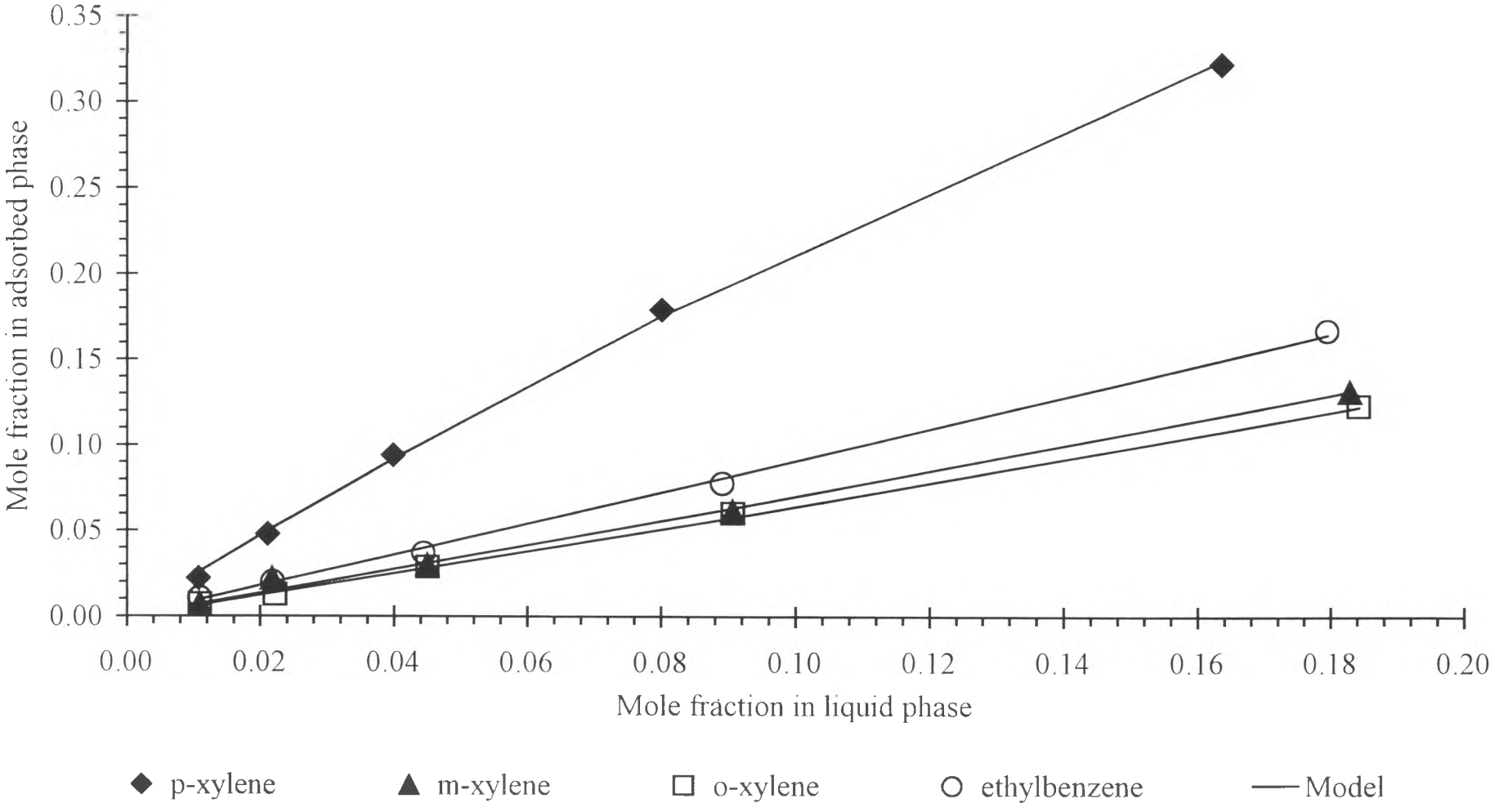

Figure 4.56 Adsorption of the C_8 aromatics on the *KY* zeolite, LOI=1.2% at 65 °C

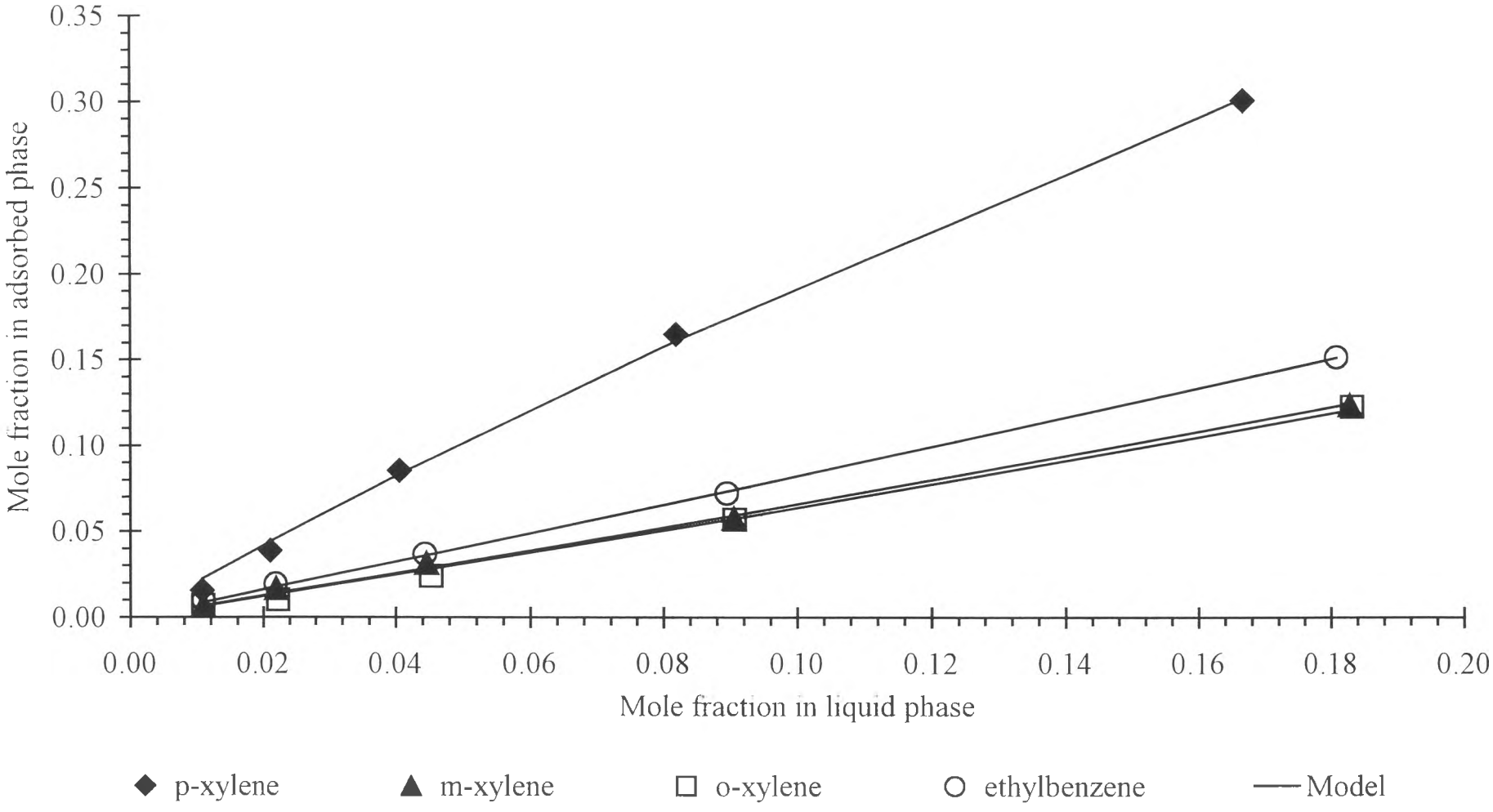

Figure 4.57 Adsorption of the C_8 aromatics on the *KY* zeolite, LOI=1.2% at 90 °C

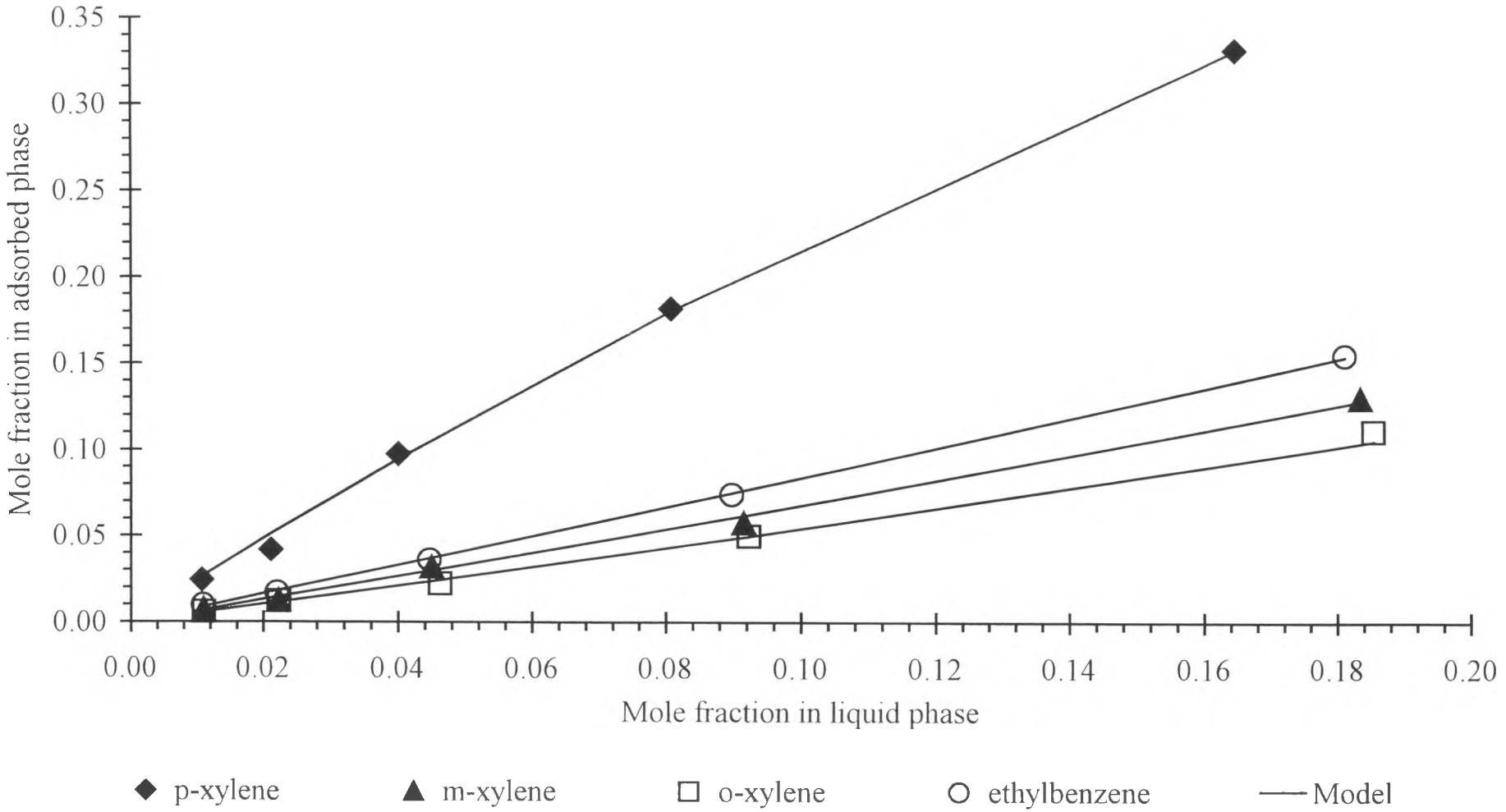

Figure 4.58 Adsorption of the C_8 aromatics on the *KY* zeolite, LOI=2.4% at 40 °C

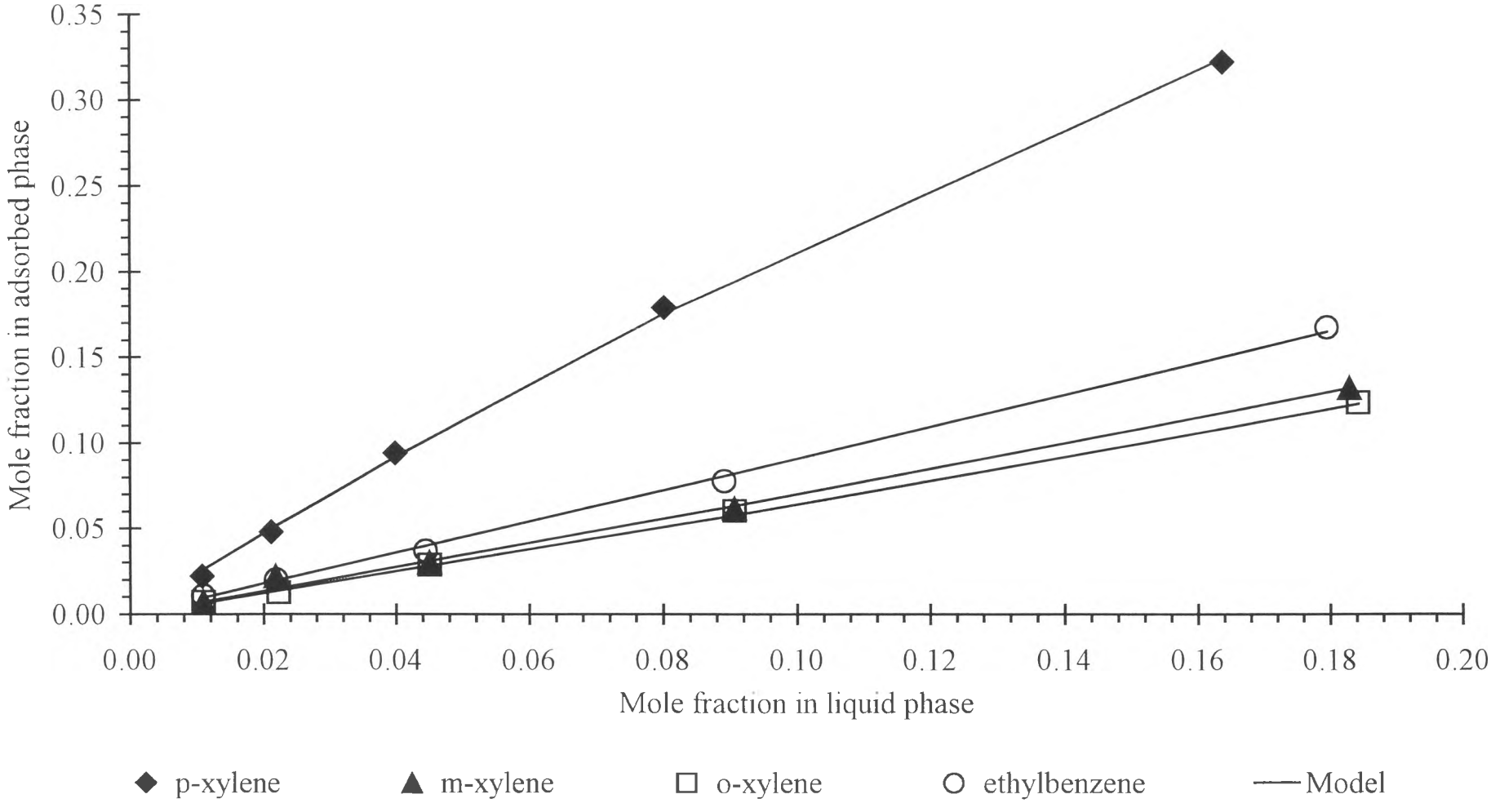

Figure 4.59 Adsorption of the C_8 aromatics on the *KY* zeolite, LOI=2.4% at 65 °C

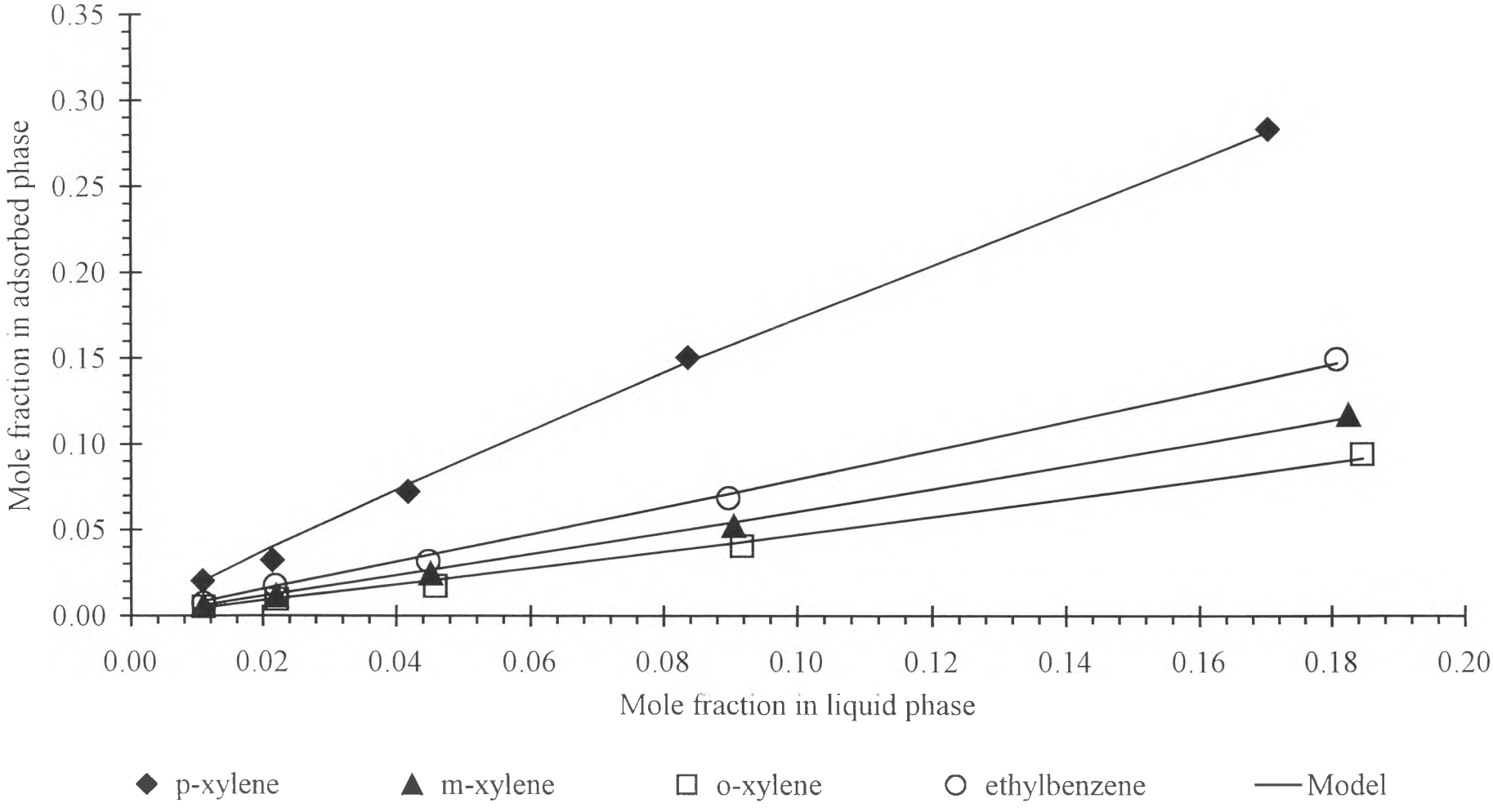

Figure 4.60 Adsorption of the C_8 aromatics on the *KY* zeolite, LOI=2.4% at 90 °C

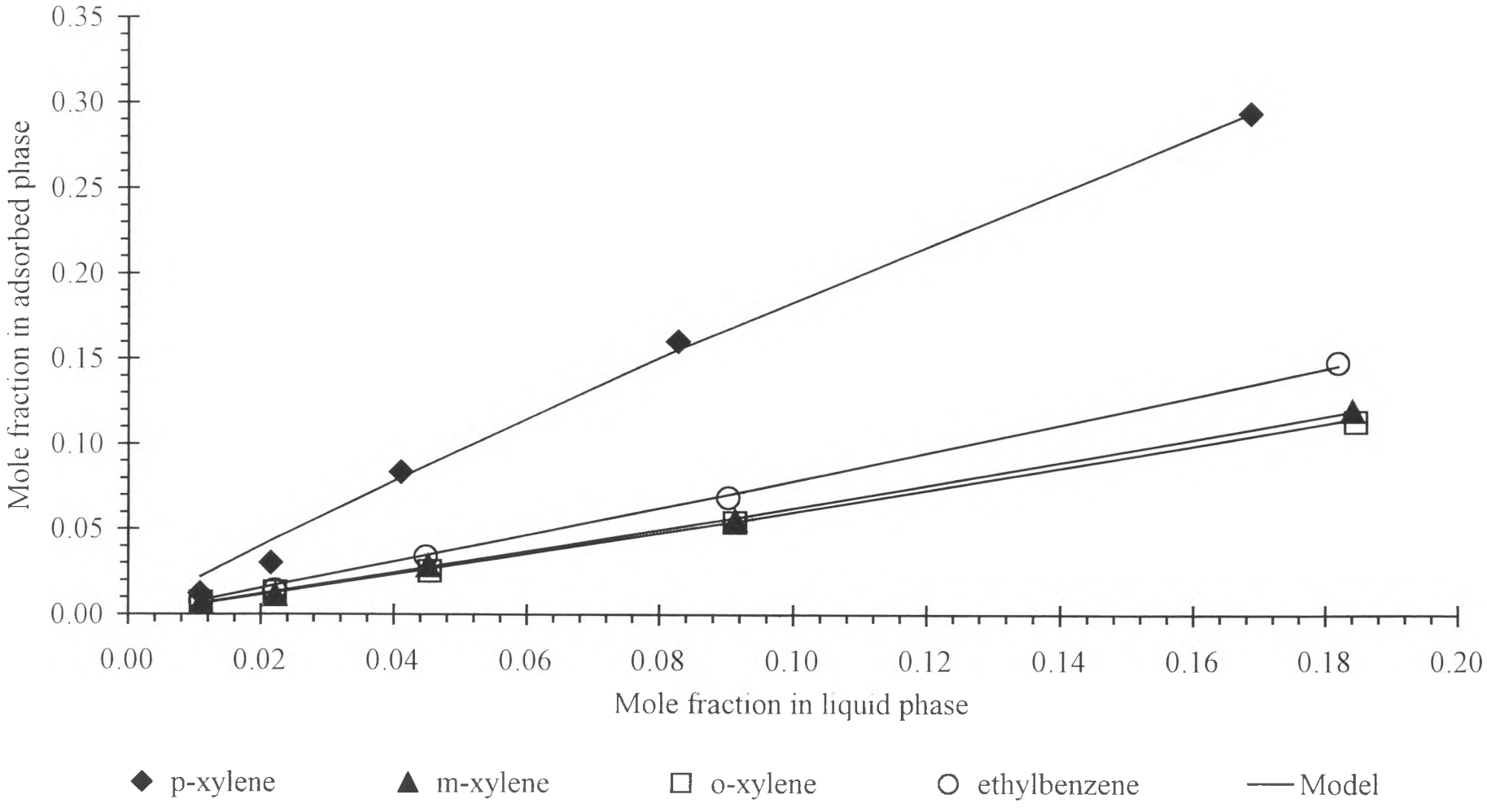

Figure 4.61 Adsorption of the C_8 aromatics on the *KY* zeolite, LOI=4.4% at 40 °C

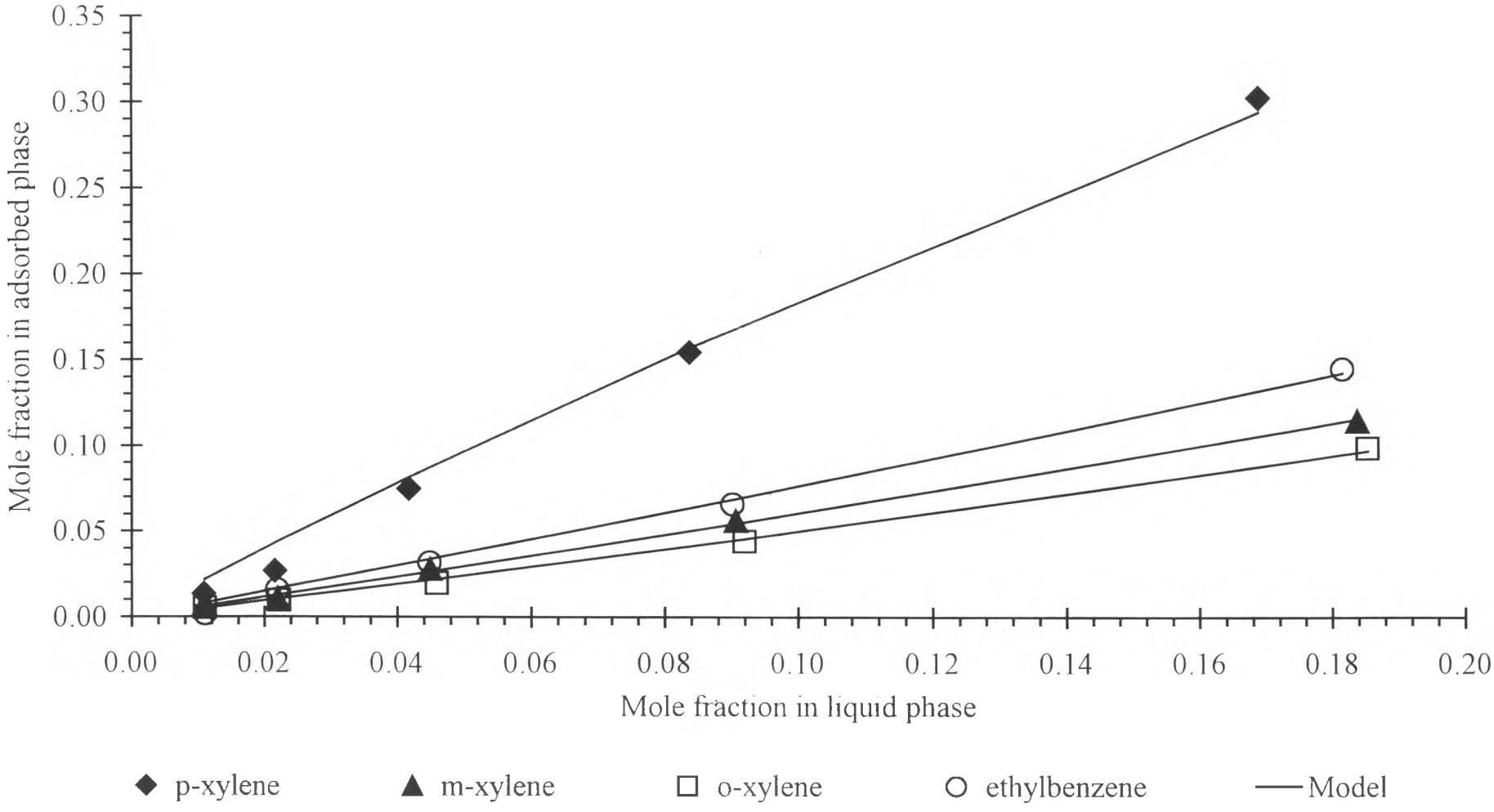

Figure 4.62 Adsorption of the C_8 aromatics on the *KY* zeolite, LOI=4.4% at 65 °C

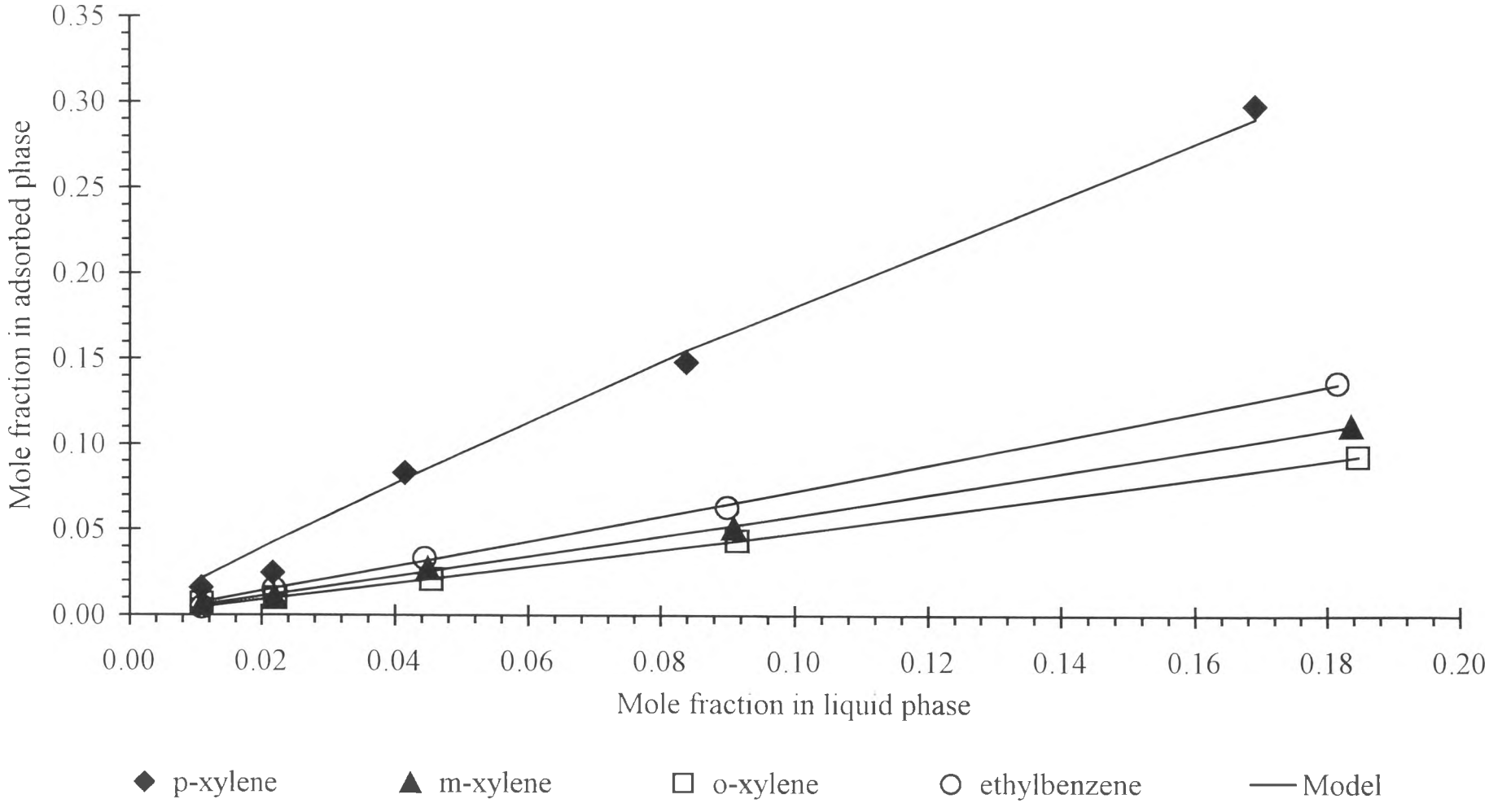

Figure 4.63 Adsorption of the C_8 aromatics on the *KY* zeolite, LOI=4.4% at 90 °C

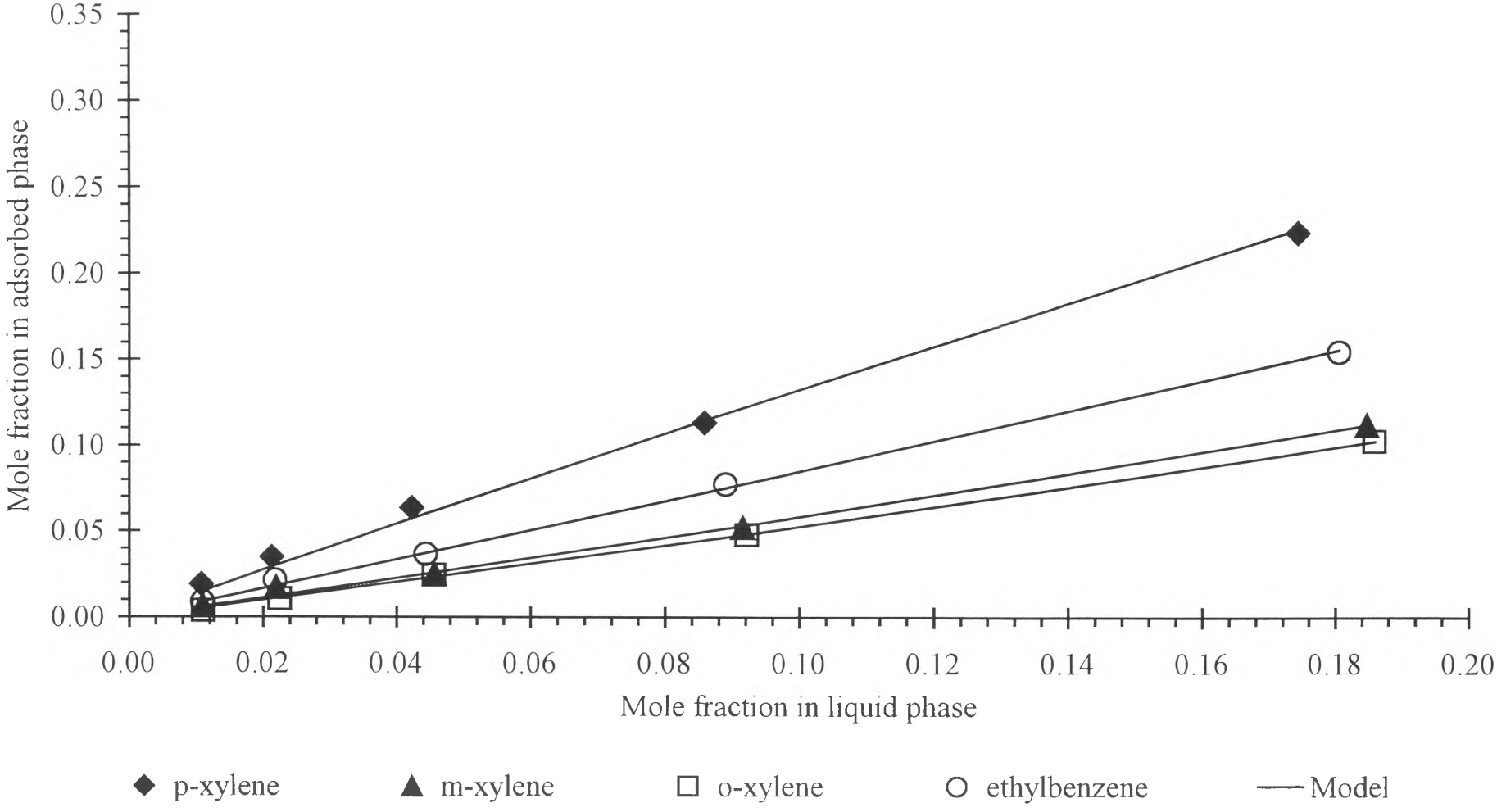

Figure 4.64 Adsorption of the C_8 aromatics on the *KBaX* zeolite, LOI=1.2% at 40 °C

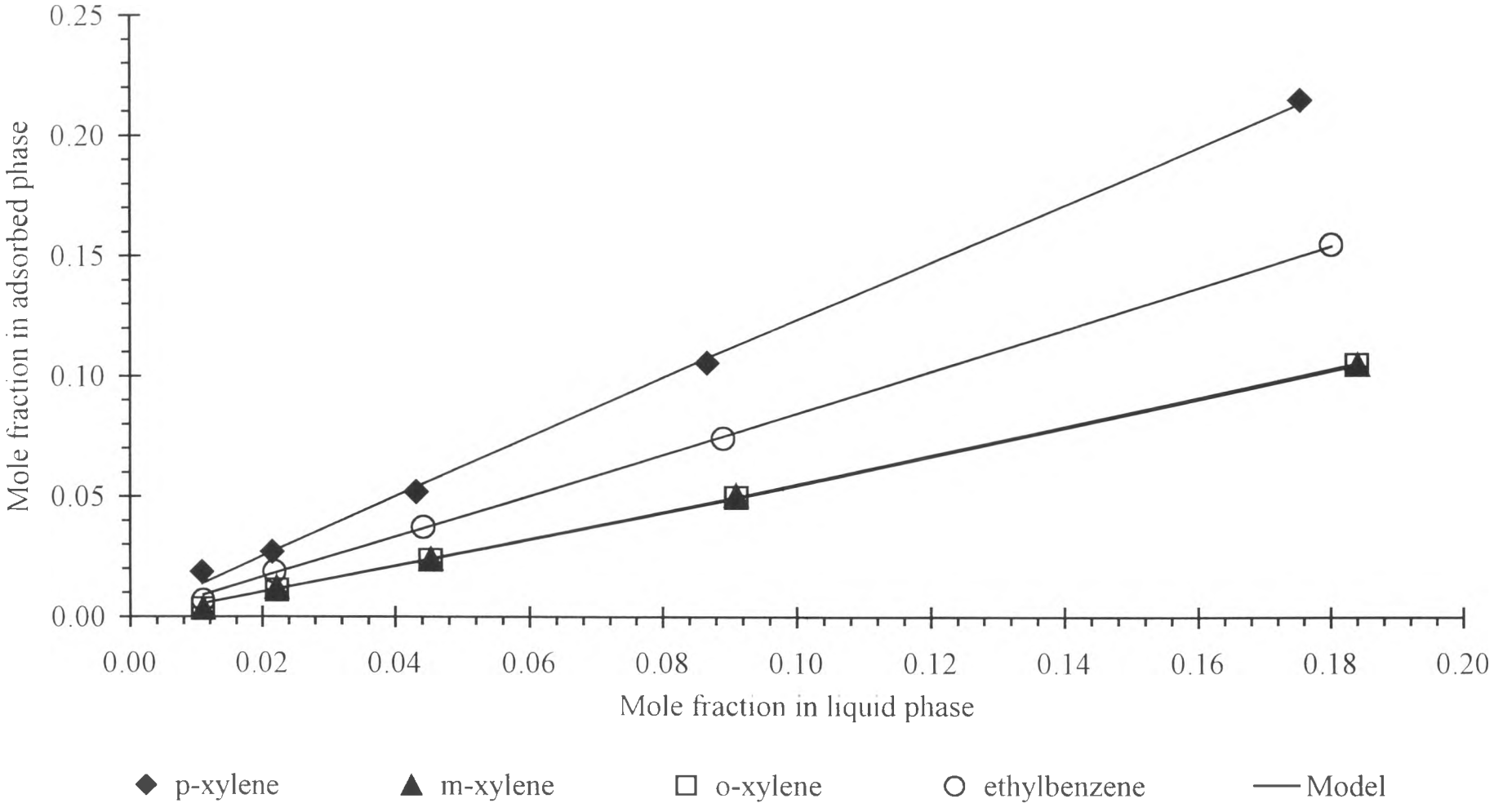

Figure 4.65 Adsorption of the C_8 aromatics on the *KBaX* zeolite, LOI=1.2% at 65 °C

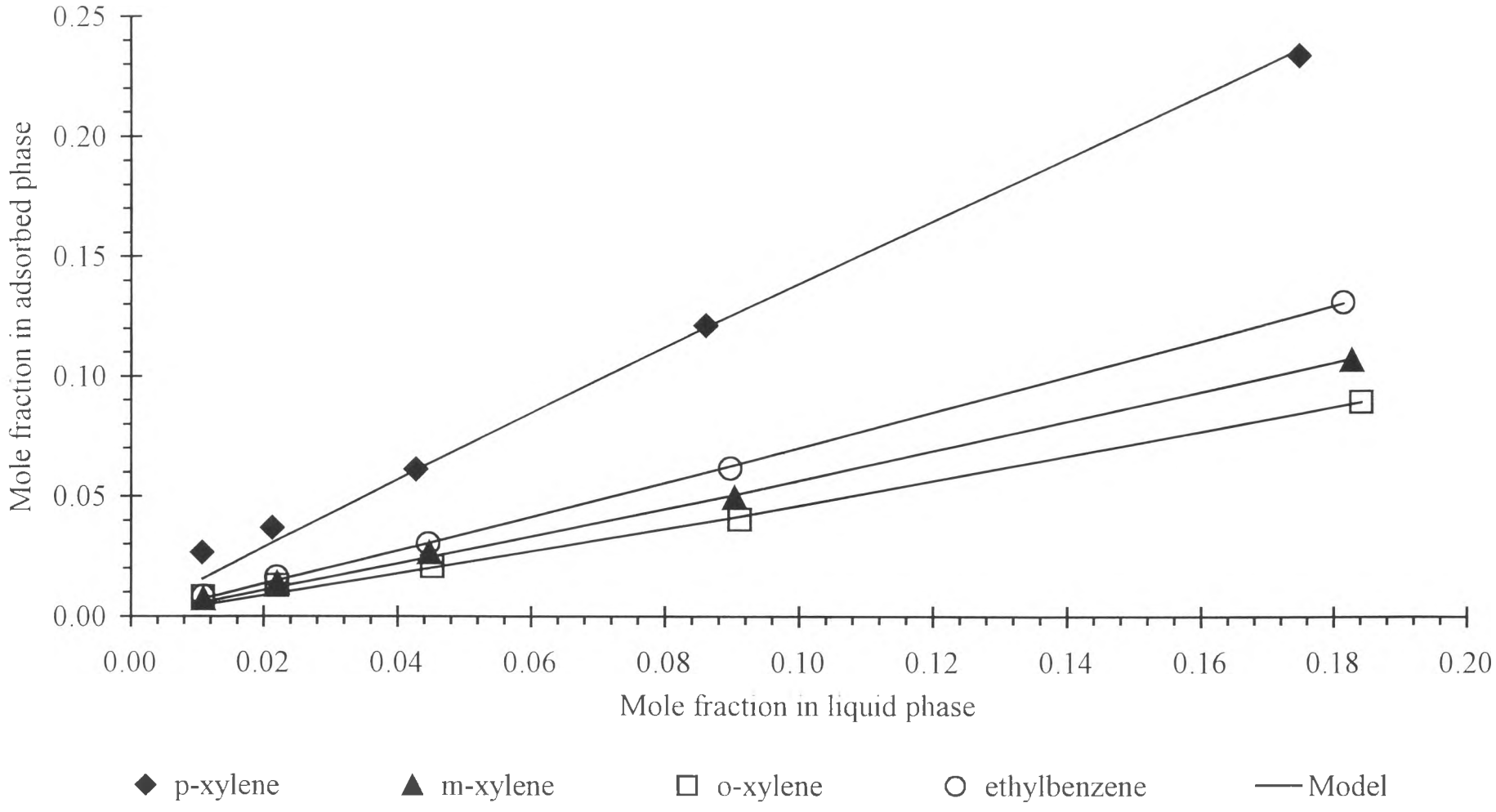

Figure 4.66 Adsorption of the C_8 aromatics on the *KBaX* zeolite, LOI=1.2% at 90 °C

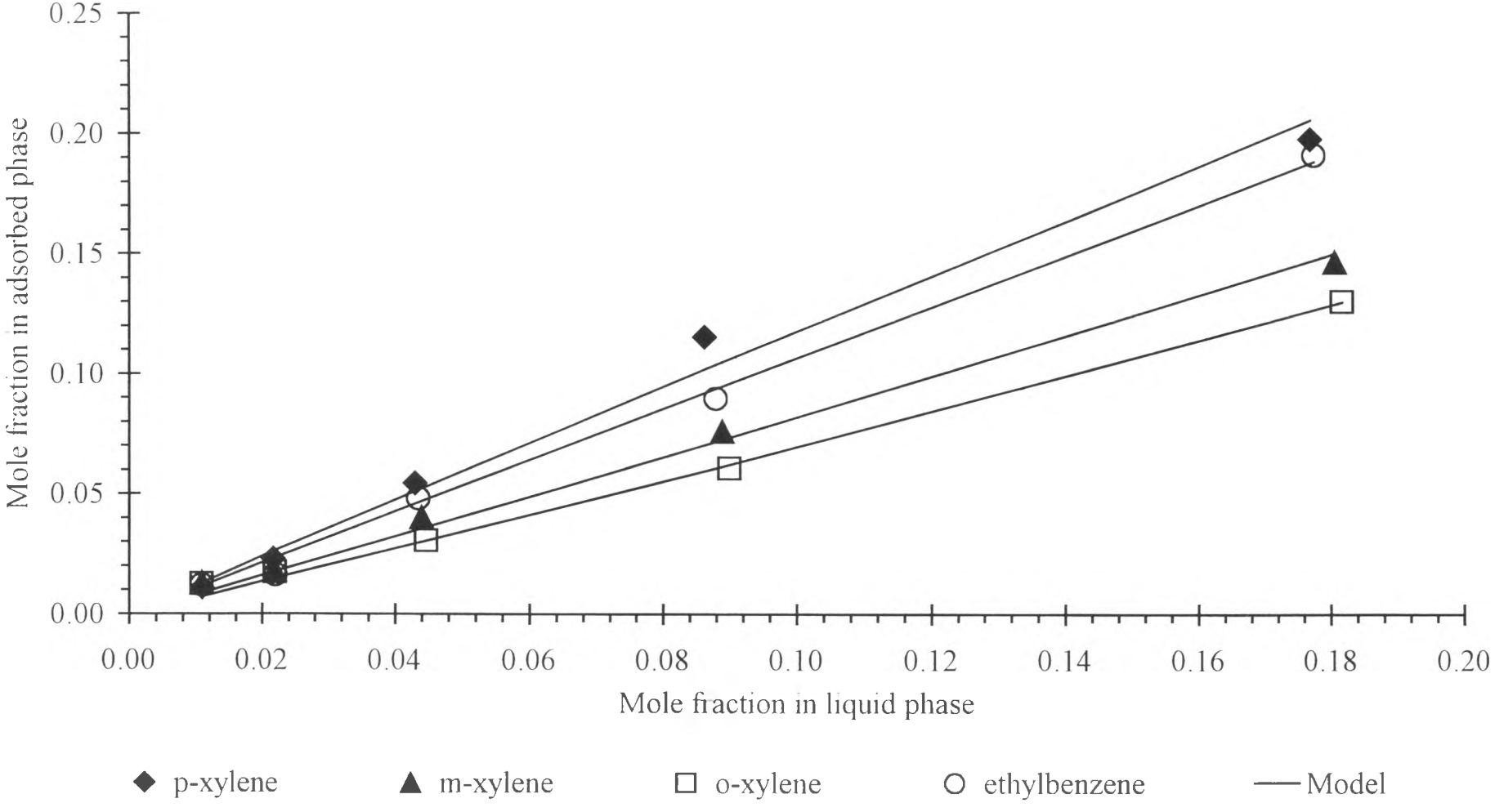

Figure 4.67 Adsorption of the C_8 aromatics on the *KBaX* zeolite, LOI=2.5% at 40 °C

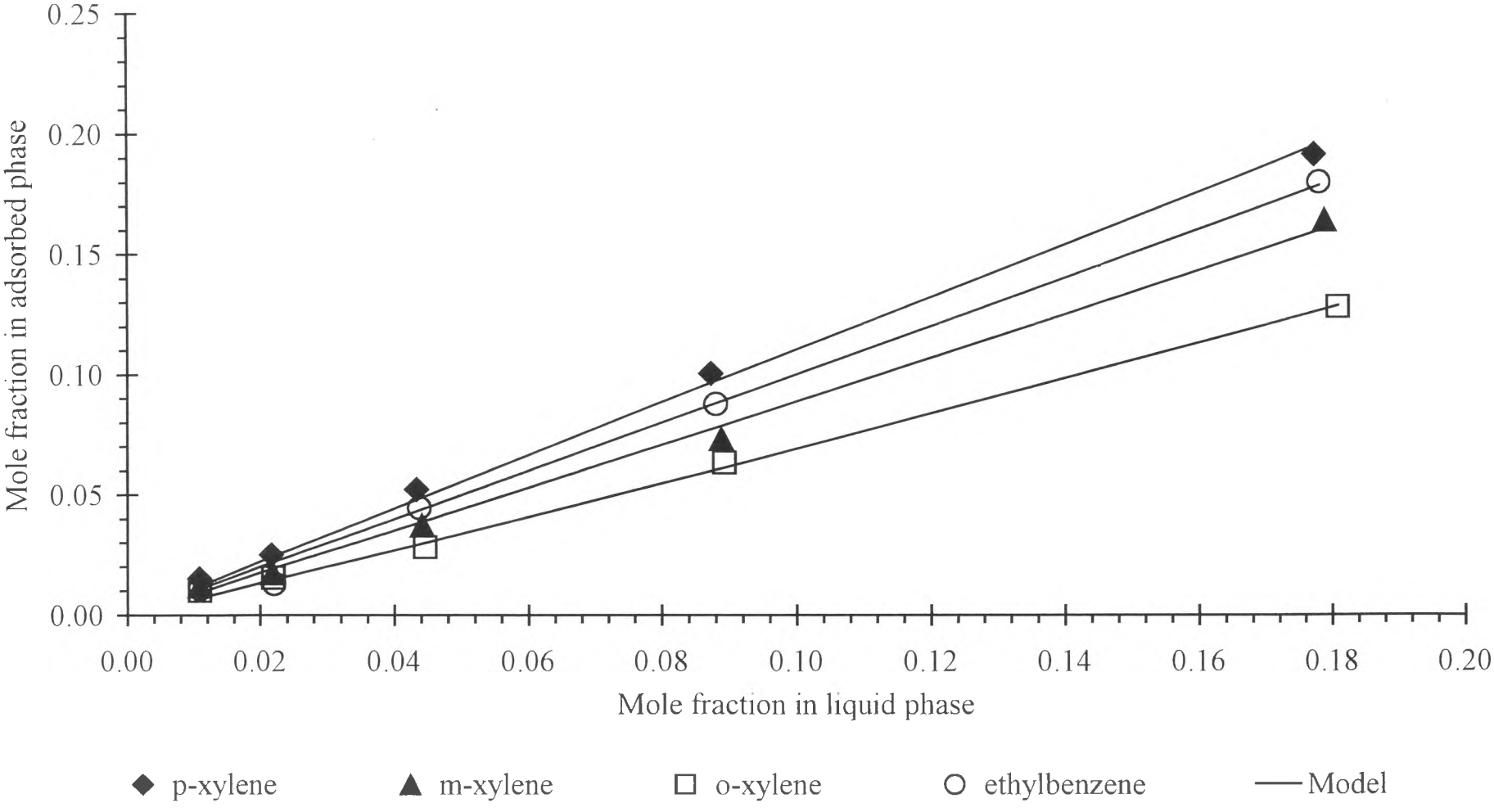

Figure 4.68 Adsorption of the C_8 aromatics on the *KBaX* zeolite, LOI=2.5% at 65 °C

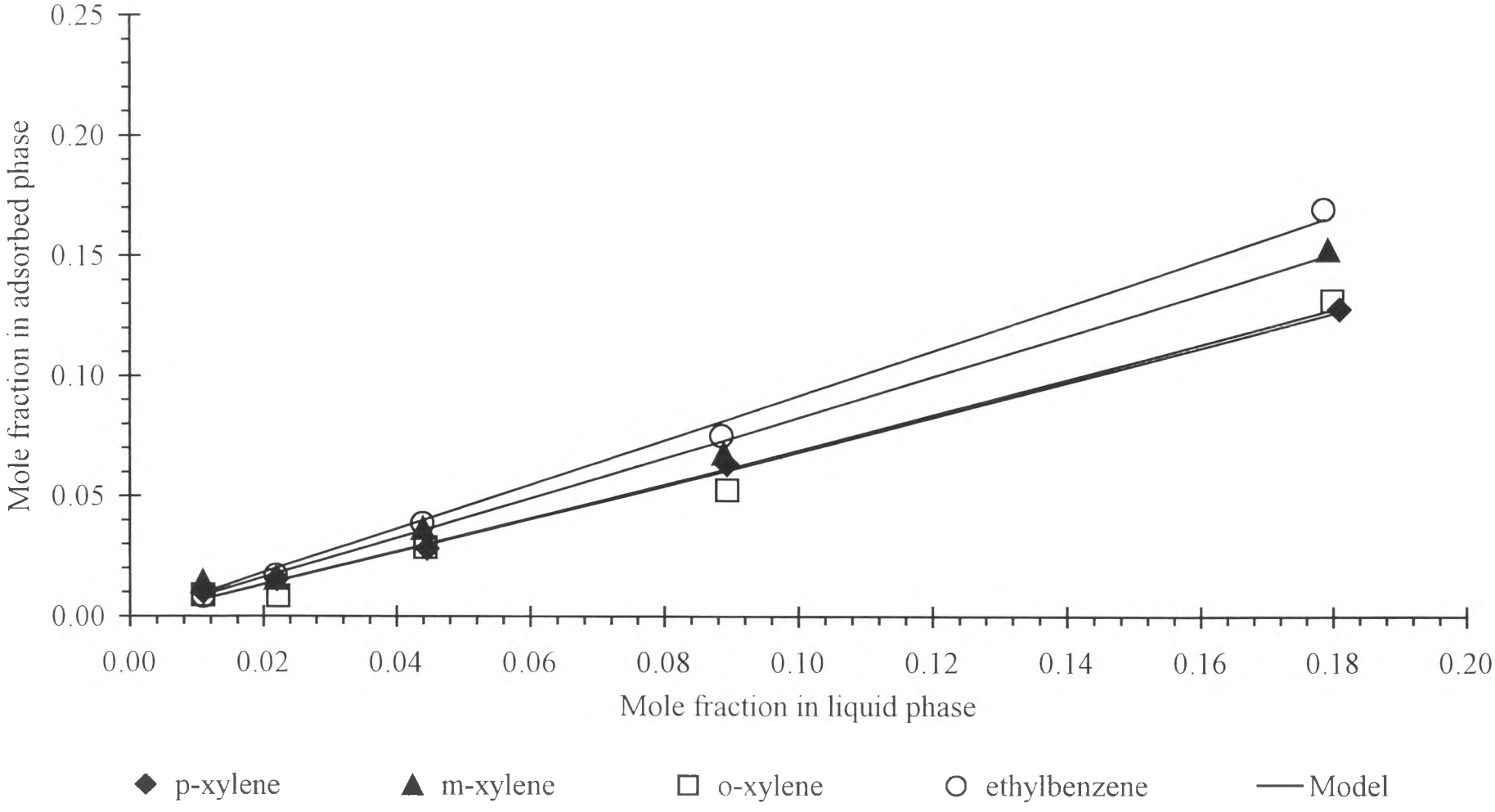

Figure 4.69 Adsorption of the C_8 aromatics on the *KBaX* zeolite, LOI=2.5% at 90 °C

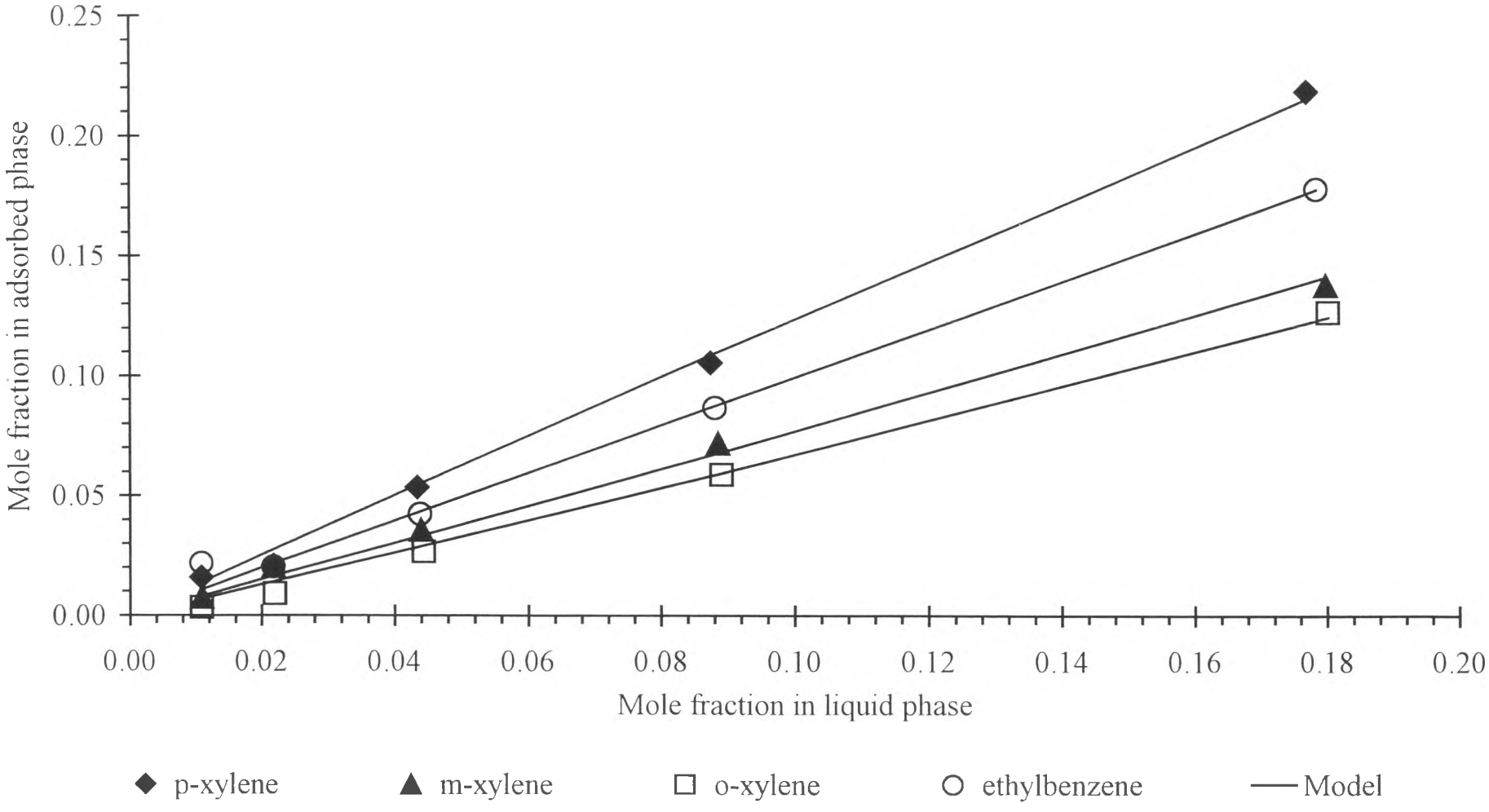

Figure 4.70 Adsorption of the C_8 aromatics on the *KBaX* zeolite, LOI=4.5% at 40 °C

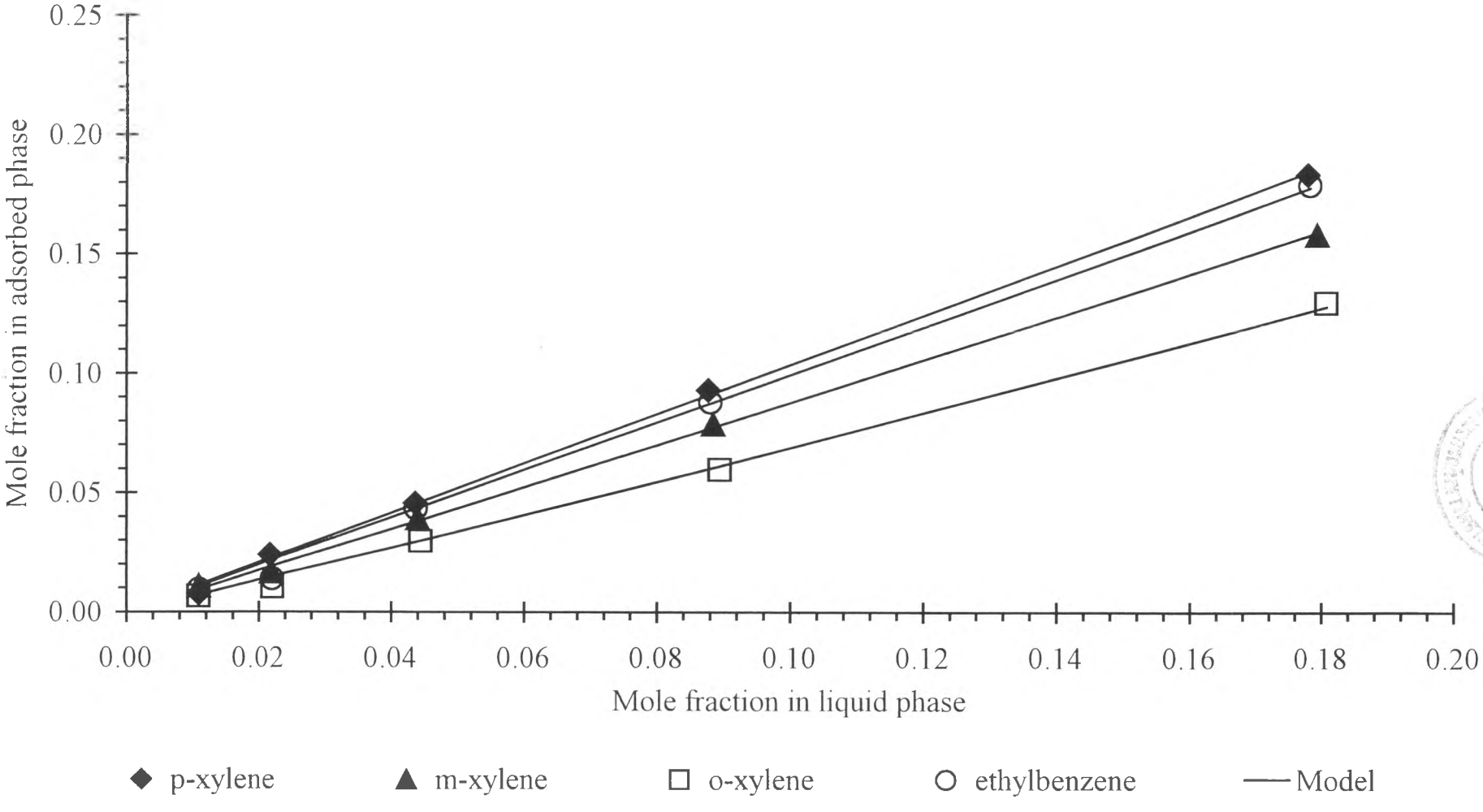

Figure 4.71 Adsorption of the C_8 aromatics on the *KBaX* zeolite, LOI=4.5% at 65 °C

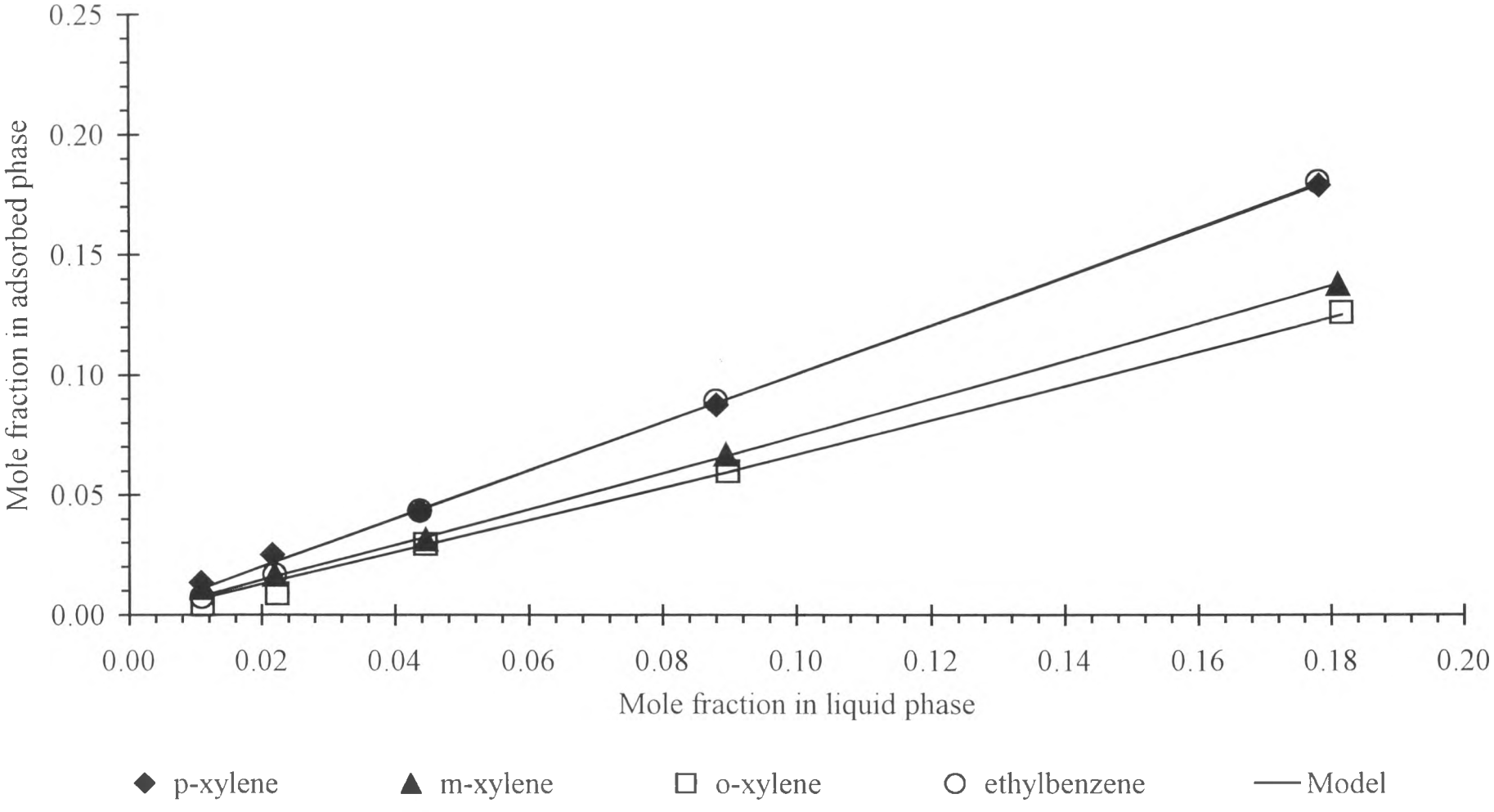

Figure 4.72 Adsorption of the C_8 aromatics on the *KBaX* zeolite, LOI=4.5% at 90 °C

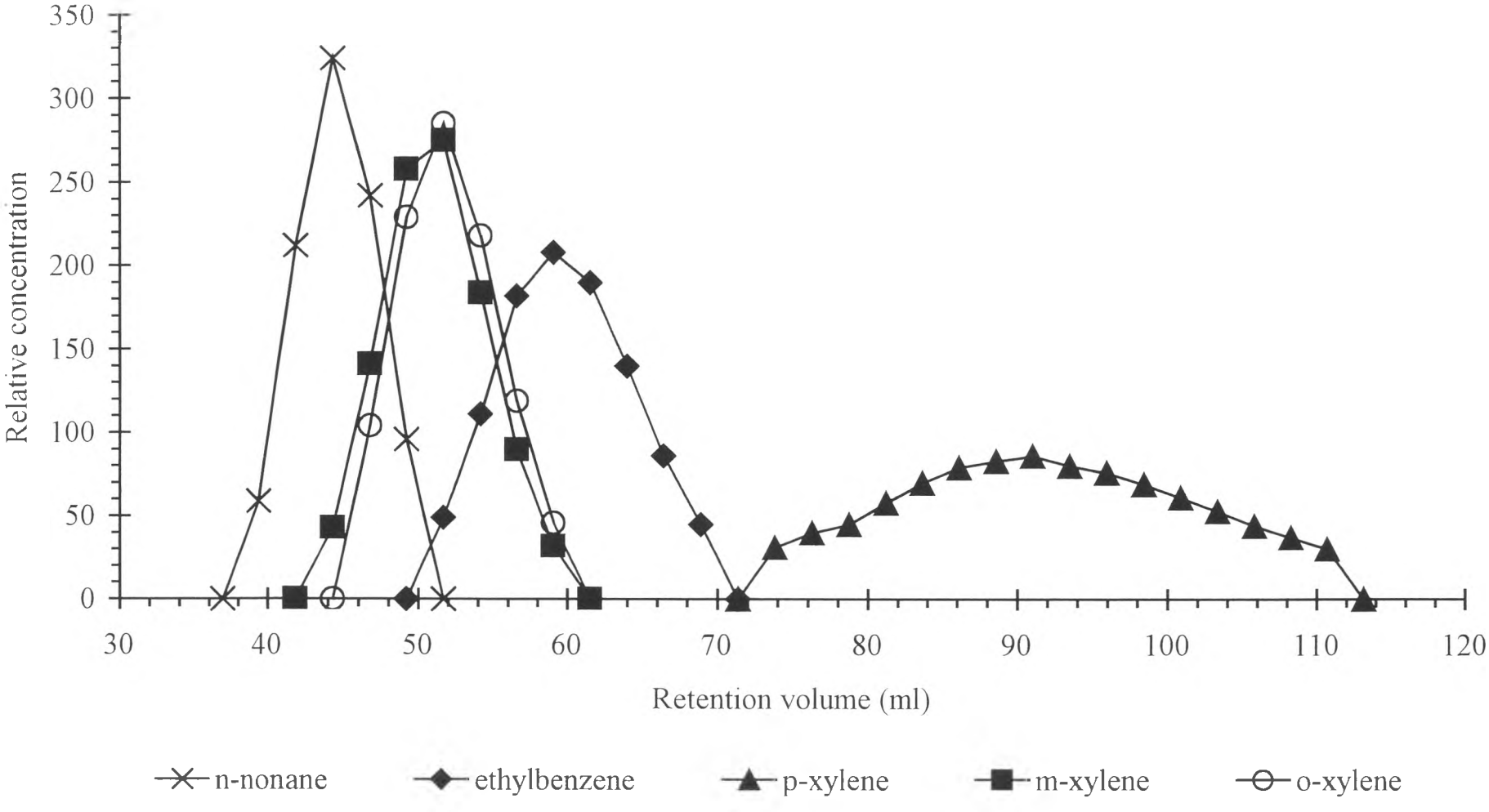

Figure 4.73 Pulse test on *KY* zeolite, LOI=1.2% at 40 °C

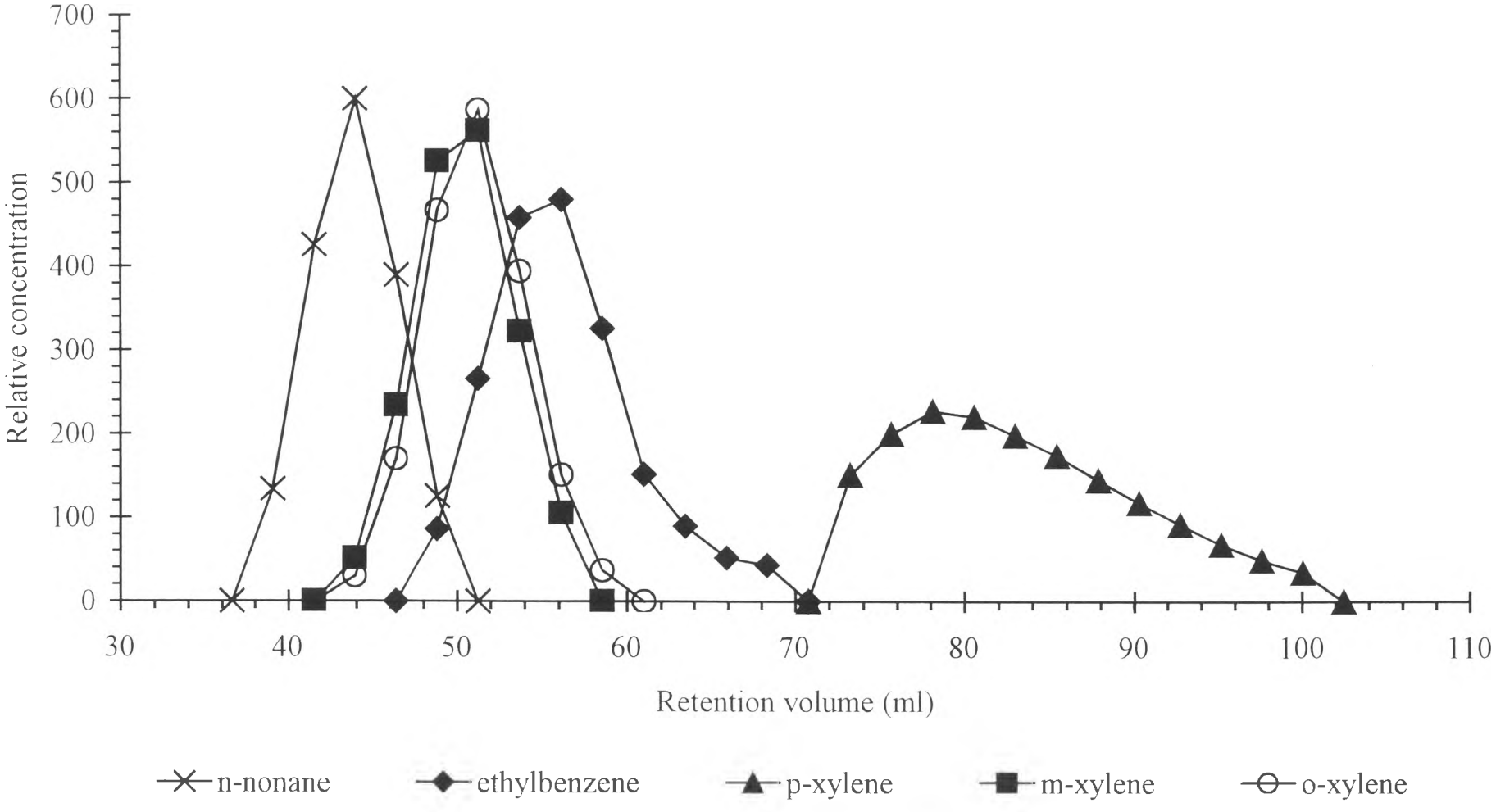

Figure 4.74 Pulse test on *KY* zeolite, LOI=1.2% at 65 °C

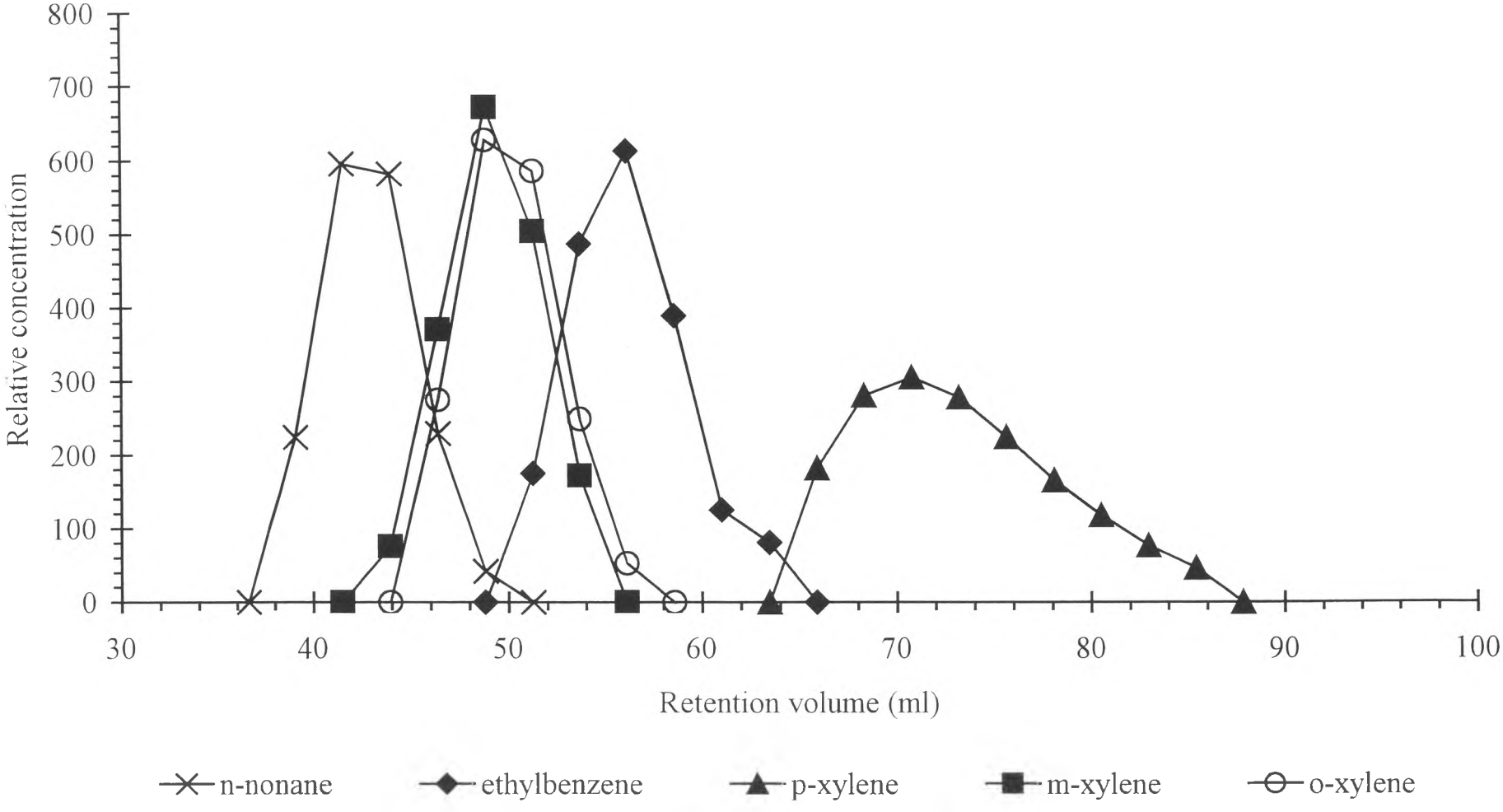

Figure 4.75 Pulse test on *KY* zeolite, LOI=1.2% at 90 °C

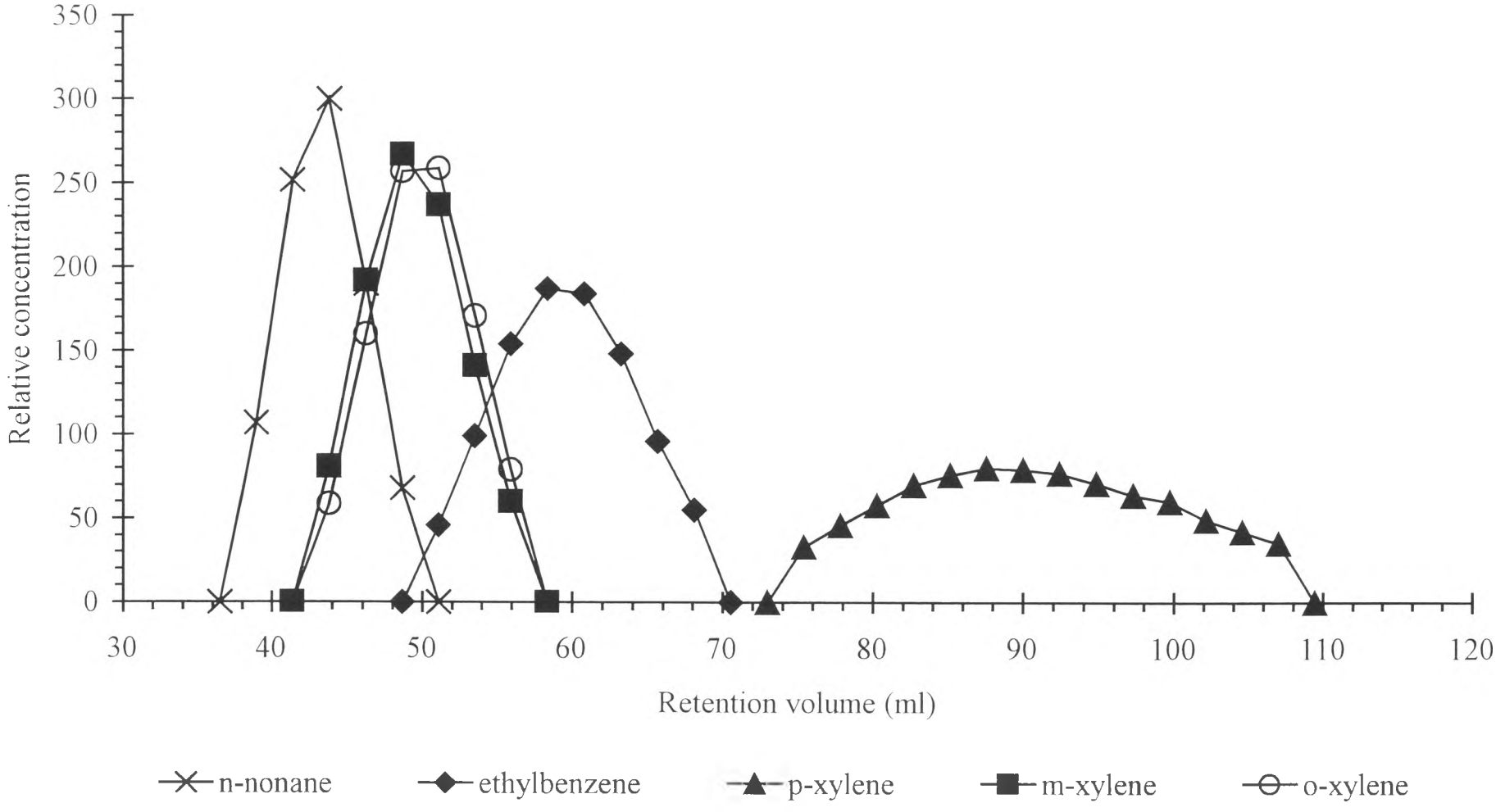

Figure 4.76 Pulse test on *KY* zeolite, LOI=2.4% at 40 °C

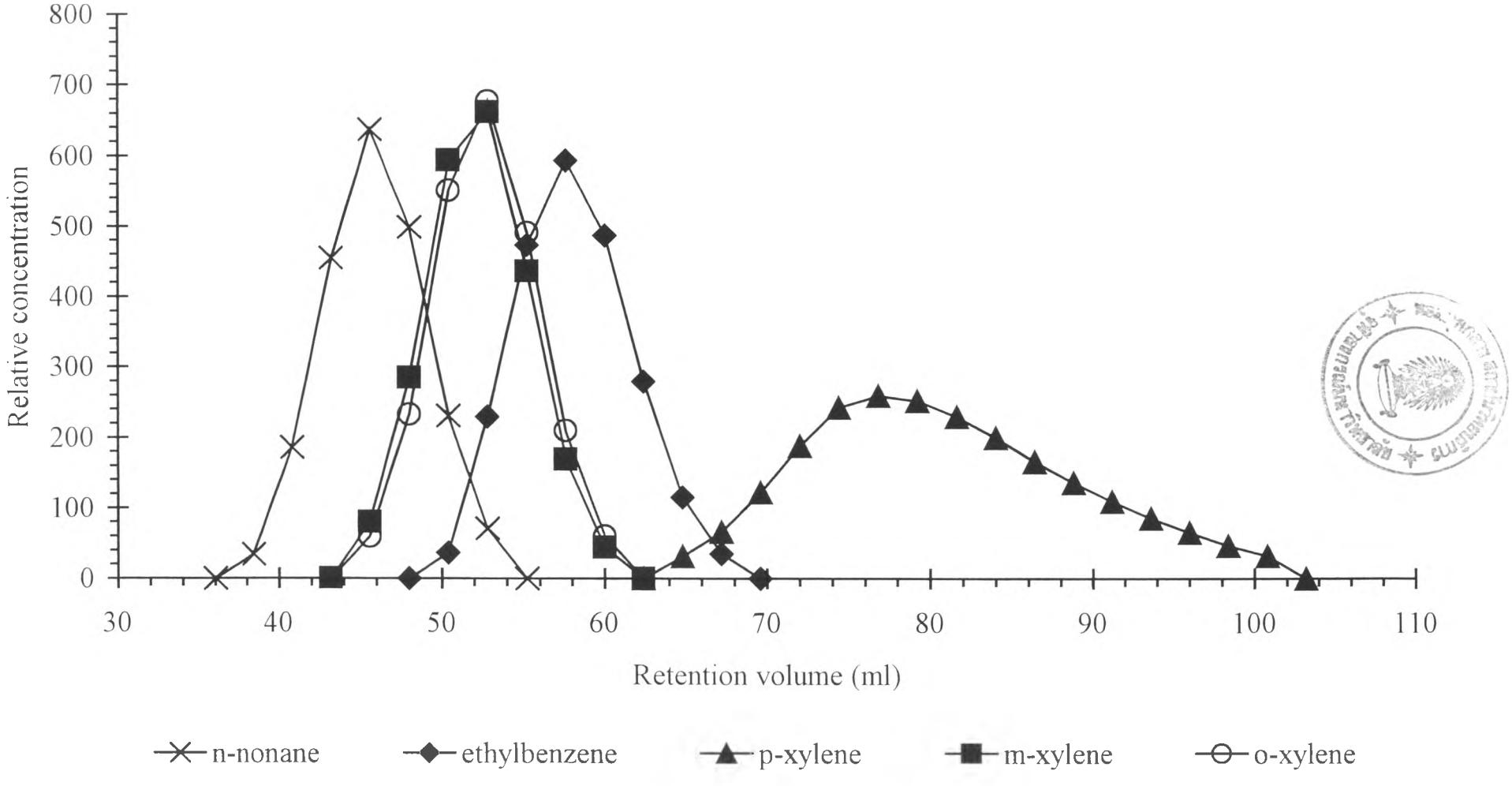

Figure 4.77 Pulse test on *KY* zeolite, LOI=2.4% at 65 °C

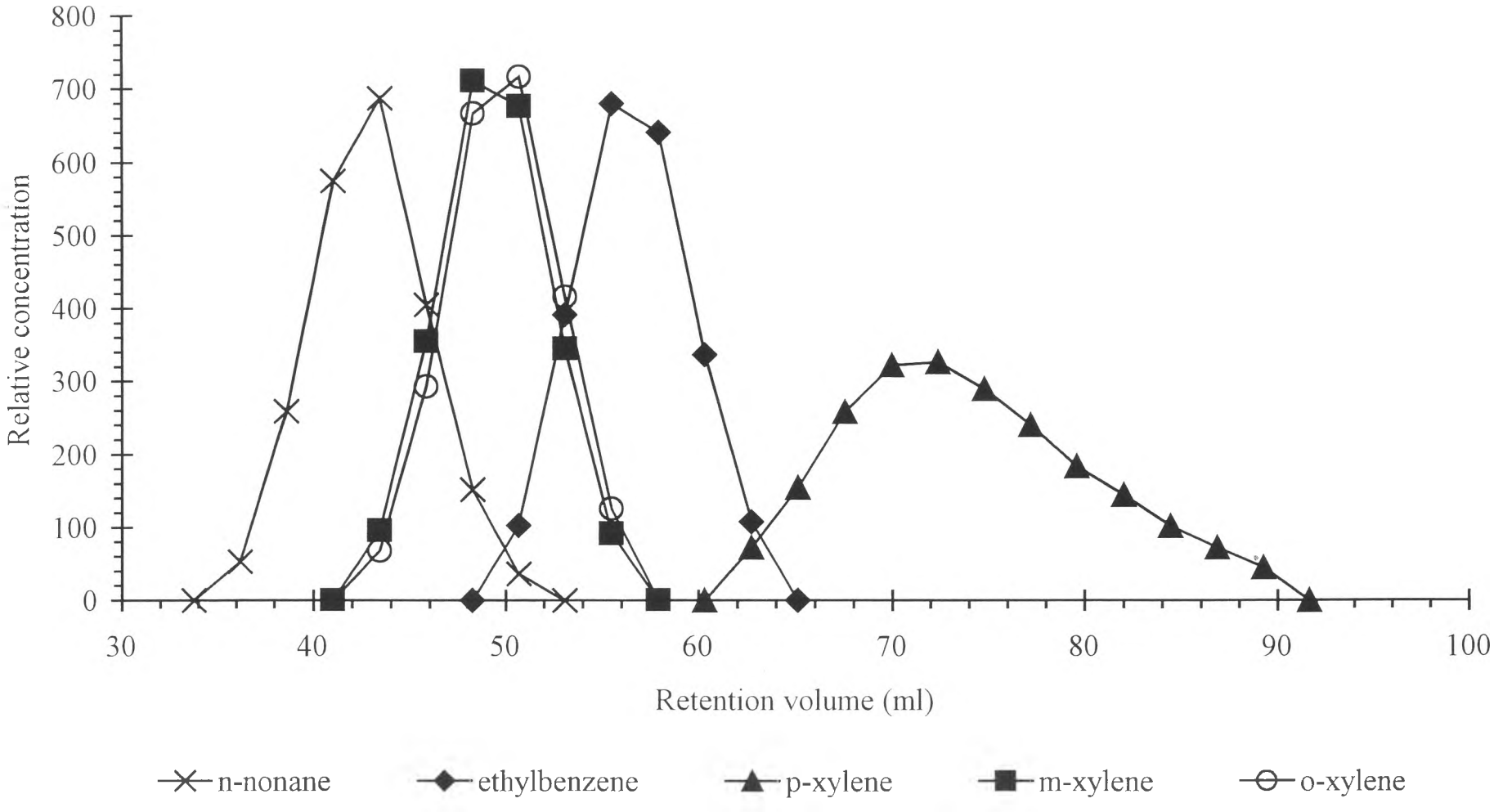

Figure 4.78 Pulse test on *KY* zeolit, LOI=2.4% at 90 °C

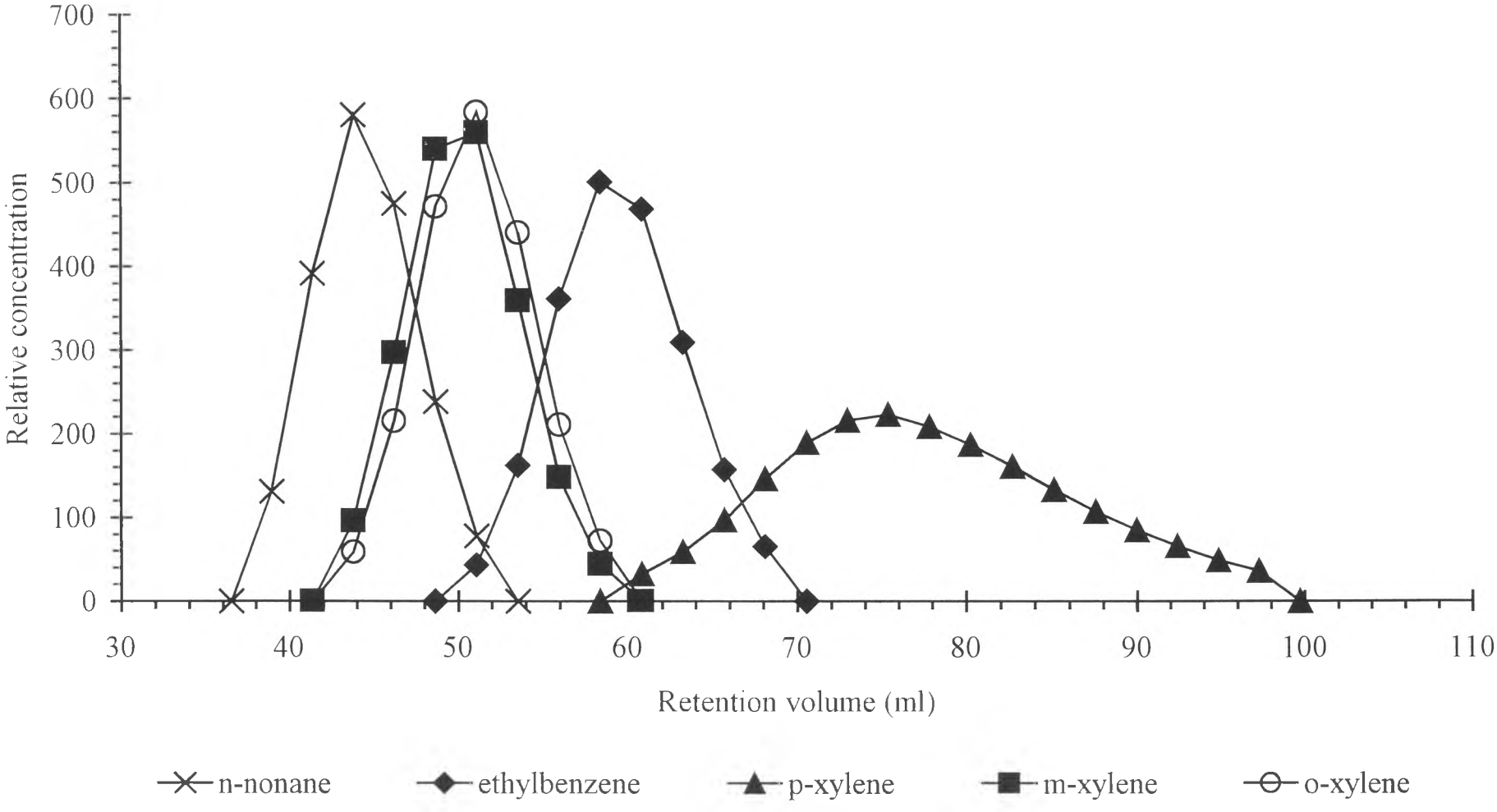

Figure 4.79 Pulse test on *KY* zeolite, LOI=4.4% at 40 °C

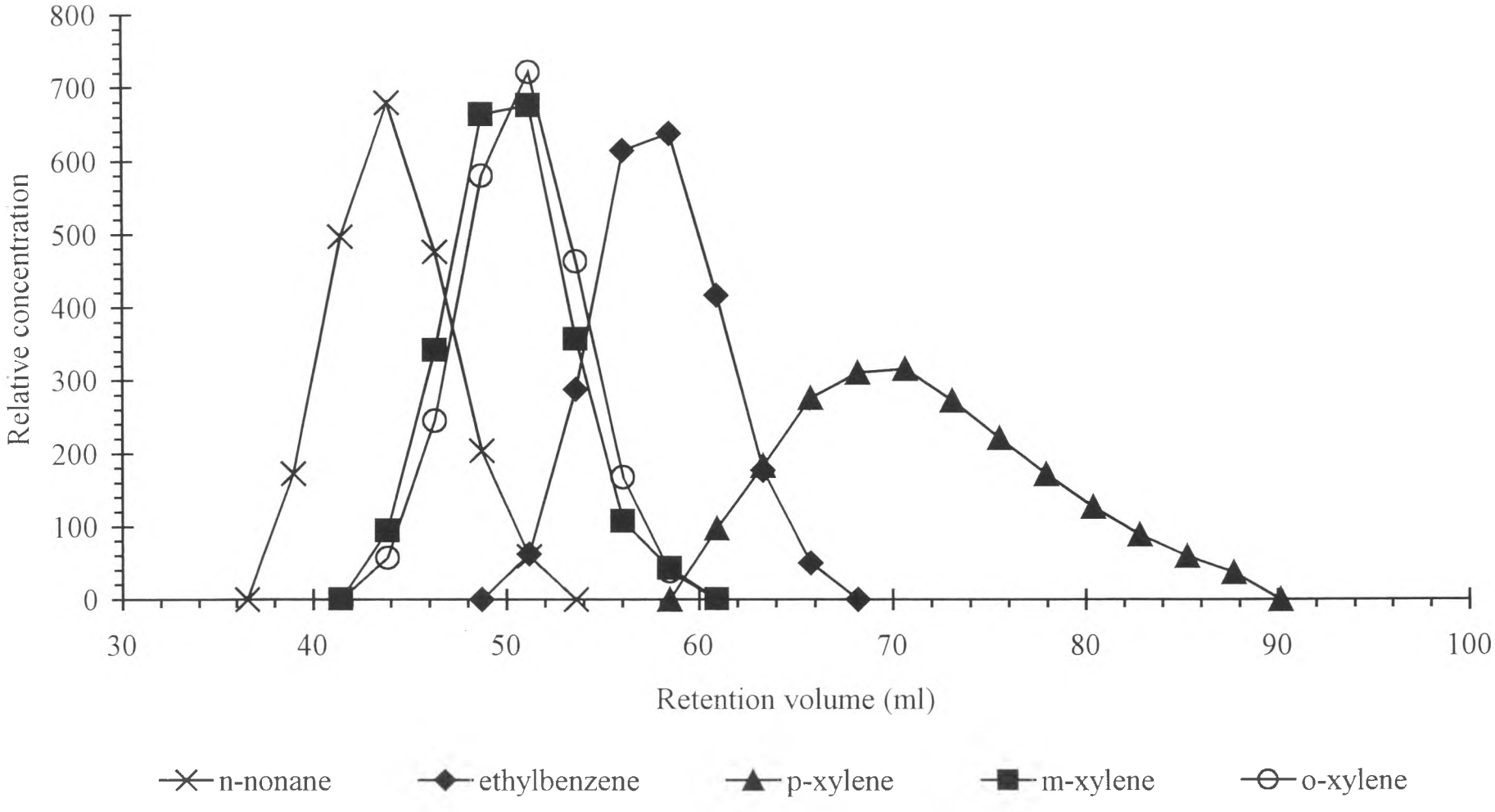

Figure 4.80 Pulse test on *KY* zeolite, LOI=4.4% at 65 °C

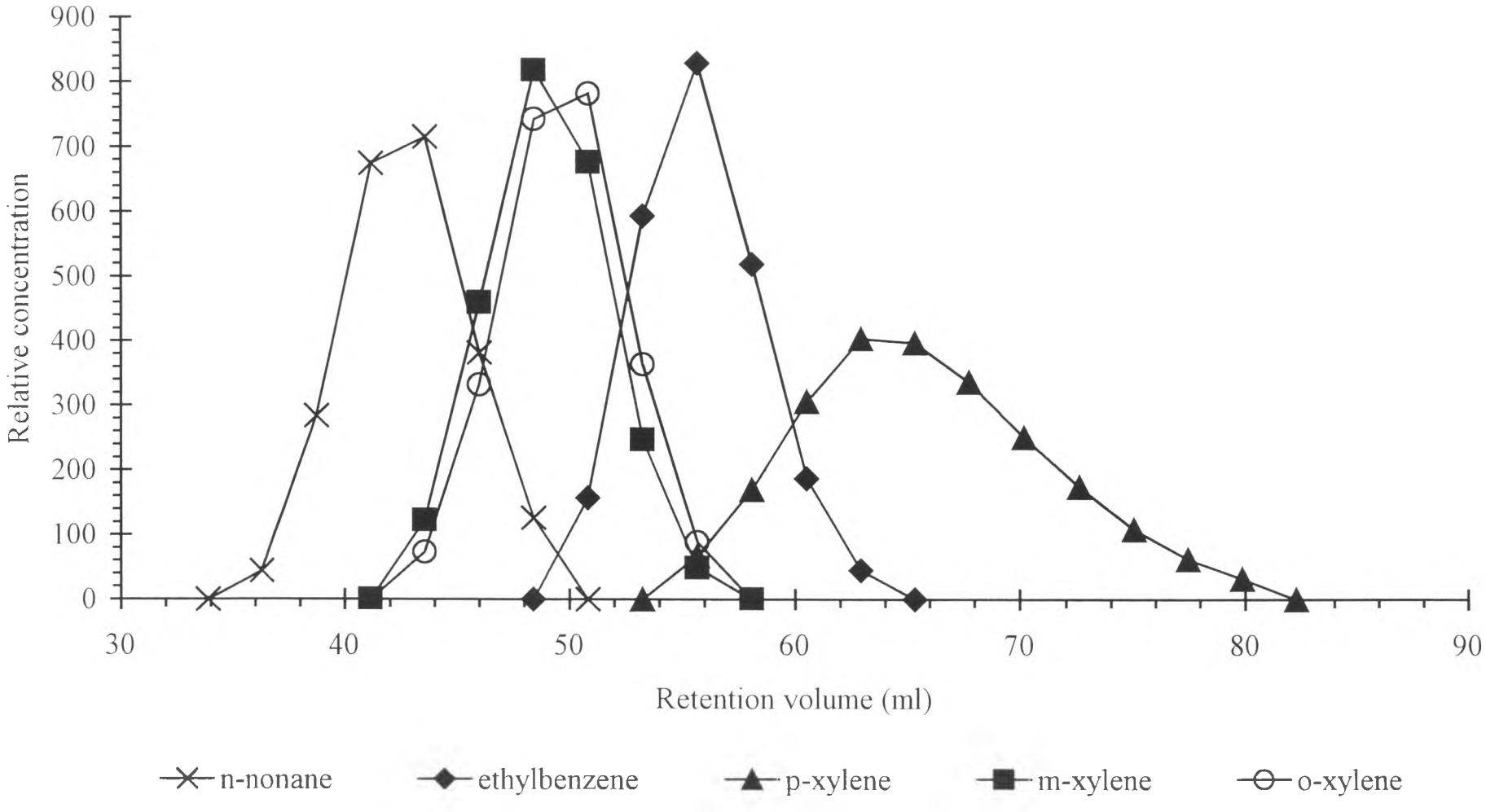

Figure 4.81 Pulse test on *KY* zeolite, LOI=4.4% at 90 °C